Article

One Earth

# Ecosystem heterogeneity is key to limiting the increasing climate-driven risks to European forests

## Graphical abstract

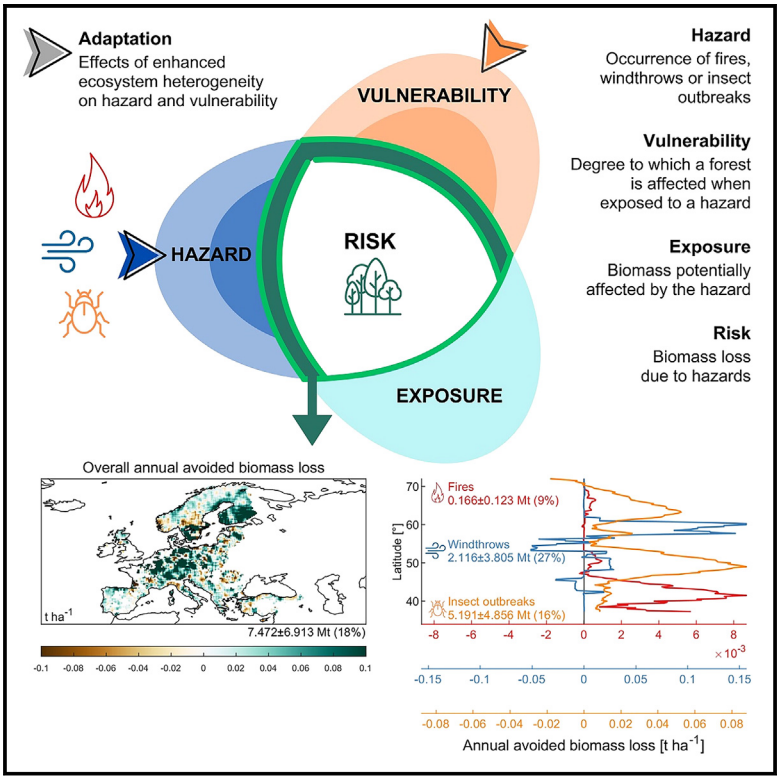


## Highlights

- Forest disturbances have led to a rise in biomass loss in Europe over 1979–2018
- Climate change has largely determined the increasing trend in risk
- The contribution of insect outbreaks is prominent compared to windthrows and fires
- Enhancing ecosystem heterogeneity reduces the climate risks to European forests

## Authors

Giovanni Forzieri, Hervé Jactel, Alessandra Bianchi, Jonathan Spinoni, Deepakrishna Somasundaram, Luc Feyen, Alessandro Cescatti

## Correspondence

giovanni.forzieri@unifi.it

## In brief

Quantifying the impact of forest disturbances and disentangling the underlying ecological processes is key to identifying effective adaptation measures and preserving the long-term stability of forests. However, knowledge and methodological gaps in observing, understanding, and predicting natural disturbances have so far hampered substantial progress. Our contribution provides an observation-based assessment of the impact of natural disturbances on European forests occurring over the period 1979–2018, elucidates their key drivers, and estimates the benefits achievable from enhanced ecosystem heterogeneity.

Forzieri et al., 2024, One Earth 7, 1–16
December 20, 2024 
https://doi.org/10.1016/j.oneear.2024.10.005

CellPress

One Earth

CellPress
OPEN ACCESS

Article

# Ecosystem heterogeneity is key to limiting the increasing climate-driven risks to European forests

Giovanni Forzieri,[1,6,*] Hervé Jactel,[2] Alessandra Bianchi,[3] Jonathan Spinoni,[4] Deepakrishna Somasundaram,[1] Luc Feyen,[5] and Alessandro Cescatti[5]

[1]Department of Civil and Environmental Engineering, University of Florence, Firenze, Italy
[2]INRAE, University of Bordeaux, BIOGECO, F-33610 Cestas, France
[3]FINCONS SPA, Vimercate, Italy
[4]Department of Management, Economics and Industrial Engineering, Polytechnic University of Milan, Milan, Italy
[5]Joint Research Centre, European Commission, Ispra, Italy
[6]Lead contact
*Correspondence: giovanni.forzieri@unifi.it
https://doi.org/10.1016/j.oneear.2024.10.005

**SCIENCE FOR SOCIETY** Forest mortality due to natural disturbances such as fires, storms, and pests has increased in Europe in recent decades and is expected to increase further due to climate change. Although important forest services may soon be seriously affected, assessments of the negative effects of natural disturbances and possible solutions to minimize them are still scarce. Ecosystem heterogeneity—the diversity of tree species and sizes—has been suggested as an option to increase forest resistance, but its effectiveness remains elusive. Here, we estimate the biomass loss due to natural disturbances on European forests from 1979 to 2018 and evaluate the benefits of increasing forest heterogeneity. We used the Intergovernmental Panel on Climate Change method for climate risk assessment by integrating disturbance records and satellite data. Results show that enhancing the ecosystem heterogeneity could reduce biomass loss by about 18%, and such action should therefore be fostered to minimize climate-related risks to European forests.

## SUMMARY

The rise in forest disturbances due to climate change poses a serious threat to key forest ecosystem services, yet impact and adaptation assessments are scarce at European scale. Here, we estimate the forest biomass loss in Europe due to fires, windthrows, and insect outbreaks over 1979–2018 and evaluate potential adaptation benefits by integrating machine learning with disturbance data and satellite products. Results show an average overall annual biomass loss of 41.6 ± 5.3 Mt at European level subject to a significant rise of 2.3 ± 0.3 Mt year$^{-1}$, largely influenced by climate change (72%–98%). The contribution of insect outbreaks appears prominent (79%) compared to windthrows (20%) and fires (1%) and linked to their upsurge after the year 2000. However, impacts vary greatly across Europe depending on local environmental conditions. We estimate that enhancing ecosystem heterogeneity could reduce biomass loss by about 18%, and such action should therefore be fostered in forest adaptation policies.

## INTRODUCTION

European forests cover about 2 million km$^2$, corresponding to 35% of the land surface.[1] They provide a large set of ecosystem services that contribute to human well-being and are considered a key element for mitigating climate change.[2] However, forests are vulnerable systems, as the long lifespan of trees limits a rapid adaptation to fast environmental changes.[3,4] Stand-replacing natural disturbances—large pulses of tree mortality that originate from abiotic and biotic agents such as fires, strong winds, or insect outbreaks—are an integral part of forest dynamics. Disturbances modify the structure, composition, and function of the ecosystem, altering the resource availability and the physical environment. In doing so, they affect biodiversity[5] and initiate ecosystem renewal or reorganization.[6] However, a sudden increase in disturbance occurrence and severity has been

Please cite this article in press as: Forzieri et al., Ecosystem heterogeneity is key to limiting the increasing climate-driven risks to European forests, One Earth (2024), https://doi.org/10.1016/j.oneear.2024.10.005



documented over the last decades at European level, causing widespread tree mortality,[7–9] and it is expected to further rise as a result of climate and global change.[10,11] Consequently, key forest ecosystem services, such as land-based climate mitigation, could be seriously reduced in the near future.[10,12,13] Quantifying the impact of forest disturbances and elucidating the underlying ecological drivers and processes is therefore of paramount importance in identifying effective adaptation measures and preserving the long-term provision of ecosystem services and stability of European forests.

Recent studies have proposed the evaluation of climate-driven risks to forests based on the integration of the widely used concepts of hazard, vulnerability, and exposure as defined by the Intergovernmental Panel on Climate Change (IPCC).[14,15] Although such a method has long been adopted in socio-economic and climate-change-related studies,[15] it has been rarely applied to forests[16–18] and has yet to be implemented comprehensively at large scales on multiple types of disturbances. In this context, the hazard represents the occurrence of a natural disturbance affecting forests (e.g., fires, windthrows, or insect outbreaks), vulnerability expresses the degree to which a forest is affected when exposed to a hazard, and exposure refers to the amount of forest resources (e.g., biomass) potentially affected by the hazard. Each of the aforementioned risk components can be modulated by changes in environmental drivers, such as background climate conditions (e.g., water stress and wind speed) and vegetation properties (e.g., structural and physiological characteristics).[19]

Forest management can influence the hazard, vulnerability, and exposure of forests to natural disturbances, ultimately affecting the overall risk levels.[16] To implement adaptive forest management measures, it is therefore crucial to provide robust spatially explicit risk estimates and understand how the changes in vegetation properties mediated by management interact with climate parameters in determining hazard, vulnerability, and exposure. Attempts to cope with climate-driven disturbances without a comprehensive assessment of the underlying drivers may lead to unintended negative consequences of adaptation plans (maladaptation) as documented in a number of studies.[20–22] However, disentangling the effect of risk components and environmental drivers is extremely challenging, due to the multivariate non-linear dynamics of forest disturbances typically characterized by strong interacting features.[4,23]

Two major approaches have been used to examine forest disturbances and their key determinants at large scales. First, process-based vegetation models, such as land surface models or dynamic global vegetation models, include an increasingly sophisticated representation of forest disturbances driven by the interplay between climate drivers and forest properties.[24–26] While such tools hold promise to quantify forest risk, they still only partially represent the complex interactions between hazard, vulnerability and exposure, due to an incomplete understanding and representation of the underlying processes, the lack of information to parameterize these processes over large areas, and the mismatch between model resolution and disturbance extent.[24,26,27] Second, empirical assessments of climate controls on forest disturbances, typically based on satellite data of forest loss[8,28] or meta-analyses of field studies,[9,29] are also exploited. These studies have provided important insights into specific aspects yet mostly lack a quantitative evaluation of the impacts (e.g., loss in ecosystem services) associated with such climate-driven disturbances. Rather, they have mainly focused on the vulnerability component,[4,30] have considered a limited set of hazards and drivers,[7,18,31,32] or have neglected the spatial variability of the phenomena because of the use of country-scale disturbance records.[7,10,33] In addition, these approaches mostly adopt a priori knowledge to identify the functional relationships that link the risk component under consideration and its potential drivers. Therefore, possible amplification or dampening effects that may emerge at local scale from interactions among multiple drivers and risk components[34] cannot be fully detected.

The European Union (EU) has adopted the first ever European Climate Law[35] with the ambitious target of achieving climate neutrality by 2050. To reach this goal, existing policies assume forests to act as a sustained net carbon sink for decades. This assumption is challenged by the sudden increase in climate-driven natural disturbances that may expose forests to widespread rises of mortality rates. A continued increase in forest disturbances will put policy targets out of reach.[36] In light of these limitations, the monitoring of climate-related risks and the development of adaptation strategies for the forest sector in Europe remain critical, especially because of the urgency imposed by the rapid changes in climate and the observed decline in forest resilience.[4,37] Ecosystem heterogeneity, resulting from compositional and/or structural diversity of vegetation, has long been suggested as a valuable strategy to increase forest resistance to natural disturbances.[38,39] However, its effectiveness with respect to multiple disturbances still needs more solid evidence[40] and has yet to be verified in the context of climate change. Empirical evidence on the benefits of enhancing ecosystem heterogeneity is scarce at large scales,[41,42] and it is unclear to what extent results based on silvicultural practices developed at stand or landscape scale[43–46] can be extrapolated to larger areas. Investigating this issue at pan-European scale would be particularly useful to support the EU in the design and development of forest adaptation strategies and to prioritize regional investments aimed at fostering the implementation of such actions at regional and national levels.

Here, we provide an observation-based and spatially explicit comprehensive assessment of the impact of fires, windthrows, and insect outbreaks in European forests that occurred over the period 1979–2018, elucidate their key risk components and environmental drivers, and estimate the benefits achievable from enhanced ecosystem heterogeneity. To this aim, we implemented a novel methodology, consistent with the IPCC risk-assessment framework, and express the biomass loss—our risk metric—as the product of hazard, vulnerability, and exposure. We use random forest (RF) as a machine learning method[47] to characterize the space-time dynamics of each risk component in response to a suite of climate and vegetation drivers. The inherent ability of RF models to detect interacting features from data avoids the prescription of specific relations between variables. We retrieve a pool of environmental drivers by integrating geocoded datasets of forest disturbance events, distinguished per agent type (fires, windthrows, and insect outbreaks), with multiple satellite-based and reanalysis products (Texts S1 and S2). The RF models—implemented for different plant

Please cite this article in press as: Forzieri et al., Ecosystem heterogeneity is key to limiting the increasing climate-driven risks to European forests, One Earth (2024), https://doi.org/10.1016/j.oneear.2024.10.005



CellPress
OPEN ACCESS

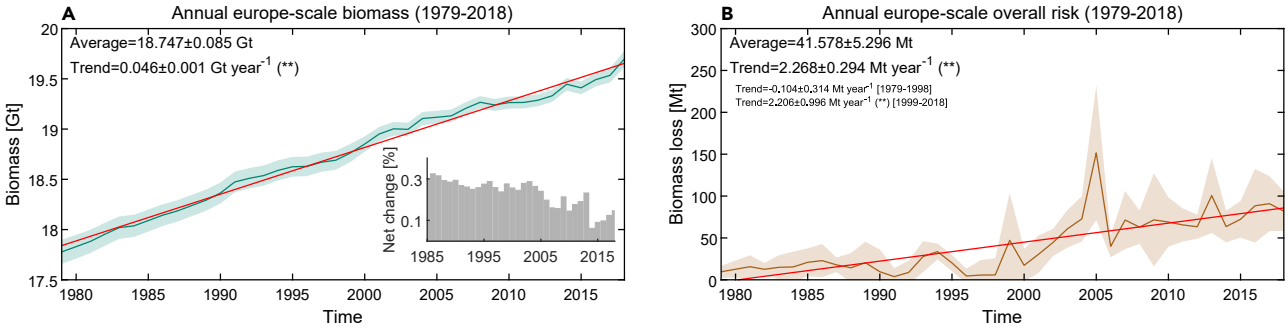


**Figure 1. Temporal variations in biomass and overall risk in European forests**

(A and B) (A) Annual changes in forest biomass aggregated at European scale (green line) and corresponding 95% confidence interval (shaded area). Inter-annual net changes in forest biomass are shown in the inset. (B) Annual changes in overall risk expressed in terms of biomass loss caused by fires, windthrows, and insect outbreaks aggregated at European scale (brown line) and corresponding 95% confidence interval (shaded area). Long-term average and trend in biomass and climate risk over the period 1979–2018 are displayed as red lines and reported (top left) together with their standard error; "**" indicates a significance level with $p$ value of <0.05 (two-sided modified Mann-Kendall test). Trends in biomass losses are computed for 1979–1998 and 1999–2018 separately and reported in smaller font in (B).

functional types (PFTs), disturbance agents, and risk components—are applied at 0.25° spatial resolution over the whole of Europe annually over the 40-year observational period (see experimental procedures). Our analysis provides data-driven evidence that changes in climate during the past four decades have largely contributed to the intensification of disturbances related to fires, windthrows, and insect outbreaks in European forests, resulting in a progressive rise in biomass loss. Such a trend appears to be largely due to the widespread upsurge of insect outbreaks after the year 2000. Results also show that promoting the heterogeneity of European forests could reduce total biomass loss by about 18%. Our findings emphasize the importance of implementing adaptation strategies to increase the level of forest heterogeneity and thus reduce the increasing climate-driven risks and their negative impacts on climate mitigation plans.

## RESULTS AND DISCUSSION

### Temporal variations in biomass and overall risk at European scale

At the European level, we estimate the average woody biomass stock at 18.747 ± 0.085 Gt with an average increment of 0.046 ± 0.001 Gt year$^{-1}$ ($p$ value <0.05) between 1979 and 2018 (Figure 1A). Central and Northern European countries contribute most in terms of both overall biomass stock and temporal changes (Figure S1 and Table S1). Estimates appear to represent reasonably well reference data[48,49] used for the exposure model development (experimental procedures and Figure S2) and are further corroborated by independent assessments reported in the literature.[50] The increase in biomass stock has been attributed to a change in management practices, $CO_2$ fertilization, N deposition, and growing season extension.[51,52] However, our analysis shows a slowing down of biomass accumulation since 2000, reflected in a reduction of biomass net annual change (Figure 1A, insect box), as confirmed by the report on the State of Europe's Forests.[1] Recent observational studies suggest that the world's forests are transitioning from a period dominated by the positive effects of $CO_2$ fertilization to a period characterized by the progressive reduction of these effects and the rise of negative climate change impacts.[53,54] Such a transitioning phase is particularly pronounced in Europe with a mean warming about twice the rate of the global mean average.[55] This is happening in forest ecosystems that have been heavily influenced by humans in the recent past. Indeed, after World War II forest management in central Europe was mainly oriented at increasing forest yields (e.g., even-aged monoculture plantations) to the detriment of their climatic suitability and vulnerability.[56] The increase in climate-driven natural disturbances has been hypothesized as a plausible cause of carbon sink saturation in Europe.[57] In this study, by integrating hazard, vulnerability, and exposure metrics in a consistent data-driven risk-assessment framework, we provide further evidence in support of such a hypothesis. Our climate risk assessment indicates—at the European level—an average and trend in overall biomass loss due to climate-driven disturbances of 41.578 ± 5.296 Mt and 2.268 ± 0.294 Mt year$^{-1}$ ($p < 0.05$), respectively, between 1979 and 2018, with a strong upsurge after the year 2000 (Figure 1B). The area affected by such disturbances is rapidly increasing and may affect the dynamics of the growing stock, the land carbon budget, and potentially the supply chain of forest biomass.

### Biomass loss caused by forest disturbances and underlying ecological mechanisms

To better elucidate the underlying ecological mechanisms that caused disturbances, we analyzed the spatial and temporal variations of biomass loss due to fires, windthrows, and insect outbreaks separately. These analyses have been complemented by a series of factorial simulations to disentangle the marginal effect of each risk component (hazard, vulnerability, exposure) and quantify the effects of vegetation properties and climate drivers on biomass loss (experimental procedures).

We estimated that the average overall impact of natural disturbances on forest biomass (Figure 1B) has been largely caused by insect outbreaks, which have damaged annually 31.855 ± 3.811 Mt of biomass (77% of the total damaged biomass) followed by the impact of windthrows and fires, which have led to 7.864 ± 2.735 Mt and 1.859 ± 0.086 Mt of biomass loss, respectively (19% and 4% of the total). Similarly, in terms of

Please cite this article in press as: Forzieri et al., Ecosystem heterogeneity is key to limiting the increasing climate-driven risks to European forests, One Earth (2024), https://doi.org/10.1016/j.oneear.2024.10.005



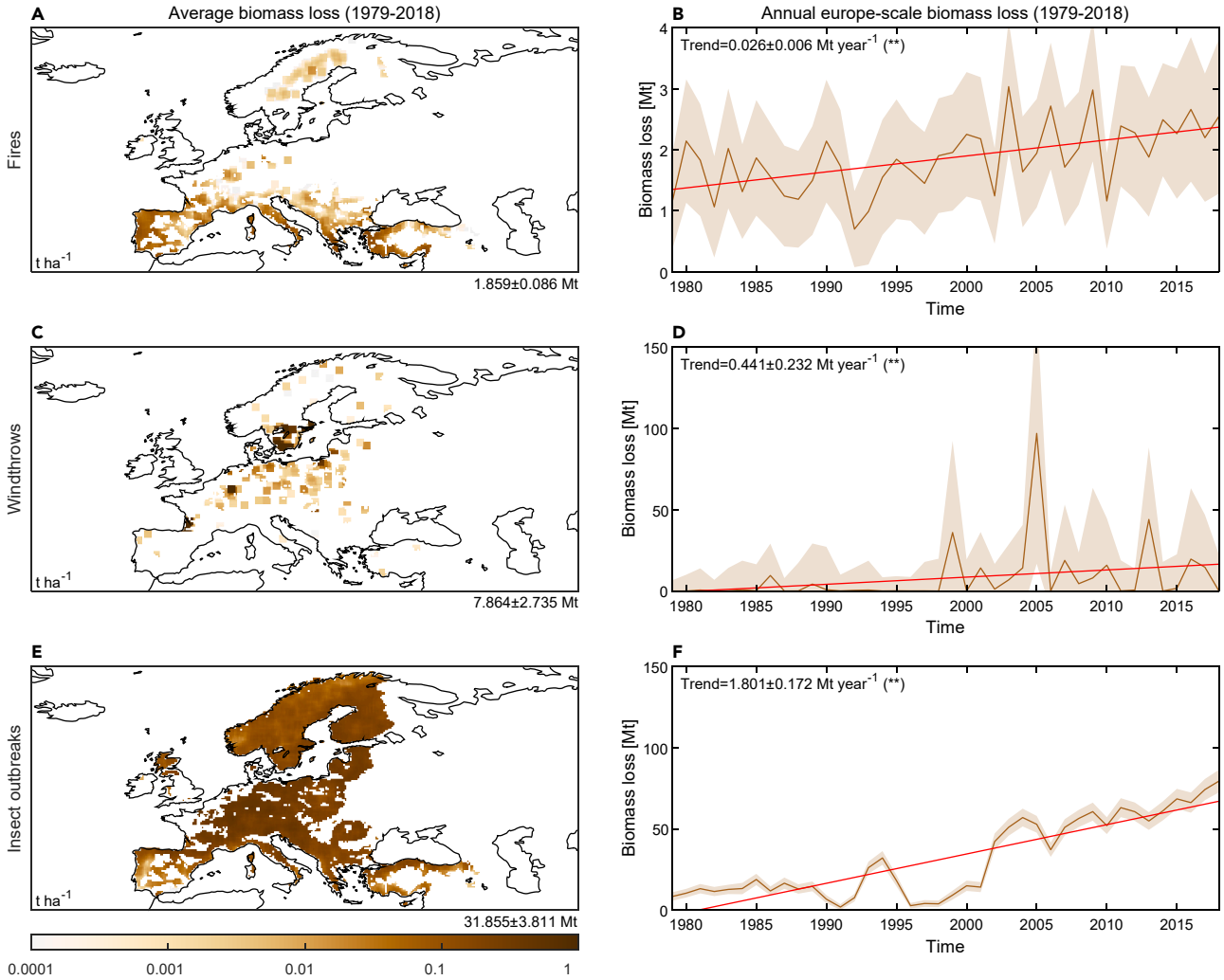


**Figure 2. Spatial and temporal variations of biomass loss caused by fires, windthrows, and insect outbreaks**

(A–F) (A) Spatial map of annual average of biomass loss caused by fires over the period 1979–2018 and corresponding value aggregated at European scale reported as average ± SE (bottom right). Forests with cover fraction lower than 0.1 are masked in white. (B) Annual changes in biomass loss caused by fires aggregated at European scale (brown line) and corresponding 95% confidence interval (shaded area). Long-term trend in biomass loss is displayed as red line and reported together with its SE; "**" indicates a significance level with $p$ value of <0.05 (two-sided modified Mann-Kendall test). (C–F) As (A) and (B) but for windthrows (C and D) and insect outbreaks (E and F). Confidence intervals in (F) are multiplied by a factor of 5, and values in (A), (C), and (E) are averaged over a 1.25° × 1.25° moving window for visual purposes.

temporal variability, damage due to insect outbreaks has contributed most to the long-term variations in the overall biomass loss, explaining 79% of its trend, whereas windthrows and fires explain the remaining 20% and 1%, respectively. However, substantial differences emerged across geographic regions for the three climate-driven disturbances, reflecting their strong dependence on local environmental conditions (Figure 2).

As expected, forest fires show a prominent spatial gradient of biomass loss toward southern Europe (Figure 2A and Table S2). Severe aridity (Figures S3A–S3D) led to high average levels of hazard and vulnerability[58] (Figures S4A and S4B), making fires the most important natural disturbance in most Mediterranean forests (Figure S5). Over the observational period, Europe—and particularly southern countries—has experienced a significant increase in fire-induced biomass loss (0.026 ± 0.006 Mt year$^{-1}$, $p < 0.05$) (Figure 2B and Table S3). Such an emerging positive trend was largely driven by change in the hazard component (97%, $p < 0.05$, Figure 3A). Climate change, and particularly the increase in aridity (Figures S6A–S6D), that affects both triggering and susceptibility mechanisms,[58] was the primary underlying driver for the rise in biomass loss from forest fires (72%, $p < 0.05$, Figure 3B). Changes in the structural properties of forests (e.g., amount of woody biomass and leaf area index) played an important role as well (27%, Figure 3B) by affecting a series of processes, such as the amount of fuel loads and the probability of fire ignition.[59,60] However, these effects are significant ($p < 0.1$) only when aggregated at European scale (Figure S7B). Noteworthy, temporal changes in single risk components and underlying environmental drivers did not lead to a systematic increase

Please cite this article in press as: Forzieri et al., Ecosystem heterogeneity is key to limiting the increasing climate-driven risks to European forests, One Earth (2024), https://doi.org/10.1016/j.oneear.2024.10.005



CellPress
OPEN ACCESS

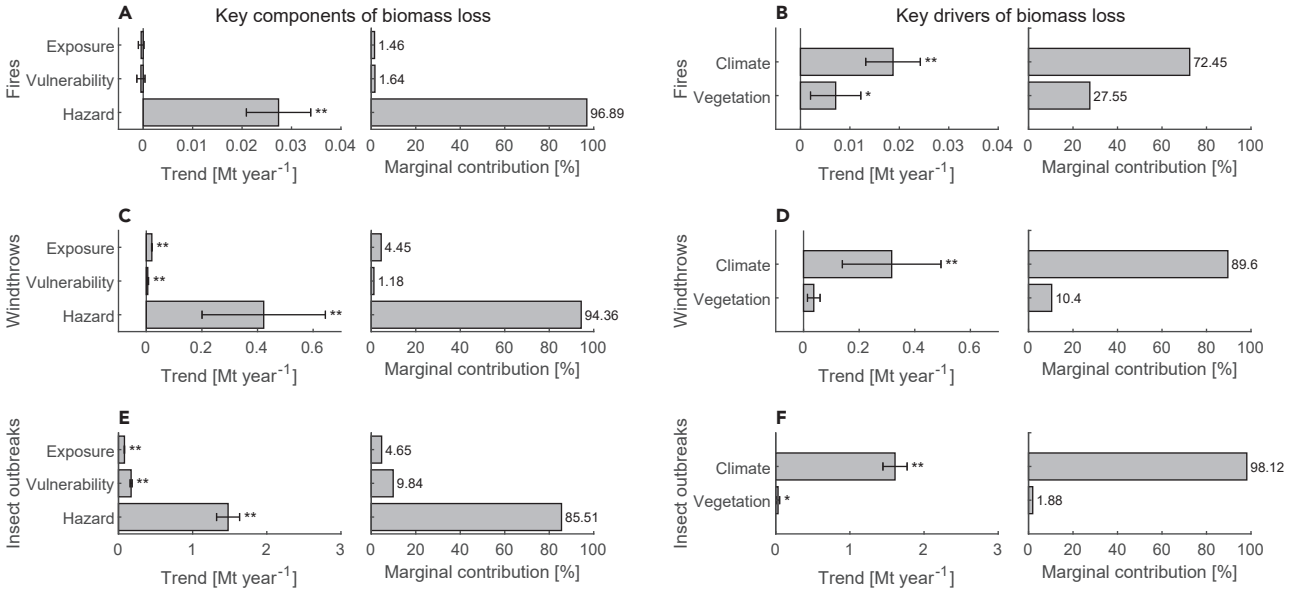


**Figure 3. Key determinants of natural disturbances**

(A–F) (A) Long-term trend in biomass loss (average ± SE) due to fires, aggregated at European scale, owing to changes in each risk component (hazard/vulnerability/exposure) and corresponding marginal contribution to the overall trend (left and right panel, respectively). "**" and "*" indicate trend statistically significant with $p$ values of <0.05 and <0.1, respectively (two-sided modified Mann-Kendall test). (B) As (A), but for trend in biomass loss due to fires, owing to changes in certain key drivers (vegetation/climate). (C–F) As (A) and (B), but for windthrows (C and D) and insect outbreaks (E and F).

in disturbance regimes. For instance, the variations in vulnerability and exposure over the period 1979–2018 in southern Europe have led to a reduction in biomass loss due to fires (Figure S7A). These patterns, whose statistical significance remains largely elusive, can be associated with a decline in available fuel loads (Figure S1B). However, the large increase in the hazard component, as mentioned above, offsets the mild negative trends in biomass loss, ultimately leading to an increase in risk levels also in these regions.

Windthrows, being an extreme event strongly dependent on exceptional weather conditions modulated by local orography,[61] showed a discontinuous spatial pattern with larger biomass loss in northern and western Europe (Figure 2C and Table S2). Biomass loss due to such hazards experienced a significant increase ($0.441 \pm 0.232$ Mt year$^{-1}$, $p < 0.05$) over the observational period, although the temporal dynamics were dominated by strong inter-annual variability (Figure 2D), with impacts being locally much larger than any other disturbance type (Figure S5). For example, we estimated that ~97 Mt of biomass was damaged in 2005 by the windstorm Gudrun in Sweden, equivalent to about 2 years of harvesting at national scale. In 2007, the windstorm Kyrill caused the loss of ~19 Mt of biomass in Germany and the Czech Republic. In 2009, the windstorm Klaus hit forests in France and caused biomass losses of about 16 Mt. Temporal variations in biomass loss due to windthrows were dominated by change in the hazard component (94%, $p < 0.05$, Figure 3C), whereas variations in vulnerability and exposure showed minor contributions but were still statistically significant. Climate factors were the dominant underlying drivers (90%, $p < 0.05$, Figure 3D). The damaging effect of wind gusts, a key determining factor of windthrows, is also amplified by soil water content, as captured by precipitation, and snow load on the crown. Storm impacts are amplified in regions with increasing amounts of rainfall and snowfall (Figures S6E–S6G), which tend to favor tree overturning and stem breakage.[61,62] Biomass accumulation, by increasing bending moment and exposure,[63] also contributed to an increase in risk levels (10%, Figure 3D), although such effects are not statistically significant ($p > 0.1$) across the European regions (Figure S7D).

Insect outbreaks caused a high average loss of forest biomass across most of Europe (Figures 2E and S5), predominately resulting from a widespread distribution of the hazard component (Figure S4E). Biomass loss due to insect outbreaks significantly increased from south to north (Figure 2E and Table S2), closely following the distribution of certain tree species such as Norway spruce,[64] typically more vulnerable to insect outbreaks. In addition, this pattern likely reflects a strong dependence of disturbance processes on average temperature[19] (Figures S3H–S3J), because bark beetles are poikilothermic organisms that respond favorably to global warming by improving winter survival, multiplying the number of generations per year and expanding their natural range northward in Europe.[65,66] In addition, high-biomass monospecific coniferous forests of central and northern Europe are notoriously at higher risk of bark beetle outbreaks.[67,68] Biomass loss due to insect outbreaks significantly increased over the observational period ($1.801 \pm 0.172$ Mt year$^{-1}$, $p < 0.05$, Figure 2F), with a strong rise since the year 2000 in northern and central Europe (Table S3). This is consistent with the abrupt increase in vulnerability of forests to insect outbreaks observed for warming levels larger than +0.5°C (referring to 1970–1990) that occurred around the year 2000 at European scale and documented in previous studies.[4,9] Further increases in temperature above such a threshold (Figures S6H–S6J) have likely reduced plant defense mechanisms by ultimately favoring

Please cite this article in press as: Forzieri et al., Ecosystem heterogeneity is key to limiting the increasing climate-driven risks to European forests, One Earth (2024), https://doi.org/10.1016/j.oneear.2024.10.005



triggering processes and making forests more vulnerable to insect attacks. This is confirmed by the significant and dominant role of the changes in climate factors, including temperature and aridity (98%, $p < 0.05$, Figure 3F), and in the hazard and vulnerability components (86% and 10%, $p < 0.05$, Figure 3E) in determining the biomass loss dynamics. Furthermore, the concurrent increase in windthrow and insect outbreaks seems to suggest a possible amplification generated from the interaction effect between these two disturbances (Figures 2D–2F). Uprooted trees from strong winds are virtually defenseless breeding material, supporting the buildup of bark beetle populations and the consequent increase in insect outbreaks.[23] However, it is difficult to disentangle such interactions in our assessment due to the lack of reference observational data of compound events, and therefore they can be represented only to the extent that they are reflected in the environmental predictors of the RF models (experimental procedures). Such a climate-driven abrupt increase in insect disturbances after year 2000 could be an important cause of the slowdown in biomass growth observed at European level (Figure 1A), in parallel to direct climate effects on tree growth.[69] Changes in exposure with higher standing volume of susceptible forests, and in vegetation structural properties, have also contributed to intensified risk levels, although their effects remain limited compared to climatic determinants (Figures 3E and 3F).

The estimates of biomass losses reported above have been confronted with independent disturbance databases, including emissions from burned biomass,[70] salvage logging data,[71] and compilations of reports on past tree mortality events based on extensive literature search[9,29] (Text S3). While recognizing that the cross-comparison analysis is not fully consistent in terms of damage reported, we believe that the reasonable agreement in terms of correlations and long-term trends between the investigated datasets—especially for fires and insect outbreaks—support the overall framework proposed here (experimental procedures, Text S4, and Figure S8). Furthermore, a careful validation of each single risk component (hazard, vulnerability, and exposure) has been conducted (experimental procedures; Figures S2 and S9–S12), and possible extrapolation errors of RF models beyond the training range have been evaluated (experimental procedures; Tables S4 and S5). Although our modeling framework is not exempt from limitations in methodological and data aspects (Text S5), the obtained model performances corroborate the robustness of our modeling framework and the validity of our findings.

Overall, our results show univocally that changes in climate that occurred over the last four decades have acted as primary drivers of the observed increase in biomass loss due to forest disturbances in Europe, influencing prominently the hazard component. The detrimental effect of climate drivers on risk levels obtained here appears substantially larger compared to previous estimates that have reported climate and forest conditions to contribute almost equally.[33] Differences in datasets and methods may explain such discrepancies. In our study, we develop a spatially explicit framework to quantify risk levels due to forest disturbances over the period 1979–2018. In the aforementioned work (Seidl et al.[33]), the assessment focuses on the vulnerability component only (thus neglecting hazard and exposure components) based on country-scale disturbance records over the period 1951–2001. Therefore, the marginal effect of key drivers cannot be directly compared between these two studies. Furthermore, the crossing of a warming level in the last two decades, documented in this work as the prominent process underlying the abrupt shift in biomass loss (Figures 1B, 2E, and 2F), has likely made European forests much more sensitive to changes in climate drivers compared to the period before 2000. This is of great concern because projected warming scenarios and the resulting alteration in climate variability will likely further exacerbate these climate-driven risks[10,11] and, thus, the impact on the carbon budget of forests. The combination of increased stand-replacing forest disturbances and the climate-driven reduction of forest growth may undermine the effectiveness of nature-based climate solutions that rely on a long-term forest carbon sink.[12,36]

## Potential adaptation benefits of enhanced forest heterogeneity against natural disturbances

In such a context of increasing climate risks, it is critical to develop forest management strategies to reduce the negative impact of abiotic and biotic disturbances. Local-scale studies have shown that species-rich forests are likely to have a greater functional diversity, increasing the probability that one tree species can compensate for the negative responses of other species to disturbance.[72,73] Spatial diversity of ecosystem structure and composition across the landscape can strongly influence the extent and effect of forest disturbance processes as well, depending on agent type and characteristic of spread.[74] To elucidate the underlying mechanisms associated with ecosystem heterogeneity, we explored the relative biomass losses observed over approximately 150,000 records of disturbed forest patches across Europe, along a gradient of biomass and spatial homogeneity. Homogeneity has been derived from satellite data at 1-km spatial resolution (Tuanmu and Jetz[75]) and quantifies the spectral similarity of ecosystem spatial patterns; therefore, it is a metric negatively correlated with heterogeneity. The strong negative relationships that emerge between this metric and independent datasets on forest compositional and structural diversity (experimental procedures, Spearman rank $< -0.98$, $p < 0.05$, Figure S13), show that spectral homogeneity in forested landscapes is largely driven by the spatial heterogeneity in forest types and biomass. This is further corroborated by the high correlation between homogeneity metrics computed by including all land-cover types and those derived by accounting for forest land covers only (experimental procedures, Spearman rank >0.75, $p < 0.05$, Figure S14).

Results show that areas characterized by lower spatial homogeneity (i.e., higher heterogeneity) systematically experience lower relative biomass losses across all the disturbance types considered in this study (Figures 4A–4C). High-heterogeneity patterns, reflecting high structural or compositional diversity of ecosystems, show an enhanced forest resistance to climate-driven disturbances. This is likely thanks to the complementarity in ecological traits and climate responses among ecosystems, reduction of availability and accessibility to host species and food resources for insect herbivores,[76] and disruption of propagation processes limiting fire spread[77] and domino fall caused by windstorms.[61,62] The relationships between ecosystem heterogeneity and resistance to climate-driven disturbances is

Please cite this article in press as: Forzieri et al., Ecosystem heterogeneity is key to limiting the increasing climate-driven risks to European forests, One Earth (2024), https://doi.org/10.1016/j.oneear.2024.10.005





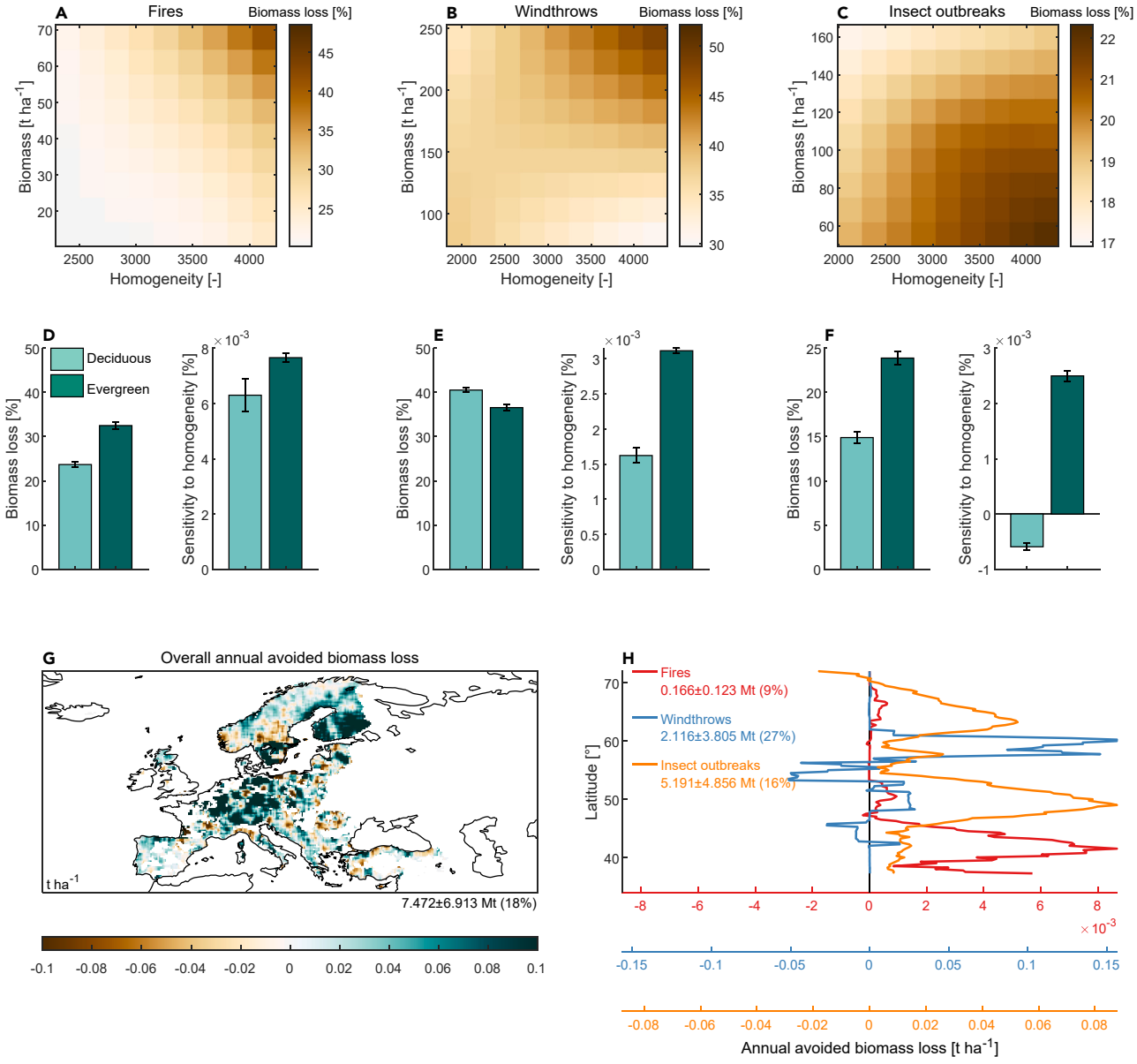


**Figure 4. Effects of enhanced heterogeneity on forest resistance against natural disturbances**

(A–H) Relative biomass loss due to fires (A), windthrows (B), and insect outbreaks (C) expressed as a function of homogeneity (inverse of heterogeneity) and biomass. Average relative biomass loss due to fires (D), windthrows (E), and insect outbreaks (F) (left panels) and its sensitivity to homogeneity (right panels) for deciduous and evergreen functional types (average ± SE). (G) Spatial map of the changes in overall biomass loss following a potential increase in ecosystem heterogeneity. Benefits (in terms of avoided biomass losses) and detrimental effects (in terms of exacerbated damages) are shown as positive and negative values, respectively. Values are averaged over a 1.25° × 1.25° moving window for visual purposes, and forests with cover fraction lower than 0.1 are masked in white. (H) Latitudinal gradient of the changes in biomass loss, separately for each natural disturbance considered, following a potential increase in ecosystem heterogeneity. Annual avoided biomass loss aggregated at European scale is shown as average ± SE (left) together with the relative variation of the actual risk estimate.

discussed in more detail in Text S6. For fire and windthrow events, these processes were more evident in high-biomass areas (Figures 4A and 4B), suggesting larger benefits of enhanced heterogeneity in forests typically more vulnerable to these disturbances.[59–61] For insect outbreaks, the benefits of increased heterogeneity appeared more evident in low-biomass patterns, such as northern conifer forests (Figure 4C). These forests in Europe show high vulnerability to insect attacks,[4] possibly because of a limited adaptation to increasing water stress and a reduced defense capacity related to tree aging. Regardless of biomass loss, the vulnerability of evergreen forest types appears more influenced by homogeneity compared to deciduous forests for all disturbance types considered (Figures 4D–4F). This signal may be driven by specific traits of

Please cite this article in press as: Forzieri et al., Ecosystem heterogeneity is key to limiting the increasing climate-driven risks to European forests, One Earth (2024), https://doi.org/10.1016/j.oneear.2024.10.005



these forests, such as root morphology, wood density, and the extended phenology, which affect the vulnerability to multiple disturbances (windthrows, droughts, bark beetles), particularly in even-aged, homogeneous stands. Therefore, an increase in structural and/or compositional diversity in evergreen forests would be particularly beneficial for these functional types of trees, enhancing their resistance against climate-driven natural disturbances. It is worth noting that deciduous forests exposed to insect outbreaks represents the only case in this study that shows a negative sensitivity to homogeneity (Figure 4F). This would suggest that heterogeneity leads to higher vulnerability of this plant functional type to insects. Deciduous forests in Europe are typically not affected by bark beetles, whereas they are vulnerable to defoliators, which are mostly primary pests feeding on healthy trees. Results seem, therefore, to suggest that diversity in deciduous forests by promoting productivity[78,79] and forest cover (canopy packing; Jucker et al.[80]) could ultimately favor the development of primary pests exploiting foliage.

We then quantify the potential benefits achievable from forest management aimed at increasing ecosystem heterogeneity. To this aim, we developed an idealized scenario, which simulates the impact of higher ecosystem heterogeneity while preserving the consistency with the local environmental conditions (Figure S15). Such a new value of increased heterogeneity has been used as predictor in the hazard and vulnerability models in place of the actual value. The high variable importance scores of ecosystem heterogeneity metrics in the hazard and vulnerability models (Figures S9–S11 and Forzieri et al.[4]) confirm their key role in influencing both triggering and susceptibility mechanisms of disturbances. Differences in risk levels generated under the actual and idealized scenarios have been ultimately used to quantify the potential reduction in biomass loss achievable with this adaptation measure (experimental procedures).

Overall, we found that about 18% of the actual overall climate-driven risk to European forests, corresponding to an annual biomass loss of 7.472 ± 6.913 Mt, could be avoided by increasing the ecosystem heterogeneity under current climate conditions (Figure 4G). This represents an important gain, which could potentially limit the carbon sink saturation effect.[57] The avoided biomass losses potentially resulting under the idealized scenario of enhanced ecosystem heterogeneity appear largely associated with the widespread reduction in the hazard component (Figures S16A, S16D, and S16G). The vulnerability component is affected as well by changes in heterogeneity. However, its response differs across geographic regions and disturbance types and may show contrasting patterns with possible amplification or dampening of risk levels (Figures S16B, S16E, and S16H). Averaged at European scale, we found that biomass loss due to fires could be reduced by 9% (annual avoided biomass loss of 0.166 ± 0.123 Mt) with larger values in Mediterranean countries (Figure 4H). Damage due to windthrows could be dampened by 27% (2.116 ± 3.805 Mt) with particularly high benefits in regions affected by destructive events (e.g., Gudrun, Kirill). Biomass loss due to insect outbreaks could be reduced by 16% (5.191 ± 4.856 Mt) with higher percentages in central and northern regions. This level of reduction is very close to that estimated at the stand level, with an average reduction of damage in mixed forests of 23% compared to pure forests.[39] Thus, consistent with previous analyses (Figures 4A–4C), larger benefits could be reached in those forests at higher risk. Considering the climate sensitivity of the risk and the forecasted climate trajectory for the 21$^{st}$ century, it is likely that the relative importance of this adaptation measure will increase under future climate conditions of European forests.

Despite the net gain in terms of overall annual avoided biomass loss, it is important to point out that an enhanced heterogeneity would not lead to a reduction of risk levels everywhere, depending on the background environmental conditions and current level of heterogeneity. For instance, an increase in ecosystem heterogeneity in most Nordic regions seems to increase the biotic risks (Figure 4H). This effect could be triggered by shallow soils that may limit positive complementarity processes, such as root stratification, while on the contrary exacerbating competition for water among species[81,82] and ultimately leading to an increase in vulnerability to insect outbreaks (Figure S16H). The considerable spatial variability emerging from the analysis highlights the complexity of the problem and the importance of assessing the effectiveness of adaptation strategies within a multi-dimensional framework designed for local environmental conditions and to account for amplification and dampening effects that may emerge from the non-linear interactions of multiple factors.[34] The effects associated with enhanced heterogeneity may go beyond the reduction in biomass loss due to natural disturbances. For instance, changes in forest heterogeneity influence the provision of various ecosystem services important for human societies, such as wood production, climate regulation, biodiversity conservation, and cultural values.[83,84] Further research is urgently needed to identify optimal local adaptation strategies offering the best compromise in terms of resilience to climate change and delivery of ecosystem services.

## Conclusions

Our analysis provides data-driven evidence that changes in climate during the past four decades have had an important role in intensifying disturbance events related to fires, windthrows, and insect outbreaks in European forests, ultimately leading to increasing biomass loss. Such a rising trend in forest disturbances is plausibly contributing to the recent slowdown of the European carbon sink[57] and corroborates previous studies, which have highlighted the progressive saturation of the positive effects of $CO_2$ fertilization on carbon sequestration and the rise of negative impacts of climate change on the accumulation of forest biomass.[53,54] We found that enhanced ecosystem heterogeneity would be particularly effective in reducing climate-driven risks at European scale, yet local environmental conditions play an important role in modulating these potential benefits. Given the spatial aggregation at 0.25° used in our modeling framework, our results may support relevant stakeholders and managers acting at municipality, regional, and national levels. In addition, our findings could also be of interest for those working on land-based climate policy and on the implementation of climate-smart forest management strategies. Considering that current climate policies heavily rely on stable carbon capture by forests,[85] our results can contribute to the development of more integrated and effective land-based mitigation and adaptation strategies based on ecosystem diversification, particularly urgent in view of the expected intensification of disturbance

Please cite this article in press as: Forzieri et al., Ecosystem heterogeneity is key to limiting the increasing climate-driven risks to European forests, One Earth (2024), https://doi.org/10.1016/j.oneear.2024.10.005



regimes due to global warming.[10,11,18] The results may also serve as a benchmark for forest/vegetation models to improve their capacity to represent natural disturbances and ultimately enhance the reliability of future land-climate predictions. This is particularly important, as the ability of forests to keep absorbing $CO_2$ is one of the greatest sources of uncertainty in climate projections.[2] Finally, our findings—by disentangling the effects of the various components and drivers of risk and unraveling the underlying ecological processes—contribute to a better understanding of the dynamics by developing concepts at the interface between remote sensing, landscape ecology, forestry, and climate science.

## EXPERIMENTAL PROCEDURES

### Observed forest disturbances

We focused on the risks to European forests caused by three major natural disturbances: forest fires, windthrows, and insect herbivore outbreaks (e.g., bark beetles, defoliators, and sucking insects). More than 150,000 spatially explicit records of disturbed forest areas collected over the period 2000–2017 were used to develop hazard and vulnerability models (see following sections). Fires were retrieved from the European Forest Fire Information System (EFFIS, https://effis.jrc.ec.europa.eu/), windthrows from the European Forest Windthrow dataset[86] (FORWIND, https://doi.org/10.6084/m9.figshare.9555008), and insect outbreaks from the National Insect and Disease Survey (IDS, http://foresthealth.fs.usda.gov) database of the United States Department of Agriculture (USDA). The use of IDS-USDA data to the European context follows the rationale and approach described in Forzieri et al.[4] and is further detailed in Text S5.

Each disturbance record (EFFIS, FORWIND, IDS-USDA) is characterized by the georeferenced spatial extent of the corresponding affected forest and the timing of the disturbance occurrence, the latter defined with an annual time resolution. The use of such spatially explicit databases of forest disturbances—in combination with satellite data—allowed retrieval for each record of the corresponding observed biomass loss. For each observed forest disturbance occurring at the time $t$, the corresponding relative biomass loss ($BL_{rel}$) was quantified based on the difference between pre- and post-disturbance biomass ($B$), as follows:

$$BL_{rel} = \left[\frac{\max(B_{t-n},\ldots,B_t) - \min(B_t,\ldots,B_{t+m})}{\max(B_{t-n},\ldots,B_t)}\right] \quad \text{(Equation 1)}$$

where $n$ and $m$ represent the backward and forward time lags (in years), respectively, and express the time window over which a biomass loss can be reasonably attributed to a given disturbance. For fires and windthrows, $n$ and $m$ were both set to 1, as these disturbances typically cause an abrupt loss in vegetation. For insect outbreaks, $n$ and $m$ were set to 2 and 5, respectively, in order to characterize the progressive and slow change in biomass following an insect infestation.[87] Annual $B$ time series are reconstructed at the disturbance record level by integrating a static 100-m above-ground biomass map acquired for the year 2010 from multiple Earth Observation systems[48] with forest cover changes derived from the Global Forest Change maps recorded at 30-m spatial resolution from Landsat imagery.[28] The methodological details of this approach have been described in Forzieri et al.[4]

Furthermore, as complementary disturbance databases, we exploited: the Database on Forest Disturbances in Europe[9,29] (DFDE, https://efi.int/articles/database-forest-disturbances-europe); the database of forest disturbances provided by the Food and Agriculture Organization (FAO) of the United Nations (https://fra-data.fao.org/EU/fra2020/disturbances/); the collection of salvage logging data provided by the Joint Research Center (JRC) of the European Commission[71] (https://data.jrc.ec.europa.eu/dataset/2100b612-a4b0-4897-829b-72b7b1e5782c); and estimates of dry matter emissions of boreal and temperate forest fires acquired from the Global Fire Emission Database[70] (GFED, https://www.geo.vu.nl/~gwerf/GFED/GFED4/). These additional disturbance databases have been used in a cross-comparison analysis to evaluate our estimates against independent retrievals. Additional details are reported in Text S3.

### Detection of undisturbed forest areas

For each disturbance type, in addition to the disturbance records we used two sets of records of undisturbed conditions to train the machine learning algorithm implemented for the hazard component (the model development is described in the following sections). The first set of undisturbed records refers to the spatially explicit disturbed areas, described above (EFFIS, FORWIND, IDS), before the occurrence of the disturbance event. A given forest patch can be undisturbed for long time until certain critical conditions in climate and forest manifest. Under such critical conditions the disturbance can occur. To capture such evolving hazard conditions in the same area, for each observed forest disturbance occurring at the time $t$, we retrieved the corresponding records of undisturbed conditions over the four preceding years (from $t-5$ to $t-1$). For such records, the timing is therefore different from the one referring to the disturbance events. We avoid sampling years after $t$ because environmental conditions could be still affected by the past disturbance (e.g., partial recovery of vegetation) and not properly represent the undisturbed conditions of the forest. The second set of undisturbed records was derived at different locations from the disturbed records by generating randomly over the 2000–2017 period 200,000 circular areas of extents equal to the average area of the disturbed forest patches and excluding those that overlapped with disturbance records. This second set of records, therefore, presents random geographical location and timing. The average area size was derived separately for agent type. To identify areas with stable vegetation conditions, only records with relative changes in biomass over the observational period lower than 5%, estimated following Forzieri et al.,[4] were retained and, together with the first set of records, used as reference sample of undisturbed forests. The use of two datasets of undisturbed records was required to inform the RF algorithms about environmental conditions both in areas that have not been interested by disturbances during the observation periods and in areas that have been affected by disturbances at a different time. In this way both the spatial and the temporal variability of the phenomenon is properly captured in the training datasets. The relevance of this issue is further explored in Text S7.

### Environmental drivers

A comprehensive set of climate and vegetation variables collected from satellite and reanalysis products were used as predictors of the hazard, vulnerability, and exposure models (see following sections). Climate features include annual values of key climatic variables (e.g., temperature, precipitation, snow), their long-term averages, and extreme event indicators. Vegetation features include structural variables (e.g., leaf area index, spatial heterogeneity, vegetation optical depth) and phenological metrics. The full list of climate and vegetation variables exploited in this study is reported in Table S6. The products used for describing the selected environmental variables have spatial resolutions ranging between 100 m and 0.5° and can be static or dynamic with annual time step. Missing years in the environmental predictors were reconstructed by linear interpolation over time at the grid-cell level to cover the whole observational period 1979–2018. Such temporal extrapolation was conducted for the dynamic variables included in the models (e.g., LAI, population density, phenological metrics), whereas static variables (e.g., tree density, tree age, tree height, homogeneity, coefficient of spatial variation, elevation, slope) were kept constant for the whole period. Additional details on the datasets used are reported in Texts S1 and S2.

Specifically for the hazard and vulnerability models, environmental variables were spatially averaged over the forest area of each disturbance record and undisturbed record and refer to the climate conditions occurring at the timing of the record. Vegetation variables were similarly spatially averaged; however, as their satellite-derived estimates could be affected by disturbance occurrences, the sampling of vegetation characteristics refers to the conditions occurring 1 year before the timing of the record. Such an approach enabled us to extract for each record climate and vegetation characteristics that can be effectively used as predictors of triggering and susceptibility mechanisms of natural disturbances. When models are used in prediction mode over the period 1979–2018, environmental predictors have been spatially averaged to a common spatial resolution (0.25°) by masking out non-forest areas.

Furthermore, the cover fractions of different PFTs, including broadleaved deciduous (BrDc), broadleaved evergreen (BrEv), needle leaf deciduous (NeDc), and needle leaf evergreen (NeEv), were retrieved from the land-cover

Please cite this article in press as: Forzieri et al., Ecosystem heterogeneity is key to limiting the increasing climate-driven risks to European forests, One Earth (2024), https://doi.org/10.1016/j.oneear.2024.10.005



maps of the European Space Agency Climate Change Initiative (ESA-CCI, https://www.esa-landcover-cci.org/).

### Methodological framework for climate risk assessment

To express the impact of climate-driven disturbances to forests, we adopted the IPCC risk assessment framework widely used in climate impact studies.[15] In the context of climate change impacts, risks result from dynamic interactions between climate-related hazards (*H*) with vulnerability (*V*) of the affected human or ecological system to the hazards and its exposure (*E*).[15] Risk in this study is expressed in terms of biomass loss (*R*) due to natural disturbances and is derived as the product of hazard, vulnerability, and exposure as follows:

$$R = H \cdot V \cdot E \quad \text{(Equation 2)}$$

The three risk components reflect different processes. *H* represents the fraction of forest area affected by a given disturbance. It is derived as a function of its probability of occurrence and expressed by a continuous number ranging between 0 and 1: 0 means a forest is not exposed to disturbance, and 1 means the whole forest cover is exposed to disturbance. We focused on disturbances originating from three hazards: fires, windthrows, and insect outbreaks. For insect outbreaks, we merge bark beetles, sucking insects, and defoliators in a unique insect hazard class consistently with Forzieri et al.[4] *V* defines the degree to which a forest ecosystem is affected when exposed to a given disturbance (*H*), and it is expressed by the potential relative biomass loss when a forest is exposed to a natural disturbance. *V* is a continuous number ranging between 0 and 1: 0 means a forest is not vulnerable to the given disturbance, and 1 means a forest is completely damaged when exposed to the given disturbance. *E* refers to the amount of biomass exposed to (and potentially damaged by) a hazard, and it is quantified in terms of tons per hectare of available above-ground biomass. The combination of the three risk components (*H*,*V*, and *E*) provides the amount of biomass loss, expressed in tons per hectare caused by a certain disturbance type. When risk estimates are integrated in space, they are expressed in cumulated tons of biomass loss.

Each risk component depends on multiple spatially and temporally varying environmental drivers (e.g., climate features and vegetation properties), and changes in one driver can also influence multiple risk components. For instance, water stress enhances the likelihood of fire ignition and—at the same time—makes forest more susceptible to large and rapid fire spread once triggered.[58] The combined increase in hazard and vulnerability in this case amplifies the risk. However, prolonged water stress conditions may also lead—in the long term—to reduced fuel loads and a consequent reduction in forest vulnerability. In this case, hazard and vulnerability show opposite sensitivity to water stress with a possible dampening effect on biomass loss.[60] The dynamic interplay between *H*, *V*, and *E* present complex and non-linear patterns that need to be evaluated in a multi-dimensional framework that is able to account for the interactions among risk components and underlying environmental drivers.

To address this issue, we developed a series of RF models[47] and express each of the risk components (*H*,*V*, and *E*) as a function of climate and vegetation drivers. Machine learning in general, and RF in particular, accounts for non-linear feature interactions and does not require unrealistic assumptions about the functional form relating the key drivers and the response functions. Specifically, for the hazard and vulnerability components, RF models were developed for major PFTs, namely BrDc, BrEv, NeDc, and NeEv. Exploring the ecosystem response to natural disturbances for different PFTs enabled us to characterize ecosystem-specific behaviors.

We adopted a common modeling setup across the risk components. RF models were implemented with 500 classification (*H*) and regression (*V*, *E*) trees, whose depth and number of predictors to sample at each node were identified using Bayesian optimization. The algorithm allows for the optimal selection of machine learning hyperparameters that strongly control model performance. For each year over the observational period 2000–2017, we randomly extracted 60% of the records to use as training set and the remaining 40% as validation set. Once calibrated/validated, the RF models were used to reconstruct each risk component (and corresponding uncertainties) annually for the period 1979–2018 for the domain covering EU27 countries plus the United Kingdom, Iceland, Norway, Switzerland, Turkey, and the Balkan area at 0.25° spatial resolution. To this aim, RF models were used in predictive mode using as input spatial maps of environmental predictors. Annual estimates of a given risk component were obtained as the average from all trees in the RF ensemble and the corresponding grid-cell uncertainty estimated in terms of standard deviation of the computed responses over the ensemble of the grown trees of the model. Hazard, vulnerability, exposure, and risk estimates were provided at grid-cell level and at macro-region scale (Figure S17). We consider the 0.25° spatial resolution appropriate for this work, as it allows to explore patterns and drivers of forest disturbances at the regional/national scale and, therefore, to support both the development of the science and the definition of regional/national forest strategies that aim at reducing climate risks and improving forest resilience. Furthermore, such spatial aggregation is also optimal (1) to support the data-driven estimates of the predictive models by minimizing the effects of stochasticity in the signal of forest disturbances, (2) to reduce potential spatial dependence in the pool of predictors, and (3) to facilitate the comparison of our data-driven risk levels with analogous estimates generated by process-based vegetation/forest models ultimately supporting their parameterization. Additional details are reported in Text S8.

### Hazard

Hazard (*H*) levels are quantified here in terms of expected fraction of forest area annually affected by a given disturbance (*EFAA*). It is a metric widely used in multi-risk assessment and allows for a quantitative comparison of hazards described by different process characteristics.[88] *EFAA* is expressed as a function of the probability of occurrence of a given disturbance (*P*) following the procedure described below.

For each disturbance type and for each PFT, we developed an RF classification model[47] to predict *P* (response variable) based on climate and vegetation conditions (predictors). To this aim, records of disturbed (EFFIS, FORWIND, IDS-USDA) and undisturbed forest patches previously described were used as training/testing dataset. A set of climate and vegetation variables was chosen as predictors (Table S6) based on a feature selection procedure described in Forzieri et al.[4] We used the same input variables for the hazard and vulnerability components (the latter one described in the next section) to preserve consistency with the modeling tools already developed[4] to enable the integration of multiple risk components in a coherent framework and better isolate the underlying drivers across multiple risk components. We have added only population density as additional driver in the hazard model of fires (Table S6) to capture possible human-related mechanisms, such as human ignition and fire suppression.[89] Potential effects of the spatial dependence and spatial resolution of the observational datasets were minimized by resampling the environmental drivers first to the common 0.25° spatial resolution and then along the gradients of the three principal components derived from the set of predictors. Such methodology has been originally implemented for the vulnerability component[4] and is further detailed in Text S9, complemented with new dedicated experiments designed for the hazard modeling presented in Text S7 and Table S7.

For each RF model, the optimal operating point of the receiver operating characteristic (ROC) curve was retrieved to identify the probability threshold ($P_{ROC}$) that maximizes classification accuracy. The RF models predict disturbance occurrences with overall accuracies of 88.3%, 69.4%, and 89.2% for fires, windthrows, and insect outbreaks, respectively. Variable importance scores, ROC curves, and classification performances are shown in Figures S9–S11.

The RF models were used to evaluate *P* (and corresponding uncertainty, $\sigma_P$) annually between 1979 and 2018 for each grid cell of the spatial domain. Results of PFT-specific RF models were averaged at grid-cell level with weighting based on the cover fractions of PFTs.

To express the hazard component in magnitude terms and account for the stochasticity of the disturbance processes, annual *P* values were translated into *EFAA*. To this aim, for each grid cell over the period 2000–2017, we extracted the annual *P* value and the corresponding observed fraction of forest area affected. The observed fraction of forest area affected was derived from the forest disturbance datasets available for Europe (EFFIS, FORWIND, and DFDE) gridded to the common 0.25° spatial resolution. We then clustered all grid cells in ten probability classes with a 0.1 probability bin, and for each probability class we retrieved its empirical cumulative distribution function of fraction of area affected (Figure S12). For insect outbreaks, records of European data are provided at country scale (DFDE, Text S3); therefore, the aforementioned approach was developed by linking the average probability computed at country scale and the corresponding reported fraction of forest

Please cite this article in press as: Forzieri et al., Ecosystem heterogeneity is key to limiting the increasing climate-driven risks to European forests, One Earth (2024), https://doi.org/10.1016/j.oneear.2024.10.005



affected. We recognize that DFDE likely misses important disturbance events, being uniquely based on a literature search, and may underestimate the effective impact occurred at country level.[9] Therefore, hazard levels for insect outbreaks derived in this study plausibly reflect a conservative estimate and should be viewed while considering this potential bias. We reconstructed the *EFAA* for each grid cell of our spatial domain over the whole 1979–2018 period by randomly generating its value based on its probability class-specific empirical cumulative distribution function. *EFAA* corresponding to $P < P_{ROC}$ was set to 0 for fires and insect outbreaks to reduce the occurrence of false positives. The windthrow hazard modeling required some additional processing. To incorporate in a more explicit manner the dependence of windthrow hazard on meteorological features, only *EFAA* grid cells with maximum annual wind speed greater than one standard deviation above the multi-annual mean were retained. Furthermore, to reduce the potential underestimation of the overall hazard component originating from the incompleteness of the FORWIND dataset,[86] *EFAA* maps were rescaled to preserve consistency with the cumulated area affected at the European scale for the period 2000–2017 reported by the FAO database.

The resulting maps, expressed in terms of *EFAA*, represent the hazard (*H*) component of our risk-assessment framework. The standard deviation of each class-specific distribution was quantified to assess the uncertainty of *EFAA* ($\sigma_{EFAA}$) attributable to the aforementioned random generator process and added in quadrature to $\sigma_P$ to derive the full uncertainty of the *H* component at the grid-cell level ($\sigma_H$).

### Vulnerability

Vulnerability (*V*) expresses the degree to which a forest ecosystem is affected when exposed to a given disturbance and in this study is quantified in terms of fraction of biomass losses based on the difference between pre- and post-disturbance biomass (Equation 1), further detailed in a previous study.[4] For each disturbance type and PFT, an RF regression model[47] was implemented to predict the observed relative biomass loss ($BL_{rel}$, response variable) based on climate and vegetation conditions (predictors, Table S6). Models explain on average 34%–49% of the variance in relative biomass loss ($R^2$) across the considered disturbances. More details on model development and validation can be found in Forzieri et al.[4] The PFT-specific RF models were used to evaluate the *V* of forests annually between 1979 and 2018 for each grid cell of the spatial domain and then weighted based on the cover fractions of PFTs. Grid-cell uncertainty of predicted *V* values were quantified in terms of standard deviation ($\sigma_V$) of the computed responses over the ensemble of the grown trees of the model.

### Exposure

Exposure (*E*) refers to the spatial and temporal availability of forest biomass potentially prone to hazards. We used an RF regression model[47] to reconstruct the forest biomass (response variable) as a function of a set of vegetation conditions (predictors, Text S2). To this aim, we first derived a time series of annual forest biomass maps as reference dataset by rescaling estimates of the changes in carbon stock occurring over the period 2000–2018 (Xu et al.,[49] https://zenodo.org/record/4161694#.YZ1VwvnMKUk) to the forest biomass values available for the year 2010 (Santoro et al.,[48] GlobBiomass, https://doi.org/10.1594/PANGAEA.894711). The scaling factor was derived by dividing at the grid-cell level the biomass value in 2010 by the carbon stock value in 2010. The multi-temporal biomass dataset was then generated by multiplying the scaling factor by the carbon stock changes over the period 2000–2018 and used as response variable for the development of the RF model. To this aim, we randomly extracted 60% of the pixels to use as training set and the remaining 40% as validation set. We found that the RF model explains 89% of the variance ($R^2$) of the reference biomass, with a root mean squared error of 15.13 t ha$^{-1}$ and an average overestimation of 0.128 (percent bias,[90] PBIAS) (Figures S2A and S2B).

The RF model was then used to evaluate the evolution of forest biomass annually (*E*) between 1979 and 2018 for each grid cell of the spatial domain. Estimates of biomass, representing the *E* component in our risk-assessment framework, are obtained as the average from all trees in the RF ensemble and the corresponding grid-cell uncertainty estimated in terms of standard deviation ($\sigma_E$) of the computed responses over the ensemble of the grown trees of the model. Temporal changes in *E* due to natural or human-induced factors, such as $CO_2$ fertilization effects and forest management, are implicitly incorporated in our assessment to the extents they are reflected in the satellite-based variables used as predictors in the RF model (Text S2).

We further assess the capability of the RF model to capture the observed temporal variability of biomass. To this aim, we estimated the linear trend at grid-cell level for both the reference and modeled biomass over the common temporal period 2000–2018 and found an $R^2$ of 0.63 ($p < 0.05$) between the two trend maps (Figure S2C). Furthermore, we compared the net change of modeled biomass aggregated over the whole of Europe with estimates of net changes in carbon stock derived from FAO (https://fra-data.fao.org/EU/fra2020/home/) for the temporal windows 1990–2000, 2000–2010, and 2010–2020. To increase consistency in terms of temporal coverage between the two estimates, we retrieved the FAO estimate of carbon stock in 2018, which is the last year of the modeled biomass, by assuming a linear growth rate of carbon stock between 2010 and 2020. Furthermore, we apply a 10-year centered moving window over the time series of modeled annual biomass. Net changes in our biomass values appear comparable to FAO estimates, but always lower, with a bias of about 0.4% (Figure S2D).

### Risk integration and error propagation

The three risk components described above, hazard (*H*), vulnerability (*V*), and exposure (*E*), were integrated to quantify the risk due to each of the natural disturbances considered, based on Equation 2. At the grid-cell scale, risk levels are expressed in terms of tons of biomass loss per hectare of forest area. The overall modeling framework has been specifically designed for forest ecosystems. All environmental drivers used as predictors in the RF models have been computed for the forest area of each record by masking out non-forest lands. Such methodology ensures consistency between target variables and predictors and provides estimates of biomass loss that are representative of the forest ecosystems and independent of the distribution of forest within each grid cell (e.g., forest fragmentation). The error propagation in risk estimate (*R*) is computed in terms of standard deviation by incorporating the uncertainties in single risk components and possible correlated systematic errors[91] as follows:

where *i* is a given pixel, $\frac{\partial R_i}{\partial X}$ denotes the partial derivative of *R* with respect to the *X* variable (in our case, *H*,*V*, and *E*), and $\sigma_X$ is the standard deviation operator that reflects the uncertainty in each single component, whereas $\sigma_{XY}$ is the covariance between variables *X* and *Y*. When risk levels are aggregated at macro-region scale, biomass losses are cumulated over the whole reference domain accounting for the forest area of each grid cell and finally expressed in tons. The corresponding error is derived by adding in quadrature the single-grid-cell uncertainties as follows:

$$\sigma_{R_i} = \sqrt{\left(\frac{\partial R_i}{\partial H_i}\cdot\sigma_{H_i}\right)^2+\left(\frac{\partial R_i}{\partial V_i}\cdot\sigma_{V_i}\right)^2+\left(\frac{\partial R_i}{\partial E_i}\cdot\sigma_{E_i}\right)^2+\left(2\sigma^2_{HV}\cdot\frac{\partial R_i}{\partial H_i}\cdot\frac{\partial R_i}{\partial V_i}\right)+\left(2\sigma^2_{HE}\cdot\frac{\partial R_i}{\partial H_i}\cdot\frac{\partial R_i}{\partial E_i}\right)+\left(2\sigma^2_{VE}\cdot\frac{\partial R_i}{\partial V_i}\cdot\frac{\partial R_i}{\partial E_i}\right)} \quad \text{(Equation 3)}$$

$$\sigma_R = \sqrt{\sum_i \left(\sigma_{R_i}\right)^2} \quad \text{(Equation 4)}$$

where grid cell *i* spans the considered macro-region. Inter-annual average and long-term trend in biomass loss are then analyzed both at macro-region scale and for the whole domain. Long-term trends in biomass loss are quantified

over the period 1979–2018 using linear regression models and their significance evaluated by the two-sided modified Mann-Kendall[92] test to account for possible serial correlation in the time series. Results of these analyses are shown in Figures 1 and 2. To derive average and trend values of biomass loss that are minimally affected by potential extrapolation errors beyond the training range of the RF models, we quantified spatial statistics of risk levels based solely on areas with climatological conditions analogous to those of the observational datasets. Results showed a general consistency with the estimates derived from the entire spatial domain and corroborate the robustness of our findings (Tables S2–S5).

The adopted resampling procedure (section "environmental drivers") may affect the spatial variability in environmental predictors with consequent possible local-scale effects of forest disturbances. However, such biases are minimized by constraining the hazard component on the observed fractions of the forest area affected (section "hazard").

To quantify the overall climate risk due to multiple disturbances, we cumulated biomass losses originating from single disturbances. Possible amplification/dampening effects could manifest due to dependencies among multiple disturbances (e.g., Schelhaas et al.,[23] Seidl and Rammer,[93] Meigs et al.[94]). Despite the relevance of these interactions, the lack of reference observational data of compound events hampered the explicit integration of their effects in our modeling framework. Therefore, such interplays are represented in our assessment only to the extents they are reflected in the spatially and temporally varying environmental predictors of the RF models.

To enhance the confidence of our approach, in addition to the validation of the single risk components, (hazard, vulnerability, and exposure; see previous sections), we evaluated the resulting risk estimates against independent sources of biomass losses expressed in terms of damaged volumes (DFDE), salvage loggings (JRC), and dry matter emissions (GFED) (Text S3). The agreement was assessed in terms of Spearman rank correlation ($\rho$) computed between pairs of samples of annual country-scale risk estimates. Furthermore, we compared inter-annual averages and trends of risk computed over the considered domain (Text S4 and Figure S8). While the reasonable agreement between our risk estimates and those reported in independent disturbance databases corroborates the overall hazard-vulnerability-exposure integration framework proposed here, a series of potential limitations have been critically evaluated and discussed in Text S5.

### Disentangling the key determinants of risk

To disentangle the key components and drivers of risk, we explored two sets of factorial simulations. The first experiment aims to isolate the marginal contribution of each risk component (hazard, vulnerability, and exposure) on the resulting temporal changes in risk levels. To this scope, we explored three different scenarios, each one generated from an ensemble of runs. In each scenario, a risk component $j$ (hazard, vulnerability, or exposure) is kept dynamic while the remaining two elements are fixed to a reference year. Under such configuration, we perform 40 different runs by changing the reference year over the period 1979–2018. The risk averaged over the generated 40-member ensemble is independent of the reference year used to simulate static conditions, and therefore the resulting temporal changes can be fully attributed to the component dynamic. Risk estimates are aggregated at macro-region level, and a linear regression model is used to retrieve the long-term trend in biomass loss due to the $j$ component ($T_j$). Its marginal contribution ($M_j$) to the risk dynamics is quantified as follows:

$$M_j = 100 \cdot \frac{|T_j|}{\sum_q |T_q|} \quad \text{(Equation 5)}$$

where $q$ spans the three risk components (hazard, vulnerability, and exposure). The second experiment aims to isolate the marginal contribution of climate and vegetation drivers on the resulting temporal changes in risk levels. Climate and vegetation features are used as predictors in each of the risk components, and therefore their effect needs to be separately analyzed in the hazard, vulnerability, and exposure components. To disentangle their effects, we adopted the same methodology described above and kept dynamic alternatively vegetation drivers or climate drivers. When vegetation changes are accounted for, these are expressed in terms of variations in leaf area index, biomass, phenological metrics, and vegetation optical depth, while the other vegetation drivers (e.g., tree height, tree age) are kept static because of the lack of multi-temporal information. Therefore, the marginal effect of vegetation changes due to natural effects, such as climate-mediated growth rate, and human-induced variations in forest patterns, such as even-aged management and growing of monocultures, are captured to the extent they are reflected in the changes of the mentioned time-varying parameters. Results of these analyses are shown in Figure 3.

### Relationship between ecosystem heterogeneity and forest compositional/structural diversity

Remotely sensed indicators of spectral variability have long been explored as proxies of spatial heterogeneity[95] at different scales and for various environmental applications.[96,97] Following such approaches, ecosystem heterogeneity was retrieved in this study based on 1-km texture metrics generated from 250-m Enhanced Vegetation Index (EVI) imagery acquired by the Moderate Resolution Imaging Spectroradiometer (MODIS) for the period 2001–2005[75] (http://www.earthenv.org/texture). We used homogeneity and coefficient of variation to quantify the similarity and dissimilarity, respectively, of vegetation patterns of multiple ecosystems (forest and non-forest land-cover types). Such diversity metrics work at the scales of beta and gamma diversity.[98] Beta diversity describes the diversity between two communities or ecosystems, while gamma diversity refers to the diversity between many ecosystems sampled at the landscape scale, such as the entire slope of a mountain or the entire littoral zone of a seashore. Homogeneity and coefficient of variation are inversely correlated and were selected from a pool of spectral diversity indicators based on a feature selection algorithm specifically designed to identify the environmental predictors of forest susceptibility to climate-driven disturbances.[4] While such diversity metrics cannot capture the within-stand tree species variations and fine-scale structural features such as tree sizes and forest gaps for which higher-spatial-resolution products would be required,[96,97,99] we stress that major patterns of forest spatial diversity at the landscape scale are plausibly well described.[75]

To evaluate the relationship between the selected texture metrics and the spatial diversity of forest features, we compared them against compositional and structural diversity indices retrieved from independent datasets and methods. Forest land-cover compositional diversity was quantified by the use of the Shannon Index[100] applied on forest cover types (forest land covered by trees, regional classification scheme) available at 300-m spatial resolution for the period 2001–2005 from the ESA-CCI product. For each pixel, the most frequent forest type recorded over the reference period was considered. Structural diversity was determined by computing the standard deviation of forest biomass values available at 100-m spatial resolution for the year 2010 (Santoro et al.[48]). Both compositional and structural diversity indices were quantified over 1-km spatial window to match the spatial resolution of texture metrics. Only pixels fully covered by forest cover types were retained for the following analyses; therefore, variability in spectral indices induced by non-forest land covers does not affect the analyses. Homogeneity and coefficient of variation values were then binned as a function of compositional and structural diversity across 50 equally spaced intervals, and the corresponding average and standard error were determined. The strength of the relationship between texture metrics and compositional/structural diversity was estimated separately in terms of Spearman rank over the binned values to capture possible non-linear relations between the two variables.

To further elucidate the relationship between texture-based ecosystem heterogeneity and forest characteristics, we retrieved the homogeneity and coefficient of variation using the same MODIS EVI data and algorithms described in Tuanmu and Jetz[75]—and used in previous analyses—but masking a priori non-forest land-cover pixels. Therefore, the resulting new spectral heterogeneity values are exclusively conditioned by the spatial variability in forest patterns. We then quantified the Spearman correlation between the original texture metrics (influenced by multiple land-cover types) and the new ones (dependent on forest land-cover types only) across a forest cover gradient.

The highly significant correlation observed in both experiments described above ($|\text{Spearman rank}| > 0.98$, $p < 0.05$, Figure S13; Spearman rank $>0.75$, $p < 0.05$, Figure S14) proves that in forested landscapes the ecosystem heterogeneity, quantified in terms of texture metrics, is highly driven by forest compositional and structural diversity.

### Adaptation strategies based on ecosystem heterogeneity

To assess the effect of ecosystem heterogeneity, a property that can be affected by land and forest management[43,44] and impact on the resistance against natural disturbances, we explored the relative biomass losses ($BL_{rel}$) recorded over the observed disturbed forest patches as a function of the local pre-disturbance biomass and homogeneity, separately for each disturbance type. The resulting binned data were then used to generate a fitting surface based on a modified ridge estimator to extrapolate the observed relations over the whole range of environmental gradients (Figures 4A–4C). Fitting performances were evaluated in terms of Spearman rank correlation against binned data (0.75, 0.69, and 0.45 for fires, windthrows, and insect outbreaks, respectively). Natural disturbances, in their turn, can affect ecosystem heterogeneity.[74] However, the spectral-derived indicators used as ecosystem heterogeneity metrics derived for the period 2001–2005 mostly refer to pre-disturbance conditions in the disturbance datasets (2000–2017), and therefore the proposed experiment effectively enables us to evaluate its effect on climate-driven risks.

To characterize the role of heterogeneity in influencing forest resistance across different PFTs, we derived the average value of the fitting surface and its slope across the homogeneity gradient for deciduous and evergreen forests. The first metric describes the average vulnerability expressed in terms of relative biomass loss ($BL_{rel}$). The second metric quantifies the sensitivity of biomass loss to homogeneity. To distinguish the different response of deciduous and evergreen, the fitting surface described above was generated by accounting only for records with at least 50% of forest cover of the given plant functional type, as retrieved from the ESA-CCI product. Results of this assessment are shown in Figures 4D–4F.

Indicators of ecosystem heterogeneity are included as vegetation drivers in the hazard and vulnerability models in terms of homogeneity for fires and windthrows and coefficient of variance for insect outbreaks (Table S6 and Text S1). When such models are run in prediction mode, the heterogeneity metrics are spatially averaged over forest areas at 0.25° spatial resolution to match the common grid exploited in RF simulations, as detailed in previous sections. To quantify how changes in heterogeneity control hazard and vulnerability components and may ultimately influence the resulting biomass losses, we generated an idealized scenario of enhanced heterogeneity. The rationale consists in deriving for each grid cell a lower homogeneity value (higher heterogeneity) compared to its actual (reference) value by preserving the consistency with the local background climate and biomass conditions. To this aim, for each pixel we retrieved the homogeneity values recorded in neighboring cells over a centered 1.25° × 1.25° spatial window. Records with differences in elevation larger than 500 m and average biomass (1979–2020) lower than 20% compared to the one in the centered pixel were excluded. We then computed the enhanced heterogeneity at the grid-cell level as the minimum of the sampled distribution of homogeneity values and tracked the source grid cell of the selected lowest homogeneity value. The enhanced homogeneity map (Figure S15) is directly used as input in the hazard and vulnerability models of fires and windthrows. For the hazard and vulnerability models of insect outbreaks, which instead use the coefficient of variance as heterogeneity metric, we retrieved the corresponding idealized scenario by associating to each pixel the coefficient of variance corresponding to the source grid cell of the selected lowest homogeneity value. Such an approach enables us to build scenarios of homogeneity and consistent coefficient of variance because it is based on the same source grid cells. Based on such idealized scenarios of enhanced heterogeneity, we re-run each risk component and quantify the corresponding biomass losses. Differences in biomass losses generated under the reference scenario and the idealized one are used to quantify the potential benefits of enhanced heterogeneity and are expressed in terms of avoided biomass loss (Figure 4G, 4H, and S16).

The co-occurrence of multi-dimensional environmental factors resulting from the combination of interacting physical processes (compound events) may amplify or dampen the ecosystem response.[34] Tree-based models, such as the RF approach used here, consider all variables together (Table S6) and account for non-linear feature interactions in the final model formulation.[47,101] This allows us to disentangle possible confounding factors and quantify the effective role of ecosystem heterogeneity in regulating natural disturbances. Given the aggregation level utilized in our modeling framework, such analyses should be considered informative for management decisions acting at the regional/national scale. In large parts of Europe, forest management strategies are typically quite uniform over areas of tens of kilometers.[1] This is the case, for instance, for monocultures, even-aged stands of conifers in Central Europe and Scandinavia. In this respect, the chosen 0.25° spatial resolution is appropriate to capture the emergent forest dynamics and inform stakeholders at municipality, regional, and national levels.

## RESOURCE AVAILABILITY

### Lead contact

Further information about data and code should be directed to and will be fulfilled by the lead contact, Giovanni Forzieri (giovanni.forzieri@unifi.it).

### Materials availability

The observation-driven datasets analyzed in this study are publicly available as referenced within the article.

### Data and code availability

The custom MATLAB (R2022b) code written to read and analyze data and generate figures has been made available in Figshare (https://doi.org/10.6084/m9.figshare.27089032.v1).

## ACKNOWLEDGMENTS

The study was partially funded by the Exploratory Project FOREST@RISK of the European Commission, Joint Research Centre and by DG REGIO of the European Commission as part of the "Territorial Risk Assessment of Climate in Europe" (TRACE) project (Administrative Agreement Nr JRC 36206-2022 // DG REGIO 2022CE160AT126). G.F. and D.S. were supported by the Horizon Europe Project ECO2ADAPT (grant agreement no. 101059498).

## AUTHOR CONTRIBUTIONS

G.F. and A.C. designed the study. G.F. developed the machine learning models. J.S., A.B., and D.S. assisted in data-integration tasks. G.F. and A.C. wrote the manuscript with contributions from L.F. and H.J.

## DECLARATION OF INTERESTS

The authors declare no competing interests.

## SUPPLEMENTAL INFORMATION

Supplemental information can be found online at https://doi.org/10.1016/j.oneear.2024.10.005.

Received: April 2, 2024
Revised: August 7, 2024
Accepted: October 11, 2024
Published: November 5, 2024

## REFERENCES

1. Forest Europe (2020). State of Europe's Forests 2020 (Forest Europe). https://foresteurope.org/state-europes-forests-2020/.
2. Friedlingstein, P., Meinshausen, M., Arora, V.K., Jones, C.D., Anav, A., Liddicoat, S.K., and Knutti, R. (2014). Uncertainties in CMIP5 Climate Projections due to Carbon Cycle Feedbacks. J. Clim. *27*, 511–526. https://doi.org/10.1175/JCLI-D-12-00579.1.
3. Li, D., Wu, S., Liu, L., Zhang, Y., and Li, S. (2018). Vulnerability of the global terrestrial ecosystems to climate change. Global Change Biol. *24*, 4095–4106. https://doi.org/10.1111/gcb.14327.
4. Forzieri, G., Girardello, M., Ceccherini, G., Spinoni, J., Feyen, L., Hartmann, H., Beck, P.S.A., Camps-Valls, G., Chirici, G., Mauri, A., and Cescatti, A. (2021). Emergent vulnerability to climate-driven disturbances in European forests. Nat. Commun. *12*, 1081. https://doi.org/10.1038/s41467-021-21399-7.

5. Viljur, M.-L., Abella, S.R., Adámek, M., Alencar, J.B.R., Barber, N.A., Beudert, B., Burkle, L.A., Cagnolo, L., Campos, B.R., Chao, A., et al. (2022). The effect of natural disturbances on forest biodiversity: an ecological synthesis. Biol. Rev. *97*, 1930–1947. https://doi.org/10.1111/brv.12876.

6. Thom, D., Rammer, W., and Seidl, R. (2017). Disturbances catalyze the adaptation of forest ecosystems to changing climate conditions. Global Change Biol. *23*, 269–282. https://doi.org/10.1111/gcb.13506.

7. Senf, C., Pflugmacher, D., Zhiqiang, Y., Sebald, J., Knorn, J., Neumann, M., Hostert, P., and Seidl, R. (2018). Canopy mortality has doubled in Europe's temperate forests over the last three decades. Nat. Commun. *9*, 4978. https://doi.org/10.1038/s41467-018-07539-6.

8. Senf, C., and Seidl, R. (2020). Mapping the forest disturbance regimes of Europe. Nat. Sustain. *4*, 63–70. https://doi.org/10.1038/s41893-020-00609-y.

9. Patacca, M., Lindner, M., Lucas-Borja, M.E., Cordonnier, T., Fidej, G., Gardiner, B., Hauf, Y., Jasinevičius, G., Labonne, S., Linkevičius, E., et al. (2023). Significant increase in natural disturbance impacts on European forests since 1950. Global Change Biol. *29*, 1359–1376. https://doi.org/10.1111/gcb.16531.

10. Seidl, R., Schelhaas, M.-J., Rammer, W., and Verkerk, P.J. (2014). Increasing forest disturbances in Europe and their impact on carbon storage. Nat. Clim. Change *4*, 806–810. https://doi.org/10.1038/nclimate2318.

11. Seidl, R., Thom, D., Kautz, M., Martin-Benito, D., Peltoniemi, M., Vacchiano, G., Wild, J., Ascoli, D., Petr, M., Honkaniemi, J., et al. (2017). Forest disturbances under climate change. Nat. Clim. Change *7*, 395–402. https://doi.org/10.1038/nclimate3303.

12. Anderegg, W.R.L., Trugman, A.T., Badgley, G., Anderson, C.M., Bartuska, A., Ciais, P., Cullenward, D., Field, C.B., Freeman, J., Goetz, S.J., et al. (2020). Climate-driven risks to the climate mitigation potential of forests. Science *368*, eaaz7005. https://doi.org/10.1126/science.aaz7005.

13. Pugh, T.A.M., Arneth, A., Kautz, M., Poulter, B., and Smith, B. (2019). Important role of forest disturbances in the global biomass turnover and carbon sinks. Nat. Geosci. *12*, 730–735. https://doi.org/10.1038/s41561-019-0427-2.

14. Lecina-Diaz, J., Martínez-Vilalta, J., Alvarez, A., Banqué, M., Birkmann, J., Feldmeyer, D., Vayreda, J., and Retana, J. (2021). Characterizing forest vulnerability and risk to climate-change hazards. Front. Ecol. Environ. *19*, 126–133. https://doi.org/10.1002/fee.2278.

15. Pörtner, H.-O., Roberts, D.C., Tignor, M.M.B., Poloczanska, E., Mintenbeck, K., Alegría, A., Craig, M., Langsdorf, S., Löschke, S., Möller, V., et al. (2022). IPPC 2022: Climate Change 2022: Impacts, Adaptation and Vulnerability: Working Group II Contribution to the Sixth Assessment Report of the Intergovernmental Panel on Climate Change (Cambridge University Press).

16. Jactel, H., Nicoll, B.C., Branco, M., Gonzalez-Olabarria, J.R., Grodzki, W., Långström, B., Moreira, F., Netherer, S., Orazio, C., Piou, D., et al. (2009). The influences of forest stand management on biotic and abiotic risks of damage. Ann. For. Sci. *66*, 701. https://doi.org/10.1051/forest/2009054.

17. Jactel, H., Branco, M., Duncker, P., Gardiner, B., Grodzki, W., Langstrom, B., Moreira, F., Netherer, S., Nicoll, B., Orazio, C., et al. (2012). A Multicriteria Risk Analysis to Evaluate Impacts of Forest Management Alternatives on Forest Health in Europe. Ecol. Soc. *17*, art52. https://doi.org/10.5751/ES-04897-170452.

18. Anderegg, W.R.L., Wu, C., Acil, N., Carvalhais, N., Pugh, T.A.M., Sadler, J.P., and Seidl, R. (2022). A climate risk analysis of Earth's forests in the 21st century. Science *377*, 1099–1103. https://doi.org/10.1126/science.abp9723.

19. McDowell, N.G., Beerling, D.J., Breshears, D.D., Fisher, R.A., Raffa, K.F., and Stitt, M. (2011). The interdependence of mechanisms underlying climate-driven vegetation mortality. Trends Ecol. Evol. *26*, 523–532. https://doi.org/10.1016/j.tree.2011.06.003.

20. Cao, S., Chen, L., Shankman, D., Wang, C., Wang, X., and Zhang, H. (2011). Excessive reliance on afforestation in China's arid and semi-arid regions: Lessons in ecological restoration. Earth Sci. Rev. *104*, 240–245. https://doi.org/10.1016/j.earscirev.2010.11.002.

21. Leverkus, A.B., Lindenmayer, D.B., Thorn, S., and Gustafsson, L. (2018). Salvage logging in the world's forests: Interactions between natural disturbance and logging need recognition. Global Ecol. Biogeogr. *27*, 1140–1154. https://doi.org/10.1111/geb.12772.

22. Dobor, L., Hlásny, T., Rammer, W., Zimová, S., Barka, I., and Seidl, R. (2020). Spatial configuration matters when removing windfelled trees to manage bark beetle disturbances in Central European forest landscapes. J. Environ. Manag. *254*, 109792. https://doi.org/10.1016/j.jenvman.2019.109792.

23. Stadelmann, G., Bugmann, H., Wermelinger, B., and Bigler, C. (2014). Spatial interactions between storm damage and subsequent infestations by the European spruce bark beetle. For. Ecol. Manag. *318*, 167–174. https://doi.org/10.1016/j.foreco.2014.01.022.

24. Hantson, S., Kelley, D.I., Arneth, A., Harrison, S.P., Archibald, S., Bachelet, D., Forrest, M., Hickler, T., Lasslop, G., Li, F., et al. (2020). Quantitative assessment of fire and vegetation properties in simulations with fire-enabled vegetation models from the Fire Model Intercomparison Project. Geosci. Model Dev. (GMD) *13*, 3299–3318. https://doi.org/10.5194/gmd-13-3299-2020.

25. Kautz, M., Anthoni, P., Meddens, A.J.H., Pugh, T.A.M., and Arneth, A. (2018). Simulating the recent impacts of multiple biotic disturbances on forest carbon cycling across the United States. Global Change Biol. *24*, 2079–2092. https://doi.org/10.1111/gcb.13974.

26. Chen, Y.-Y., Gardiner, B., Pasztor, F., Blennow, K., Ryder, J., Valade, A., Naudts, K., Otto, J., McGrath, M.J., Planque, C., and Luyssaert, S. (2018). Simulating damage for wind storms in the land surface model ORCHIDEE-CAN (revision 4262). Geosci. Model Dev. (GMD) *11*, 771–791. https://doi.org/10.5194/gmd-11-771-2018.

27. Huang, J., Kautz, M., Trowbridge, A.M., Hammerbacher, A., Raffa, K.F., Adams, H.D., Goodsman, D.W., Xu, C., Meddens, A.J.H., Kandasamy, D., et al. (2020). Tree defence and bark beetles in a drying world: carbon partitioning, functioning and modelling. New Phytol. *225*, 26–36. https://doi.org/10.1111/nph.16173.

28. Hansen, M.C., Potapov, P.V., Moore, R., Hancher, M., Turubanova, S.A., Tyukavina, A., Thau, D., Stehman, S.V., Goetz, S.J., Loveland, T.R., et al. (2013). High-Resolution Global Maps of 21st-Century Forest Cover Change. Science *342*, 850–853. https://doi.org/10.1126/science.1244693.

29. Schelhaas, M.-J., Nabuurs, G.-J., and Schuck, A. (2003). Natural disturbances in the European forests in the 19th and 20th centuries. Global Change Biol. *9*, 1620–1633. https://doi.org/10.1046/j.1365-2486.2003.00684.x.

30. Rogers, B.M., Jantz, P., and Goetz, S.J. (2017). Vulnerability of eastern US tree species to climate change. Global Change Biol. *23*, 3302–3320. https://doi.org/10.1111/gcb.13585.

31. Sommerfeld, A., Senf, C., Buma, B., D'Amato, A.W., Després, T., Díaz-Hormazábal, I., Fraver, S., Frelich, L.E., Gutiérrez, Á.G., Hart, S.J., et al. (2018). Patterns and drivers of recent disturbances across the temperate forest biome. Nat. Commun. *9*, 4355. https://doi.org/10.1038/s41467-018-06788-9.

32. Seidl, R., Honkaniemi, J., Aakala, T., Aleinikov, A., Angelstam, P., Bouchard, M., Boulanger, Y., Burton, P.J., De Grandpré, L., Gauthier, S., et al. (2020). Globally consistent climate sensitivity of natural disturbances across boreal and temperate forest ecosystems. Ecography *43*, 967–978. https://doi.org/10.1111/ecog.04995.

33. Seidl, R., Schelhaas, M.-J., and Lexer, M.J. (2011). Unraveling the drivers of intensifying forest disturbance regimes in Europe. Global Change Biol. *17*, 2842–2852. https://doi.org/10.1111/j.1365-2486.2011.02452.x.

34. Zscheischler, J., Westra, S., van den Hurk, B.J.J.M., Seneviratne, S.I., Ward, P.J., Pitman, A., AghaKouchak, A., Bresch, D.N., Leonard, M., Wahl, T., and Zhang, X. (2018). Future climate risk from compound events. Nat. Clim. Change *8*, 469–477. https://doi.org/10.1038/s41558-018-0156-3.

35. Regulation (EU) (2021). 2021/1119 of the European Parliament and of the Council of 30 June 2021 establishing the framework for achieving climate neutrality and amending Regulations (EC) No 401/2009 and (EU) 2018/1999 ('European Climate Law').

36. Korosuo, A., Pilli, R., Abad Viñas, R., Blujdea, V.N.B., Colditz, R.R., Fiorese, G., Rossi, S., Vizzarri, M., and Grassi, G. (2023). The role of forests in the EU climate policy: are we on the right track? Carbon Balance Manag. *18*, 15. https://doi.org/10.1186/s13021-023-00234-0.

37. Forzieri, G., Dakos, V., McDowell, N.G., Ramdane, A., and Cescatti, A. (2022). Emerging signals of declining forest resilience under climate change. Nature *608*, 534–539. https://doi.org/10.1038/s41586-022-04959-9.

38. Messier, C., Bauhus, J., Sousa-Silva, R., Auge, H., Baeten, L., Barsoum, N., Bruelheide, H., Caldwell, B., Cavender-Bares, J., Dhiedt, E., et al. (2022). For the sake of resilience and multifunctionality, let's diversify planted forests! Conservation Letters *15*, e12829. https://doi.org/10.1111/conl.12829.

39. Jactel, H., Moreira, X., and Castagneyrol, B. (2021). Tree Diversity and Forest Resistance to Insect Pests: Patterns, Mechanisms, and Prospects. Annu. Rev. Entomol. *66*, 277–296. https://doi.org/10.1146/annurev-ento-041720-075234.

40. Jactel, H., Bauhus, J., Boberg, J., Bonal, D., Castagneyrol, B., Gardiner, B., Gonzalez-Olabarria, J.R., Koricheva, J., Meurisse, N., and Brockerhoff, E.G. (2017). Tree Diversity Drives Forest Stand Resistance to Natural Disturbances. Curr. For. Rep. *3*, 223–243. https://doi.org/10.1007/s40725-017-0064-1.

41. Liu, D., Wang, T., Peñuelas, J., and Piao, S. (2022). Drought resistance enhanced by tree species diversity in global forests. Nat. Geosci. *15*, 800–804. https://doi.org/10.1038/s41561-022-01026-w.

42. Oliveira, B.F., Moore, F.C., and Dong, X. (2022). Biodiversity mediates ecosystem sensitivity to climate variability. Commun. Biol. *5*, 628–629. https://doi.org/10.1038/s42003-022-03573-9.

43. Messier, C., Puettmann, K.J., and Coates, K.D. (2013). Managing Forests as Complex Adaptive Systems: Building Resilience to the Challenge of Global Change (Routledge)).

44. Bauhus, J., Puettmann, K., and Messier, C. (2009). Silviculture for old-growth attributes. For. Ecol. Manag. *258*, 525–537. https://doi.org/10.1016/j.foreco.2009.01.053.

45. Marini, L., Ayres, M.P., and Jactel, H. (2022). Impact of Stand and Landscape Management on Forest Pest Damage. Annu. Rev. Entomol. *67*, 181–199. https://doi.org/10.1146/annurev-ento-062321-065511.

46. Seidl, R., Albrich, K., Thom, D., and Rammer, W. (2018). Harnessing landscape heterogeneity for managing future disturbance risks in forest ecosystems. J. Environ. Manag. *209*, 46–56. https://doi.org/10.1016/j.jenvman.2017.12.014.

47. Breiman, L. (2001). Random Forests. Mach. Learn. *45*, 5–32. https://doi.org/10.1023/A:1010933404324.

48. Santoro, M., Cartus, O., Carvalhais, N., Rozendaal, D.M.A., Avitabile, V., Araza, A., de Bruin, S., Herold, M., Quegan, S., Rodríguez-Veiga, P., et al. (2021). The global forest above-ground biomass pool for 2010 estimated from high-resolution satellite observations. Earth Syst. Sci. Data *13*, 3927–3950. https://doi.org/10.5194/essd-13-3927-2021.

49. Xu, L., Saatchi, S.S., Yang, Y., Yu, Y., Pongratz, J., Bloom, A.A., Bowman, K., Worden, J., Liu, J., Yin, Y., et al. (2021). Changes in global terrestrial live biomass over the 21st century. Sci. Adv. *7*, eabe9829. https://doi.org/10.1126/sciadv.abe9829.

50. Avitabile, V., and Camia, A. (2018). An assessment of forest biomass maps in Europe using harmonized national statistics and inventory plots. For. Ecol. Manage. *409*, 489–498. https://doi.org/10.1016/j.foreco.2017.11.047.

51. Ciais, P., Schelhaas, M.J., Zaehle, S., Piao, S.L., Cescatti, A., Liski, J., Luyssaert, S., Le-Maire, G., Schulze, E.-D., Bouriaud, O., et al. (2008). Carbon accumulation in European forests. Nat. Geosci. *1*, 425–429. https://doi.org/10.1038/ngeo233.

52. Etzold, S., Ferretti, M., Reinds, G.J., Solberg, S., Gessler, A., Waldner, P., Schaub, M., Simpson, D., Benham, S., Hansen, K., et al. (2020). Nitrogen deposition is the most important environmental driver of growth of pure, even-aged and managed European forests. For. Ecol. Manag. *458*, 117762. https://doi.org/10.1016/j.foreco.2019.117762.

53. Yuan, W., Zheng, Y., Piao, S., Ciais, P., Lombardozzi, D., Wang, Y., Ryu, Y., Chen, G., Dong, W., Hu, Z., et al. (2019). Increased atmospheric vapor pressure deficit reduces global vegetation growth. Sci. Adv. *5*, eaax1396. https://doi.org/10.1126/sciadv.aax1396.

54. Peñuelas, J., Ciais, P., Canadell, J.G., Janssens, I.A., Fernández-Martínez, M., Carnicer, J., Obersteiner, M., Piao, S., Vautard, R., and Sardans, J. (2017). Shifting from a fertilization-dominated to a warming-dominated period. Nat. Ecol. Evol. *1*, 1438–1445. https://doi.org/10.1038/s41559-017-0274-8.

55. Copernicus (2023). European State of the Climate 2023 | Copernicus. https://climate.copernicus.eu/esotc/2023.

56. EEA (2017). Climate change, impacts and vulnerability in Europe 2016.

57. Nabuurs, G.-J., Lindner, M., Verkerk, P.J., Gunia, K., Deda, P., Michalak, R., and Grassi, G. (2013). First signs of carbon sink saturation in European forest biomass. Nat. Clim. Change *3*, 792–796. https://doi.org/10.1038/nclimate1853.

58. Littell, J.S., McKenzie, D., Peterson, D.L., and Westerling, A.L. (2009). Climate and wildfire area burned in western U.S. ecoprovinces, 1916–2003. Ecol. Appl. *19*, 1003–1021. https://doi.org/10.1890/07-1183.1.

59. Fernandes, P.M. (2009). Combining forest structure data and fuel modelling to classify fire hazard in Portugal. Ann. For. Sci. *66*, 415. https://doi.org/10.1051/forest/2009013.

60. Walker, X.J., Rogers, B.M., Veraverbeke, S., Johnstone, J.F., Baltzer, J.L., Barrett, K., Bourgeau-Chavez, L., Day, N.J., de Groot, W.J., Dieleman, C.M., et al. (2020). Fuel availability not fire weather controls boreal wildfire severity and carbon emissions. Nat. Clim. Change *10*, 1130–1136. https://doi.org/10.1038/s41558-020-00920-8.

61. Mitchell, S.J. (2013). Wind as a natural disturbance agent in forests: a synthesis. Forestry (Lond) *86*, 147–157. https://doi.org/10.1093/forestry/cps058.

62. Gardiner, B. (2021). Wind damage to forests and trees: a review with an emphasis on planted and managed forests. J. For. Res. *26*, 248–266. https://doi.org/10.1080/13416979.2021.1940665.

63. Peltola, H., Kellomäki, S., Hassinen, A., and Granander, M. (2000). Mechanical stability of Scots pine, Norway spruce and birch: an analysis of tree-pulling experiments in Finland. For. Ecol. Manag. *135*, 143–153. https://doi.org/10.1016/S0378-1127(00)00306-6.

64. European Commission, Joint Research Centre, Caudullo, G., De Rigo, D., Mauri, A., Houston Durrant, T., and San-Miguel-Ayanz, J. (2016). European Atlas of Forest Tree Species (Publications Office of the European Union).

65. Deutsch, C.A., Tewksbury, J.J., Huey, R.B., Sheldon, K.S., Ghalambor, C.K., Haak, D.C., and Martin, P.R. (2008). Impacts of climate warming on terrestrial ectotherms across latitude. Proc. Natl. Acad. Sci. USA *105*, 6668–6672. https://doi.org/10.1073/pnas.0709472105.

66. Jactel, H., Koricheva, J., and Castagneyrol, B. (2019). Responses of forest insect pests to climate change: not so simple. Curr. Opin. Insect Sci. *35*, 103–108. https://doi.org/10.1016/j.cois.2019.07.010.

67. Biedermann, P.H., Müller, J., Grégoire, J.-C., Gruppe, A., Hagge, J., Hammerbacher, A., Hofstetter, R.W., Kandasamy, D., Kolarik, M., Kostovcik, M., et al. (2019). Bark Beetle Population Dynamics in the Anthropocene: Challenges and Solutions. Trends Ecol. Evol. *34*, 914–924. https://doi.org/10.1016/j.tree.2019.06.002.

68. Hlásny, T., König, L., Krokene, P., Lindner, M., Montagné-Huck, C., Müller, J., Qin, H., Raffa, K.F., Schelhaas, M.-J., Svoboda, M., et al. (2021). Bark Beetle Outbreaks in Europe: State of Knowledge and Ways Forward for Management. Curr. For. Rep. *7*, 138–165. https://doi.org/10.1007/s40725-021-00142-x.

69. Vacek, Z., Vacek, S., and Cukor, J. (2023). European forests under global climate change: Review of tree growth processes, crises and management strategies. J. Environ. Manag. *332*, 117353. https://doi.org/10.1016/j.jenvman.2023.117353.

70. van der Werf, G.R., Randerson, J.T., Giglio, L., van Leeuwen, T.T., Chen, Y., Rogers, B.M., Mu, M., van Marle, M.J.E., Morton, D.C., Collatz, G.J., et al. (2017). Global fire emissions estimates during 1997–2016. Earth Syst. Sci. Data *9*, 697–720. https://doi.org/10.5194/essd-9-697-2017.

71. Camia, A., Giuntoli, J., Jonsson, K., Robert, N., Cazzaniga, N., Jasinevičius, G., Avitabile, V., Grassi, G., Barredo Cano, J.I., and Mubareka, S. (2020). The Use of Woody Biomass for Energy Production in the EU (Publications Office of the European Union).

72. Tilman, D. (1996). Biodiversity: Population Versus Ecosystem Stability. Ecology *77*, 350–363. https://doi.org/10.2307/2265614.

73. Yachi, S., and Loreau, M. (1999). Biodiversity and ecosystem productivity in a fluctuating environment: The insurance hypothesis. Proc. Natl. Acad. Sci. USA *96*, 1463–1468. https://doi.org/10.1073/pnas.96.4.1463.

74. Mitchell, J.C., Kashian, D.M., Chen, X., Cousins, S., Flaspohler, D., Gruner, D.S., Johnson, J.S., Surasinghe, T.D., Zambrano, J., and Buma, B. (2023). Forest ecosystem properties emerge from interactions of structure and disturbance. Front. Ecol. Environ. *21*, 14–23. https://doi.org/10.1002/fee.2589.

75. Tuanmu, M.-N., and Jetz, W. (2015). A global, remote sensing-based characterization of terrestrial habitat heterogeneity for biodiversity and ecosystem modelling. Global Ecol. Biogeogr. *24*, 1329–1339. https://doi.org/10.1111/geb.12365.

76. Jactel, H., and Brockerhoff, E.G. (2007). Tree diversity reduces herbivory by forest insects. Ecol. Lett. *10*, 835–848. https://doi.org/10.1111/j.1461-0248.2007.01073.x.

77. Turner, M.G., Romme, W.H., and Gardner, R.H. (1999). Prefire heterogeneity, fire severity, and early postfire plant reestablishment in subalpine forests of Yellowstone National Park, Wyoming. Int. J. Wildland Fire *9*, 21–36.

78. Jactel, H., Gritti, E.S., Drössler, L., Forrester, D.I., Mason, W.L., Morin, X., Pretzsch, H., and Castagneyrol, B. (2018). Positive biodiversity–productivity relationships in forests: climate matters. Biol. Lett. *14*, 20170747. https://doi.org/10.1098/rsbl.2017.0747.

79. Jing, X., Muys, B., Bruelheide, H., Desie, E., Hättenschwiler, S., Jactel, H., Jaroszewicz, B., Kardol, P., Ratcliffe, S., Scherer-Lorenzen, M., et al. (2021). Above- and below-ground complementarity rather than selection drive tree diversity–productivity relationships in European forests. Funct. Ecol. *35*, 1756–1767. https://doi.org/10.1111/1365-2435.13825.

80. Jucker, T., Bouriaud, O., and Coomes, D.A. (2015). Crown plasticity enables trees to optimize canopy packing in mixed-species forests. Funct. Ecol. *29*, 1078–1086. https://doi.org/10.1111/1365-2435.12428.

81. Searle, E.B., Chen, H.Y.H., and Paquette, A. (2022). Higher tree diversity is linked to higher tree mortality. Proc. Natl. Acad. Sci. USA *119*, e2013171119. https://doi.org/10.1073/pnas.2013171119.

82. Grossiord, C., Granier, A., Ratcliffe, S., Bouriaud, O., Bruelheide, H., Chećko, E., Forrester, D.I., Dawud, S.M., Finér, L., Pollastrini, M., et al. (2014). Tree diversity does not always improve resistance of forest ecosystems to drought. Proc. Natl. Acad. Sci. USA *111*, 14812–14815. https://doi.org/10.1073/pnas.1411970111.

83. Brockerhoff, E.G., Barbaro, L., Castagneyrol, B., Forrester, D.I., Gardiner, B., González-Olabarria, J.R., Lyver, P.O., Meurisse, N., Oxbrough, A., Taki, H., et al. (2017). Forest biodiversity, ecosystem functioning and the provision of ecosystem services. Biodivers. Conserv. *26*, 3005–3035. https://doi.org/10.1007/s10531-017-1453-2.

84. Mauri, A., Girardello, M., Forzieri, G., Manca, F., Beck, P.S., Cescatti, A., and Strona, G. (2023). Assisted tree migration can reduce but not avert the decline of forest ecosystem services in Europe. Global Environ. Change *80*, 102676. https://doi.org/10.1016/j.gloenvcha.2023.102676.

85. Grassi, G., House, J., Dentener, F., Federici, S., den Elzen, M., and Penman, J. (2017). The key role of forests in meeting climate targets requires science for credible mitigation. Nat. Clim. Change *7*, 220–226. https://doi.org/10.1038/nclimate3227.

86. Forzieri, G., Pecchi, M., Girardello, M., Mauri, A., Klaus, M., Nikolov, C., Rüetschi, M., Gardiner, B., Tomaštík, J., Small, D., et al. (2020). A spatially explicit database of wind disturbances in European forests over the period 2000–2018. Earth Syst. Sci. Data *12*, 257–276. https://doi.org/10.5194/essd-12-257-2020.

87. Marini, L., Økland, B., Jönsson, A.M., Bentz, B., Carroll, A., Forster, B., Grégoire, J.-C., Hurling, R., Nageleisen, L.M., Netherer, S., et al. (2017). Climate drivers of bark beetle outbreak dynamics in Norway spruce forests. Ecography *40*, 1426–1435. https://doi.org/10.1111/ecog.02769.

88. Forzieri, G., Feyen, L., Russo, S., Vousdoukas, M., Alfieri, L., Outten, S., Migliavacca, M., Bianchi, A., Rojas, R., and Cid, A. (2016). Multi-hazard assessment in Europe under climate change. Climatic Change *137*, 105–119. https://doi.org/10.1007/s10584-016-1661-x.

89. Migliavacca, M., Dosio, A., Kloster, S., Ward, D.S., Camia, A., Houborg, R., Houston Durrant, T., Khabarov, N., Krasovskii, A.A., San Miguel-Ayanz, J., and Cescatti, A. (2013). Modeling burned area in Europe with the Community Land Model. JGR. Biogeosciences *118*, 265–279. https://doi.org/10.1002/jgrg.20026.

90. Gupta, H.V., Sorooshian, S., and Yapo, P.O. (1999). Status of Automatic Calibration for Hydrologic Models: Comparison with Multilevel Expert Calibration. J. Hydrol. Eng. *4*, 135–143. https://doi.org/10.1061/(ASCE)1084-0699(1999)4:2(135).

91. Clifford, A.A. (1973). Multivariate Error Analysis;: A Handbook of Error Propagation and Calculation in Many-Parameter Systems (Wiley)).

92. Hamed, K.H., and Ramachandra Rao, A. (1998). A modified Mann-Kendall trend test for autocorrelated data. J. Hydrol. *204*, 182–196. https://doi.org/10.1016/S0022-1694(97)00125-X.

93. Seidl, R., and Rammer, W. (2017). Climate change amplifies the interactions between wind and bark beetle disturbances in forest landscapes. Landsc. Ecol. *32*, 1485–1498. https://doi.org/10.1007/s10980-016-0396-4.

94. Meigs, G.W., Zald, H.S.J., Campbell, J.L., Keeton, W.S., and Kennedy, R.E. (2016). Do insect outbreaks reduce the severity of subsequent forest fires? Environ. Res. Lett. *11*, 045008. https://doi.org/10.1088/1748-9326/11/4/045008.

95. Rocchini, D., Balkenhol, N., Carter, G.A., Foody, G.M., Gillespie, T.W., He, K.S., Kark, S., Levin, N., Lucas, K., Luoto, M., et al. (2010). Remotely sensed spectral heterogeneity as a proxy of species diversity: Recent advances and open challenges. Ecol. Inf. *5*, 318–329. https://doi.org/10.1016/j.ecoinf.2010.06.001.

96. Wood, E.M., Pidgeon, A.M., Radeloff, V.C., and Keuler, N.S. (2013). Image Texture Predicts Avian Density and Species Richness. PLoS One *8*, e63211. https://doi.org/10.1371/journal.pone.0063211.

97. Wood, E.M., Pidgeon, A.M., Radeloff, V.C., and Keuler, N.S. (2012). Image texture as a remotely sensed measure of vegetation structure. Rem. Sens. Environ. *121*, 516–526. https://doi.org/10.1016/j.rse.2012.01.003.

98. Whittaker, R.H. (1972). Evolution and Measurement of Species Diversity. Taxon *21*, 213–251. https://doi.org/10.2307/1218190.

99. Skidmore, A.K., Coops, N.C., Neinavaz, E., Ali, A., Schaepman, M.E., Paganini, M., Kissling, W.D., Vihervaara, P., Darvishzadeh, R., Feilhauer, H., et al. (2021). Priority list of biodiversity metrics to observe from space. Nat. Ecol. Evol. *5*, 896–906. https://doi.org/10.1038/s41559-021-01451-x.

100. Shannon, C.E. (1948). A mathematical theory of communication. The Bell System Technical Journal *27*, 379–423. https://doi.org/10.1002/j.1538-7305.1948.tb01338.x.

101. Hastie, T., Tibshirani, R., and Friedman, J. (2009). The Elements of Statistical Learning: Data Mining, Inference, and Prediction, Second Edition (Springer-Verlag).

**One Earth, Volume *7***

## Supplemental information

# Ecosystem heterogeneity is key to limiting the increasing climate-driven risks to European forests

**Giovanni Forzieri, Hervé Jactel, Alessandra Bianchi, Jonathan Spinoni, Deepakrishna Somasundaram, Luc Feyen, and Alessandro Cescatti**

**Text S1. Environmental predictors used for the hazard and vulnerability models**

Vegetation features

- Biomass. Time series of forest biomass were derived by rescaling estimates of the changes in carbon stock occurring over the period 2000-2018 (ref. ([1]), https://zenodo.org/record/4161694#.YZ1VwvnMKUk) to the forest biomass values available for the year 2010 (ref. ([2])), (GlobBiomass, https://doi.org/10.1594/PANGAEA.894711). The methodology is described in the method section (Exposure).
- Tree height. Tree height values were retrieved from 1-km spaceborne light detection and ranging (lidar) data acquired in 2005 by the Geoscience Laser Altimeter System (GLAS) aboard ICESat (Ice, Cloud, and land Elevation Satellite)[3]. Data source: https://webmap.ornl.gov/wcsdown/dataset.jsp?ds_id=10023.
- Tree age. Tree age was retrieved from the global forest age dataset (GFAD) describing the age distributions of plant functional types (PFT) on a 0.5-degree grid and represents the 2000-2010 period[4]. The mode of the distribution for each PFT was retrieved and then used for PFT-specific hazard and vulnerability models. Data source: https://doi.pangaea.de/10.1594/PANGAEA.889943.
- Leaf Area Index (LAI). Growing season averages of LAI were retrieved from MODIS Terra+Aqua data provided at 500-meter spatial resolution over the 2002-2017 period (MCD15A3H.006, data source: https://doi.org/10.5067/MODIS/MCD15A3H.006). The growing season spans from June to September. Missing LAI values for years 2000-2001 were reconstructed from NDVI values by interpolation of a quadratic polynomial fitting function calibrated over the overlapping period 2002-2017. NDVI values were retrieved from MODIS Terra data at 250-meter spatial resolution over the 2000-2017 period (MOD13Q1.006, data source: https://doi.org/10.5067/MODIS/MOD13Q1.006). When Random Forest models are used in prediction mode, we used LAI retrieved from the Global Inventory Modeling and Mapping Studies Normalized Difference Vegetation Index (GIMMS3g v.1) covering the period 1982-2018 and provided at 15-day temporal frequency and 1/12° spatial resolution[5]. Data source:,http://sites.bu.edu/cliveg/datacodes/.
- Tree density. Tree densities were retrieved from a database of predictive regression models that link tree density observed over a multitude of plots at global scale with spatially explicit information on climate, topography, vegetation characteristics, and anthropogenic land use[6]. Tree density data were provided as a static map at 1-km spatial resolution and refer to the last two decades. Data source: https://doi.org/10.6084/m9.figshare.3179986.
- Coefficient of spatial variation (CV) and Homogeneity Index (Homogeneity). CV and Homogeneity are metrics quantifying the ecosystem heterogeneity of vegetated patterns based on the textural features of Enhanced Vegetation Index (EVI) imagery acquired by the Moderate Resolution Imaging Spectroradiometer (MODIS)[7]. Such spatial diversity metrics were provided at 1-km spatial resolution, are static and refer to the 2001-2005 period. Data source: http://www.earthenv.org/texture.

Climate features

- Annual cumulated precipitation (Pcum) and annual maximum temperature (Tmax). Pcum and Tmax were retrieved from the TerraClimate dataset, which combines high-spatial resolution climatological normals from the WorldClim dataset with time-varying coarser data from CRU Ts4.0 and the Japanese 55-year Reanalysis (JRA55)[8]. Pavg and Tmax were provided at 4-km spatial resolution over the period 1979-2018. Data source: http://www.climatologylab.org/terraclimate.html.
- Short-term average anomaly in cumulated precipitation (avg aPcum) and average temperature (avg aTavg). avg aPcum (avg aTavg) were quantified as the average of the annual anomalies in cumulated precipitation (average temperature) over a six-year time window [t-5,t]. Annual anomalies in cumulated precipitation (average temperature) were computed as the difference between the annual cumulated precipitation (average temperature) and its climatological value over the period 1970-1990. Temperature and precipitation were retrieved from the TerraClimate database[8] at 4-km spatial resolution over the period 1979-2018. Data source: http://www.climatologylab.org/terraclimate.html.
- Long-term average temperature (Long-term Tavg). Long-term Tavg was quantified as the average of annual temperature over the period 1979-2018. Temperature values are retrieved from the TerraClimate[8] database at 4-km spatial resolution over the period 1979-2018. Data source: http://www.climatologylab.org/terraclimate.html.
- Annual moisture index (MI). MI was quantified as the minimum of the seasonal MIs in a year, which were derived as (seasonal cumulated precipitation)/(seasonal maximum temperature + 30). The approach is based on a modified version of the De Martonne index[9], where the constant 30 at the denominator is introduced to avoid negative values in cold climates. Temperature and precipitation were retrieved from the TerraClimate[8] database at 4-km spatial resolution over the period 1979-2018. Data source: http://www.climatologylab.org/terraclimate.html.
- Short-term average standardized precipitation evapotranspiration index (avg SPEI). avg SPEI was quantified as the average of the annual 12-month SPEI computed over a six-year time window [t-5,t]. Monthly SPEI-12 follows the computation approach described in ref. ([10]) and is based on the difference between precipitation and potential evapotranspiration. To characterize prolonged period of water stress conditions before the occurrence of a given disturbance, we first isolated the SPEI-12 ≤ -0.5 values and summed them (in absolute values) over the 12 monthly values. No positive SPEI-12 or just-negative (between -0.5 and 0) values have been included in the annual summed values. Input climate variables were derived from reanalysis data at 0.25° spatial resolution over the period 1979-2018. Data source: https://www.ecmwf.int/en/forecasts/datasets/reanalysis-datasets/era5.
- Fire Weather Index (FWI). The FWI is composed of three moisture codes and three fire behaviour indices. The moisture codes describe the moisture content of three generalized fuel classes, while the behaviour indices represent the spread rate, fuel consumption and intensity of a fire if it were to start[11]. FWI calculations require measurements of temperature at 2m, relative humidity at 2m, and wind speed at 10m, daily snow-depth, and precipitation cumulated over the previous 24 hours. FWI was provided from the Global Fire WEather Database (GFWED) at 0.5° spatial resolution over the 1980-2018 period. Fire danger is typically mapped in classes (very low, low, medium, high, very high and extreme) according to FWI values. In our study, we used as predictor the number of days within a year with FWI above the “high danger” level. Data source: https://data.giss.nasa.gov/impacts/gfwed/.

- Cumulated annual snow (Snow). Snow values were retrieved from the NCEP-DOE Reanalysis 2 project at 0.5° spatial resolution over the 1979-2018 period[12]. Data sources: https://www.esrl.noaa.gov/psd/data/gridded/data.ncep.reanalysis2.html.
- Annual maximum wind speed (Wind speed). Wind speed values were retrieved from the ERA5 Reanalysis project at 0.25° spatial resolution over the 1979-2018 period. Data sources: https://cds.climate.copernicus.eu/cdsapp#!/dataset/reanalysis-era5-single-levels?tab=overview.

Landscape features

- Population density. Human population density depicts the distribution of population, expressed as the number of people per unit surface and has been produced within a framework tested with a large set of sensors including radar and optical public and commercial missions[13]. The original spatial resolution of 250 meter was resampled to 0.25° to better capture features of probability ignition and fire suppression[14,15]. Data source: http://ghsl.jrc.ec.europa.eu/ghs_pop.php.
- Elevation and Slope. Elevation and slope describe key geomorphic features and were derived from the Global Multi-resolution Terrain Elevation Data (GMTED2010) provided at 250-meter spatial resolution. Data source: https://www.usgs.gov/land-resources/eros/coastal-changes-and-impacts/gmted2010.

**Text S2. Environmental predictors used for the exposure model**

- Leaf area index (LAI). LAI values were retrieved from the Global Inventory Modeling and Mapping Studies Normalized Difference Vegetation Index (GIMMS3g v.1) covering the period 1982-2018 and provided at 15-day temporal frequency and 1/12° spatial resolution[5]. Data were initially aggregated at monthly scale and then average (avg), integral (int) and range (ran) values were derived for each year. Data source: http://sites.bu.edu/cliveg/datacodes/.
- Land surface phenology. A set of annual land surface phenological metrics, including start of season (SOS), end of season (EOS), length of season (LOS), day of peak season (DPS), rate of greening season (RGS), rate of senescence season (RSS), maximum of vegetation index season (MVI), cumulative vegetation index (CMI), average vegetation index (AVI) and background vegetation index (BVI), were derived from the AVHRR satellite platform for the period 1981-2016 and provided at 0.05° spatial resolution. Data source: https://vip.arizona.edu/viplab_data_explorer.php#.
- Tree cover (TC). TC values were derived from vegetation continuous fields acquired from the AVHRR satellite platform for the period 1982-2016 and provided at 0.05° spatial resolution. Data source: https://e4ftl01.cr.usgs.gov/MEASURES/VCF5KYR.001/.
- Plant cover fraction. Annual cover fractions of deciduous forests (DF) and evergreen forests (EF) were retrieved from the land cover maps of the European Space Agency Climate Change Initiative[16] provided for the period 1992-2018 at 0.05° spatial resolution. Data source: https://www.esa-landcover-cci.org/.
- Vegetation optical depth (VOD). Global daily estimates of VOD (Ku-band) were derived from multiple microwave satellite data for the period 1987-2017 at 0.25° spatial resolution[17]. Data were initially aggregated at monthly scale and then average (avg), integral (int) and range (ran) values were derived for each year. The vegetation optical depth (VOD) parameterizes the extinction (attenuation & scattering) effects due to the vegetation affecting the microwave radiations propagating through the vegetation canopy. It is a function of vegetation water content and its structure.

Data source: https://zenodo.org/record/2575599#.Ycm5kCDMKUk.

- Year (year). The temporal change is explicitly accounted for by using as additional predictor the time variable.

Vegetation variables reported above were averaged over a preceding 5-year moving temporal period prior their use in the exposure model to filter short-time variations.

**Text S3. Complementary observational datasets of forest disturbances**

- Database on Forest Disturbances in Europe (DFDE). The DFDE reports forest damages in terms of area affected and corresponding volume of biomass loss, derived from agent-specific conversion factors, aggregated at country level associated to single disturbance events occurring over the period 1981-2018 (ref. ([18,19])). Data are retrieved from a literature search. Data source: https://efi.int/articles/database-forest-disturbances-europe.
- Database of forest disturbances provided by the Food and Agriculture Organization (FAO) of the United Nations. The FAO database reports annual estimates of affected area aggregated at country level for the period 2000-2017 was used as well as complementary source. Data source: https://fra-data.fao.org/EU/fra2020/disturbances/.
- Database of salvage loggings provided by the Joint Research Centre (JRC) of the European Commission. The JRC database reports data of total salvage logging and the corresponding marginal contributions associated to windthrows and insect outbreaks expressed in volume of biomass, aggregated at country level for the period 2004-2018 for 17 Member States, including Austria, Bulgaria, Croatia, Cyprus, Czech Republic, Estonia, France, Finland, Germany, Hungary, Latvia, Lithuania, Romania, Poland, Slovakia, Slovenia and Sweden[20]. Data source: https://data.jrc.ec.europa.eu/dataset/2100b612-a4b0-4897-829b-72b7b1e5782c.
- Global Fire Emission Database (GFED). GFED reports monthly estimates of dry matter emissions of boreal and temperate forest fires acquired from the Global Fire Emission Database[21] at 0.25° spatial resolution for the 1997-2016 period. Data source: https://www.geo.vu.nl/~gwerf/GFED/GFED4/.

**Text S4. Cross-comparison analysis of risk estimates**

The lack of a systematic monitoring system of climate-driven risks to European forests did not allow a standard validation of our analysis. The approach to assess the validity of our risk estimates therefore consisted in evaluating the plausibility of the spatial and temporal distribution of biomass losses across Europe against independent datasets. To this aim, we compared our results with estimates of biomass volume losses collected in the DFDE database (for fires, windthrows, insect outbreaks and overall climate risk), salvage logging volumes collected in the JRC repository (for windthrows, insect outbreaks and overall climate risk) and GFED dry matter emissions of burning forest biomass (for fires). To increase the comparability, volume estimates (DFDE, JRC), originally expressed in cubic meters, have been approximately converted to tons by multiplying by a factor of 0.5, and all data were aggregated at country and annual scale. We compared risk estimates generated by our modelling framework separately with each of the above-mentioned databases limitedly to the common spatial and temporal domain. The agreement was assessed in terms of Spearman rank correlation ($\rho$) computed between pairs of samples of annual-country scale risk estimates. Furthermore, we compared inter-annual averages and trends of risk computed over the considered domain (Figure S8).

Significant positive correlation were found between our estimates and those provided from DFDE, GFED and JRC data for fires and overall climate risk with $\rho$ values ranging between 0.35 and

0.41 (p-values < 0.05) (Figure S8a,b,j,k). We found an underestimation of interannual averages of biomass losses in DFDE compared to our estimates, particularly for fires and insect outbreaks (Figure S8a,d,g,j), and an overall agreement in the sign of interannual trends (Figure S8c,f,i,l), yet their significance and magnitude may differ largely. When compared to GFED and JRC data, our estimates appear comparable in terms of interannual averages (Figure S8b,e,h,k). Trends based on JRC data also show a good agreement in sign with our estimates but tend to underestimate the magnitude of the temporal variations (Figure S8f,i,l), while trends based on GFED indicate an opposite tendency compared to our results (Figure S8c). Interestingly, we found that the trends in risk due to insect outbreaks emerge positive and significant (p-value<0.05) across all the considered datasets. This corroborates the transfer of models for insect outbreaks developed on US data to the European context. We point out that DFDE likely misses important disturbance events, being uniquely based on a literature search and thus related statistics may plausibly underestimate the effective spatial distribution and magnitude of biomass losses[19]. In contrast, the GFED and JRC dataset are collected based on more systematic acquisition tools and therefore - although they too are not free from uncertainties - may represent more solid benchmarks compared to DFDE in terms of interannual averages.

**Text S5. Main limitations in methodological and data aspects**

While the reasonable agreement between our risk estimates and those reported in independent disturbance databases (Text S4 and Figure S8) corroborates the overall hazard-vulnerability-exposure integration framework proposed here, a series of potential limitations should be carefully considered.

Differences in spatial accuracy across records. The spatial accuracy of the observed forest disturbances (EFFIS, FORWIND, IDS-USDA) varies across datasets and records. The patches of forest areas affected by disturbances, represented as polygons, have been collected using different techniques (e.g., visual interpretation of remote sensing imagery or aerial photographs, ground observations), by multiple actors and under different monitoring protocols. Despite a certain level of data harmonization in each product and independent validations (e.g., ref. ([22])), some differences in spatial accuracy may persist across disturbance records. To minimize these effects, we complement each record with a series of quantitative attributes derived from satellite and reanalysis products ensuring a consistent multi-dimensional characterization of each disturbance record in terms of relative biomass loss and environmental drivers used as input in our modelling framework.

Incompleteness of the disturbance datasets. The disturbance datasets are not comprehensive of all disturbance events that have occurred in the region during the observation period. Therefore, the development of the RF models may be partially affected by an under-sampling of the forest disturbances in Europe. This is particularly the case for the windthrows events collected in the FORWIND dataset[22]. Major events are mostly included, but minor events, such as those originating from smaller scale convective storms, which have caused relevant impacts for some regions of Europe[23,24], are only partially reported in the current version of the database. Consequently, the spatial and temporal dynamics of the damages caused by microbursts are likely underestimated in our assessment. To reduce the potential underestimation of the overall hazard component originating from the incompleteness of the FORWIND dataset[22], the expected fraction of forest area annually affected by windthrows ($EFAA$) were rescaled to preserve consistency with the cumulated area affected at the European scale for the period 2000-2017 reported by the FAO database.

Application of the RF models calibrated on the IDS-USDA database to the European context. No systematic spatially explicit monitoring system of insect disturbances, such as the IDS-USDA, are

currently available for Europe. Therefore, we opted to develop hazard and vulnerability models to insect outbreaks based on IDS-USDA records. To increase the transferability of the models to the European context, we developed them for functional groups instead of working on species-specific models, following the approach presented in ref. ([25]). For this purpose, we classified records based on functional groups of the pest (bark beetles, defoliators, and sucking insects) and on the plant functional type (PFT) of the host tree species. Records were considered if the host plant belonged to the following PFTs: broadleaved deciduous (BrDc), broadleaved evergreen (BrEv), needle leaf deciduous (NeDc) and needle leaf evergreen (NeEv).

Correlative approach. The developed RF models are based on a correlative approach and do not explicitly account for causal relationships between target and predictor variables[26]. To enhance the confidence of our inferences we carefully analyzed for each disturbance agent the functional relationship between biomass loss and the environmental predictors and quantified the relations via partial dependence plots (PDP). The latter were analyzed in combination with a detailed study of the literature that allowed us to understand and interpret the response functions to natural disturbances. Such analyses have been documented in a previous study (ref. ([25])).

Extrapolation of RF models beyond the training range. We note that some climate regions are poorly represented in the observational databases of forest disturbances. For instance, cold–wet and warm–dry zones are largely missing in the windthrows dataset (FORWIND), and we have few fire records from cold–dry zones (EFFIS). Forest disturbances utilized in our modelling framework are collected for the period 2000-2017, hence represent disturbances only for this period. Although we cannot fully evaluate model performance outside the range of the training sets, we stress that dedicated checks were performed on the PDPs at the boundaries of the observational ranges to reduce potential extrapolation errors as described in a previous study (ref. ([25])). Furthermore, to quantify such potential errors, we derived spatial statistics of biomass loss based solely on areas with climatological precipitation and temperature analogous to those of the observational datasets and confronted these with statistics derived for the whole spatial domain (Table S2-S5).

The development of continuous and systematic monitoring systems of forest disturbances in Europe would allow to further refine our risk models. Ongoing improvements of existing disturbance databases[22], the release of new harmonized spatially-explicit collections of biotic disturbances at the pan-European scale[27] and the advances on satellite-based detection and attribution techniques of forest disturbances hold promising opportunities for large-scale applications[28–30]. Furthermore, more sophisticated approaches, based for instance on causal modelling frameworks[31], would allow to more explicitly account for the causal relationships existing between target variable (biomass loss, in our case) and environmental predictors.

**Text S6. Relationships between ecosystem heterogeneity and resistance to climate-driven disturbances**

Increasing the diversity of ecosystems can lead to a reduction in the forest vulnerability to biotic and abiotic hazards via two main mechanisms: reduction in the amount of substrate and disruption of propagation processes[32]. The resource concentration hypothesis predicts that herbivory should increase with host plant density, as this optimizes foraging by insect herbivores. They have a greater probability of locating the resource and can stay longer to exploit it and build up their population. Recent large-scale epidemics of bark beetles in Europe and North America can be largely explained by the availability of forests of uniform age and composition[33–37]. Scolytid strategy of mass attack to exhaust the defences of host trees is also favoured by the presence of numerous congeners in the vicinity. In addition, the dispersal of herbivorous insects increases with increasing connectivity between patches of suitable habitat, which favours their successful

colonization[38]. The movement of insect populations and their colonization of forest patches can also be slowed by landscape diversity[38–40]. The presence of forest patches with high concentrations of non-hosts can in fact hinder or reduce the successful colonization of suitable stands on a landscape scale[41]. Similarly, forest fires are more likely to occur in homogeneous forest landscapes where fuel is not only more abundant, but also where there are no natural breaks limiting their spread, such as open habitats or patches of forest composed of low-flammability species[42,43]. The amount of standing forest biomass exposed to gales largely explains the extent of storm damage[44]. However, heterogeneity of the forest landscape can also play an important role, limiting domino fall caused by windstorms[45,46] or – on the contrary – increasing the risk of windthrow at exposed edges in the proximity of open areas such as clear-cuts[47].

At the landscape scale, additional factors, such as standing forest adjacent to logging coupes (edge effect), can affect the heterogeneity and consequently forest resistance against natural disturbances. For windstorms, consistent results have shown an increase in windthrow damage at the interface between forest stands and open areas (e.g. cultivated fields or clear-cuts), mainly due to the acceleration of wind speed in the absence of tall vegetation. As far as fires are concerned, the opposite trend is expected, since open areas represent an interruption in the continuity of fuel resources (e.g. firebreaks). With regard to insect pests, several studies have shown an increase in bark beetle damage at the edge of coniferous forests, mainly due to more favorable temperature conditions for insects and more stressful drought conditions for trees[48]. On the other hand, the greater fragmentation of the landscape associated with a higher edge density should be unfavorable to forest insects with a low dispersal capacity, such as defoliator Lepidoptera, resulting in a lower occurrence of pests at forest edges. Nevertheless, the effect of tree diversity has been shown to be just as effective in controlling insect damage at forest edges as within forests[49]. However, we point out that our analysis did not assess the edge effect specifically. The overall modelling framework has been specifically designed for forest ecosystems. Resulting estimates of biomass loss are representative of the forest ecosystems and independent on the distribution of forest within each grid-cell (e.g., forest fragmentation).

### Text S7. Space and time components in the hazard modelling

The use of the two sets of undisturbed records for the hazard modelling is crucial to better capture the dependence of the hazard component on the changes in climate drivers and increase the generality of the hazard models. To further explore this issue, we performed two experiments which combined in different ways the records used for training and testing the random forest classifier.

We used three different training/testing sets of records for the hazard modelling briefly described below and further detailed in the Experimental procedures section.

- Set A refers to disturbance records collected in the databases EFFIS, FORWIND and IDS-USDA.
- Set B refers to undisturbed records retrieved in disturbed areas before the occurrence of the disturbance event.
- Set C refers to undisturbed records retrieved at different locations than the disturbed records.

For each year and set (A, B, and C) we randomly extracted the records to use as training/testing and binned in the PC space as detailed in Text S9.

The two experiments have been conducted using different training sets.

- Experiment 1, hereafter referred to as EXP-SPACE-TIME represents the modelling experiment used as a reference in our study and detailed in the Experimental procedures section. In this experiment, the random forest classifier has been trained using records from sets A, B and C. In EXP-SPACE-TIME we quantify the probability of occurrence of a disturbance explicitly accounting for changes in environmental drivers (c.a., climate, LAI) that may occur in both space and time. Changes in environmental drivers in the space domain are captured in the combination of sets A and C, whereas changes in environmental drivers in the time domain are captured in the combination of sets A and B.
- Experiment 2, hereafter referred to as EXP-SPACE, represents a new modelling experiment to complement the reference run mentioned above. In this experiment, the random forest classifier has been trained using records only from sets A and C. In EXP-SPACE we quantify the probability of occurrence of a disturbance accounting only for changes in environmental drivers that may occur in space. Such variations are represented in the combination of sets A and C.

In both experiments, EXP-SPACE-TIME and EXP-SPACE, the sets A, B and C are used as testing sets. From the comparison of these two runs, we aim to evaluate to what extent the inclusion of undisturbed records retrieved in disturbed areas before the occurrence of the disturbance event (set B) contributes to capturing the dependence of the probability of occurrence of a disturbance on the variations in environmental drivers.

The results of these simulations are expressed in terms of overall accuracy and are reported in Table S7 for each disturbance and plant functional type (PFT). We found a systematic higher overall accuracy in EXP-SPACE-TIME than in EXP-SPACE for both windthrows and insect outbreaks across all PFTs. These results indicate that for the two major disturbances in European forests, the explicit integration of records conveying multi-temporal information of environmental drivers contributes to improving classification performance. Indeed, the dependency of wind and insect disturbances on changing climate factors is better captured when both space and time information were represented, compared to the case when only space variations were included. The characterization of time-varying climate conditions is particularly relevant for the model representation of these disturbances. In fact, these features are key to predicting the local sensitivity and critical climate thresholds associated to environmental triggers, such as extreme wind speeds determining tree overturning and stem breakage[45] or warm temperature anomalies leading to insect outbreaks[25,50].

In the case of fire disturbances, the overall accuracy in EXP-SPACE-TIME is lower than that one obtained in EXP-SPACE across all PFTs. In this case, the integration of records conveying multi-temporal information about environmental drivers reduces the classification performance. While fire disturbance also shows a high sensitivity to climate factors, as documented in factorial simulations shown in Figure 3, the probability of occurrence of fire disturbance is better represented when ingesting environmental factors derived from the space domain and ignoring the multi-temporal information. This may suggest that factors discriminated in the space domain most likely play a critical role on the triggering mechanisms of the disturbance. For instance, human factors can substantially influence suppression ignition processes and are likely more spatial than temporal dependent[51]. In the modelling frame, we account for these components by including the population density as a predictor. While this variable is dynamic, its temporal variations are relatively limited in the time span of the analysis compared to its spatial gradients and to the inter-annual variations in climate factors. We hypothesize that the discriminant information of human components on the probability of fire occurrence can be better disentangled from the pool of predictors when ingesting only space variations in environmental factors. However, we point out that the use of a modelling based on EXP-SPACE could likely

underestimate the effect of time-varying aridity and temperature on fire disturbance under projected climate change conditions.

To better capture time-varying climate effects of disturbance processes, increase the overall performance, ensure consistency across the different disturbance types, and develop prediction models suited in the context of climate change, we identify the EXP-SPACE-TIME set up as benchmark simulation in our study and used such modelling framework to ultimately estimate the probability of fires, windthrows and insect outbreaks.

### Text S8. Modelling patterns and drivers of forest disturbances at the regional/national scale

We consider the 0.25° spatial resolution appropriate for this work as it allows to explore patterns and drivers of forest disturbances at the regional/national scale and, therefore, to support both the development of the science and the definition of regional/national forest strategies that aim at reducing climate risks and improving forest resilience. The choice of this resolution is also optimal to support the data-driven estimates of the predictive models based on observed records of disturbances. At higher resolution, the role of stochasticity in the occurrence of disturbances is considerably larger, to the point that it may mask the role of the underlying environmental drivers. By averaging at such relatively coarse spatial resolution we could reduce the effects of stochasticity in the signal of forest disturbances and develop more robust predictive models. This allows to capture the emergent spatial and temporal patterns in biomass loss and the benefits of an enhanced ecosystem heterogeneity. Furthermore, the selected 0.25° spatial resolution is adequate to integrate the various data streams designed in our modelling framework. When we run the RF models in prediction mode, we spatially averaged all input data to the common spatial resolution of 0.25°. Such spatial resolution represents an intermediate value between the native spatial resolutions of the environmental variables which range between 100 meter and 0.5 degree. As most of the input data have finer spatial resolution, their upscaling process in the resampling procedure, together with the binning along the principal components described in Supplementary Text S9, contributes at reducing the potential effects of spatial dependence in the pool of predictors. Finally, the 0.25° spatial resolution is also useful to facilitate the comparison of our data-driven risk levels with analogous estimates generated by process-based vegetation/forest models, such as Land Surface Models (LSMs) or Dynamic Global Vegetation Models (DGVMs). While such tools hold promises to quantify forest risk, they still only partially represent the complex interactions between risk components and key drivers. These models typically run at a spatial resolution comparable to our RF-based simulations. Therefore, our results may serve as a benchmark for such large-scale vegetation/forest models to improve their capacity to represent natural disturbances and ultimately enhance the reliability of future land–climate predictions.

### Text S9. Potential effects of spatial dependence structure in the observational datasets

Potential effects of spatial dependence in the observational datasets were reduced by resampling the environmental drivers along the gradients of the three principal components (PC) derived from the set of predictors, as proposed in ref. ([25]). To this aim, we used 100 bins of equal intervals for each PC dimension spanning the full range of values. The resampling procedure was stratified by splitting the records in training and testing sets and for disturbed and undisturbed sets. For each year between 2000 and 2017, we randomly extracted 60% of the records. The extracted subset was then binned in the PC space using the average as aggregation metric. The remaining 40% of records were similarly processed and used as a separate validation set. The cover fraction of each PFT was resampled using the same approach and renormalized within each bin. The bin

values were ultimately used as input in the random forest classifier to quantify the probability of occurrence of disturbance.

The proposed methodology also mitigates the effects that may originate from the differences in the spatial resolution of environmental drivers. In fact, bin values used as training/testing sets for the random forest models do not reflect a specific geographic location nor a predefined spatial scale. Each bin is the average of multiple records with similar environmental conditions (similar PCs) that may originate from different geographical areas. Therefore, the averaging conducted at bin level implicitly contributes to harmonizing the spatial scales of training/testing sets in the PCs space.

| | Average biomass | | Long-term trend | | |
|---|---|---|---|---|---|
| **Macro-region** | avg [Gt] | SE [Gt] | slope [Gt year$^{-1}$] | SE [Gt year$^{-1}$] | p-value |
| **Central Europe (CEU)** | 4.540 | 0.038 | 0.0206 | 0.0007 | <0.05 |
| **Northern Europe (NEU)** | 6.175 | 0.025 | 0.0137 | 0.0004 | <0.05 |
| **Southern Europe (SEU)** | 3.426 | 0.010 | 0.0042 | 0.0006 | <0.05 |
| **Western Europe (WEU)** | 1.928 | 0.011 | 0.0057 | 0.0003 | <0.05 |
| **Balkans (BKS)** | 2.678 | 0.005 | 0.0023 | 0.0002 | <0.05 |
| **Europe (EU+)** | 18.747 | 0.085 | 0.0465 | 0.0008 | <0.05 |

**Table S1. Statistics of average and trend of forest biomass.** Values aggregated per macro-regions and for the full spatial domain (EU+). Metrics include annual average (avg) and its standard error (SE), interannual trend (slope) and its standard error together with the significance level computed by two-sided modified Mann–Kendall test (p-value). Macro-regions are shown in Figure S17.

| Macro-region | Fires | | Windthrows | | Insect outbreaks | | Overall risk | |
|---|---|---|---|---|---|---|---|---|
| | avg [Mt] | SE [Mt] | avg [Mt] | SE [Mt] | avg [Mt] | SE [Mt] | avg [Mt] | SE [Mt] |
| **Central Europe (CEU)** | 0.013 | 0.005 | 0.618 | 0.397 | 8.794 | 1.215 | 9.424 | 1.311 |
| **Northern Europe (NEU)** | 0.035 | 0.008 | 5.632 | 2.621 | 10.771 | 1.150 | 16.438 | 3.135 |
| **Southern Europe (SEU)** | 1.596 | 0.078 | 0.008 | 0.005 | 4.474 | 0.636 | 6.079 | 0.676 |
| **Western Europe (WEU)** | 0.133 | 0.017 | 1.599 | 0.927 | 3.654 | 0.428 | 5.386 | 1.101 |
| **Balkans (BKS)** | 0.082 | 0.015 | 0.007 | 0.005 | 4.162 | 0.647 | 4.251 | 0.651 |
| **Europe (EU+)** | 1.859 | 0.086 | 7.864 | 2.735 | 31.855 | 3.811 | 41.578 | 5.296 |

**Table S2. Annual average statistics of climate-driven risks.** Values aggregated per macro-regions and for the full spatial domain (EU+). Metrics include annual average (avg) and its standard error (SE). Macro-regions are shown in Figure S17.

| Macro-region | Fires | | | Windthrows | | | Insect outbreaks | | | Overall risk | | |
|---|---|---|---|---|---|---|---|---|---|---|---|---|
| | slope [Mt year$^{-1}$] | SE [Mt year$^{-1}$] | p-value | slope [Mt year$^{-1}$] | SE [Mt year$^{-1}$] | p-value | slope [Mt year$^{-1}$] | SE [Mt year$^{-1}$] | p-value | slope [Mt year$^{-1}$] | SE [Mt year$^{-1}$] | p-value |
| **Central Europe (CEU)** | 0.0007 | 0.0004 | 0.0624 | 0.0366 | 0.0348 | 0.2896 | 0.5426 | 0.0626 | 0.0000 | 0.5800 | 0.0688 | 0.0000 |
| **Northern Europe (NEU)** | 0.0004 | 0.0007 | 0.2840 | 0.3291 | 0.2267 | 0.1618 | 0.4445 | 0.0724 | 0.0076 | 0.7741 | 0.2487 | 0.0001 |
| **Southern Europe (SEU)** | 0.0194 | 0.0062 | 0.0138 | -0.0005 | 0.0004 | 0.1328 | 0.3021 | 0.0281 | 0.0004 | 0.3210 | 0.0300 | 0.0003 |
| **Western Europe (WEU)** | 0.0031 | 0.0015 | 0.0262 | 0.0755 | 0.0815 | 0.0725 | 0.2109 | 0.0167 | 0.0000 | 0.2895 | 0.0859 | 0.0000 |
| **Balkans (BKS)** | 0.0025 | 0.0012 | 0.0000 | 0.0002 | 0.0004 | 0.3164 | 0.3007 | 0.0305 | 0.0004 | 0.3034 | 0.0305 | 0.0003 |
| **Europe (EU+)** | 0.0262 | 0.0064 | 0.0000 | 0.4410 | 0.2323 | 0.0047 | 1.8008 | 0.1715 | 0.0002 | 2.2680 | 0.2936 | 0.0000 |

**Table S3. Long-term trends of climate-driven risks.** Values aggregated per macro-regions and for the full spatial domain (EU+). Metrics include interannual trend (slope) and its standard error (SE) together with the significance level computed by two-sided modified Mann–Kendall test (p-value). Macro-regions are shown in Figure S17.

| Macro-region | Fires | | Windthrows | | Insect outbreaks | | Overall risk | |
|---|---|---|---|---|---|---|---|---|
| | avg [Mt] | SE [Mt] | avg [Mt] | SE [Mt] | avg [Mt] | SE [Mt] | avg [Mt] | SE [Mt] |
| **Central Europe (CEU)** | 0.011 | 0.004 | 0.596 | 0.397 | 5.751 | 0.758 | 6.358 | 0.883 |
| **Northern Europe (NEU)** | 0.030 | 0.007 | 5.625 | 2.620 | 9.981 | 1.075 | 15.649 | 3.088 |
| **Southern Europe (SEU)** | 1.561 | 0.077 | 0.005 | 0.004 | 2.552 | 0.338 | 4.118 | 0.376 |
| **Western Europe (WEU)** | 0.133 | 0.017 | 1.597 | 0.927 | 2.546 | 0.297 | 4.276 | 1.040 |
| **Balkans (BKS)** | 0.082 | 0.015 | 0.005 | 0.005 | 3.259 | 0.503 | 3.346 | 0.507 |
| **Europe (EU+)** | 1.817 | 0.086 | 7.827 | 2.729 | 24.089 | 2.756 | 33.747 | 4.410 |

**Table S4. Annual average statistics of climate-driven risks over climate domains sampled by the forest disturbance databases.** As Table S2 but with spatial statistics computed on areas with climatological precipitation and temperature analogous to those of the observational datasets of forest disturbances.

| Macro-region | Fires | | | Windthrows | | | Insect outbreaks | | | Overall risk | | |
|---|---|---|---|---|---|---|---|---|---|---|---|---|
| | slope [Mt year$^{-1}$] | SE [Mt year$^{-1}$] | p-value | slope [Mt year$^{-1}$] | SE [Mt year$^{-1}$] | p-value | slope [Mt year$^{-1}$] | SE [Mt year$^{-1}$] | p-value | slope [Mt year$^{-1}$] | SE [Mt year$^{-1}$] | p-value |
| **Central Europe (CEU)** | 0.0006 | 0.0004 | 0.0797 | 0.0362 | 0.0348 | 0.2732 | 0.3255 | 0.0419 | 0.0001 | 0.3624 | 0.0519 | 0.0002 |
| **Northern Europe (NEU)** | 0.0004 | 0.0007 | 0.2533 | 0.3293 | 0.2267 | 0.1153 | 0.4199 | 0.0670 | 0.0065 | 0.7494 | 0.2460 | 0.0001 |
| **Southern Europe (SEU)** | 0.0188 | 0.0061 | 0.0131 | -0.0005 | 0.0004 | 0.1126 | 0.1548 | 0.0166 | 0.0008 | 0.1732 | 0.0182 | 0.0005 |
| **Western Europe (WEU)** | 0.0031 | 0.0014 | 0.0262 | 0.0756 | 0.0814 | 0.0946 | 0.1450 | 0.0120 | 0.0000 | 0.2238 | 0.0850 | 0.0000 |
| **Balkans (BKS)** | 0.0025 | 0.0012 | 0.0000 | 0.0003 | 0.0004 | 0.2792 | 0.2336 | 0.0237 | 0.0007 | 0.2365 | 0.0236 | 0.0006 |
| **Europe (EU+)** | 0.0255 | 0.0064 | 0.0002 | 0.4410 | 0.2318 | 0.0038 | 1.2788 | 0.1302 | 0.0000 | 1.7452 | 0.2710 | 0.0000 |

**Table S5. Long-term trends of climate-driven risks over climate domains sampled by the forest disturbance databases.** As Table S3 but with spatial statistics computed on areas with climatological precipitation and temperature analogous to those of the observational datasets of forest disturbances.

| Category | Full name | Acronym | Fires | Windthrows | Insect outbreaks |
|---|---|---|---|---|---|
| Forest | Biomass | Biomass | *X* | *X* | *X* |
| | Tree height | Tree height | *X* | *X* | *X* |
| | Tree age | Tree age | *X* | *X* | *X* |
| | Leaf Area Index | LAI | *X* | *X* | *X* |
| | Tree density | Tree density | *X* | *X* | *X* |
| Climate | Annual cumulated precipitation | Pcum | *X* | *X* | |
| | Short-term average anomaly in cumulated precipitation | avg aPcum | | | *X* |
| | Annual cumulated snow | Snow | | *X* | |
| | Short-term average anomaly in average temperature | avg aTavg | | | *X* |
| | Annual maximum temperature | Tmax | *X* | | |
| | Annual aridity index | MI | *X* | | |
| | Short-term average standardized precipitation evapotranspiration index | avg SPEI | | | *X* |
| | Fire Weather Index | FWI | *X* | | |
| | Annual maximum wind speed | Wind speed | | *X* | |
| | Long-term average cumulated precipitation | Long-term Pavg | | *X* | |
| | Long-term average temperature | Long-term Tavg | | | *X* |
| Landscape | Population density* | Population | *X* | | |
| | Coefficient of spatial variation | CV | | | *X* |
| | Homogeneity | Homogeneity | *X* | *X* | |
| | Slope | Slope | *X* | *X* | |
| | Elevation | Elevation | *X* | | *X* |

**Table S6. Environmental predictors used in hazard and vulnerability models.** Variables used to predict the hazard and vulnerability components based on the feature selection scheme described in ref. ([25]). Population density (*) was used only for the hazard component.

| Disturbance | PFT | EXP-SPACE-TIME | EXP-SPACE |
|---|---|---|---|
| Fires | BrDe | 87.8 | 89.3 |
| | BrEv | 86.7 | 88.6 |
| | NeDe | 83.8 | 89.5 |
| | NeEv | 88.2 | 89.8 |
| Windthrows | BrDe | 70.6 | 68.5 |
| | BrEv | 66.2 | 65.2 |
| | NeDe | 67.2 | 65.5 |
| | NeEv | 69.5 | 67.4 |
| Insect outbreaks | BrDe | 88.7 | 87.7 |
| | BrEv | 84.1 | 82.6 |
| | NeDe | 83.1 | 83.6 |
| | NeEv | 89.4 | 87.3 |

**Table S7. Overall classification accuracy obtained from simulations EXP-SPACE-TIME and EXP-SPACE.** Statistics are reported for different forest disturbances (fires, windthrows, insect outbreaks) and plant functional types (broadleaved deciduous (BrDe), broadleaved evergreen (BrEv), needle leaf deciduous (NeDe) and needle leaf evergreen (NeEv)).

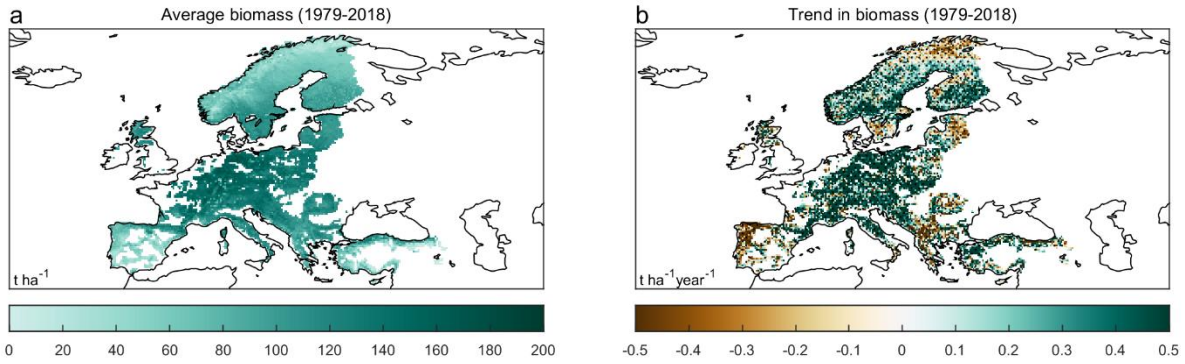


**Figure S1. Spatial and temporal variations in forest biomass.** (**a**) Annual average forest biomass computed over the 1979-2018 period. (**b**) Long-term trend in forest biomass computed over the 1979-2018 period, black dots show pixels where trends are significant (two-sided modified Mann–Kendall test; p value <0.05). Forests with cover fraction lower than 0.1 are masked in white.

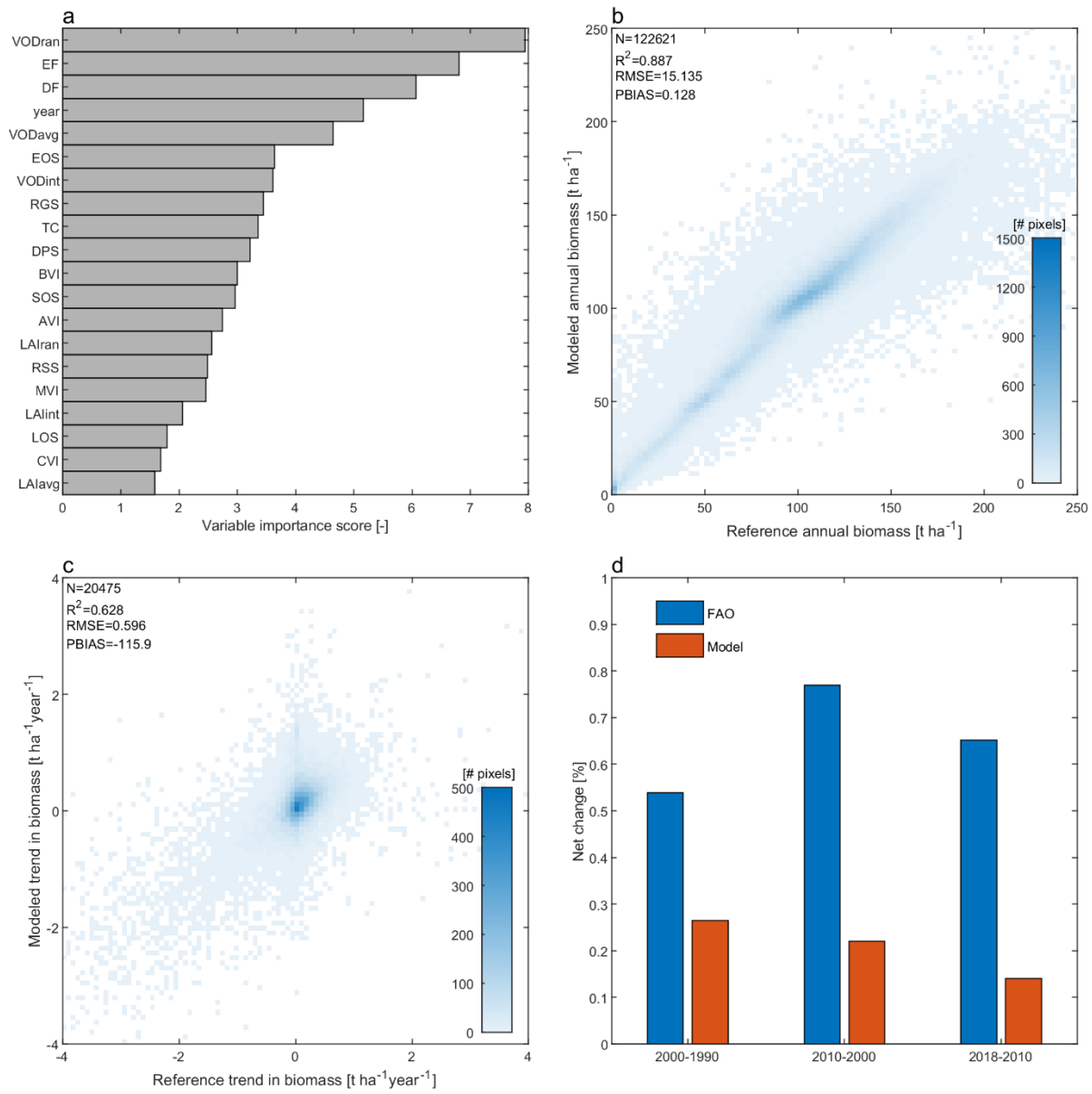


**Figure S2. Validation of the biomass (exposure) modelling.** (**a**) Selected predictors of biomass and corresponding variable importance based on the random forest (RF) regression model, acronyms reported in Text S2. (**b**) Reference versus modeled annual biomass. Number of binned records (*N*), coefficient of determination ($R^2$), root mean squared error (RMSE) and percent bias (PBIAS) are shown in labels, while the frequency distribution in color. (**c**) as (**b**) but for the trend in biomass. (**d**) Net change in biomass aggregated at European scale for different time periods and derived from the RF model and FAO estimates of carbon stock (Experimental procedures).

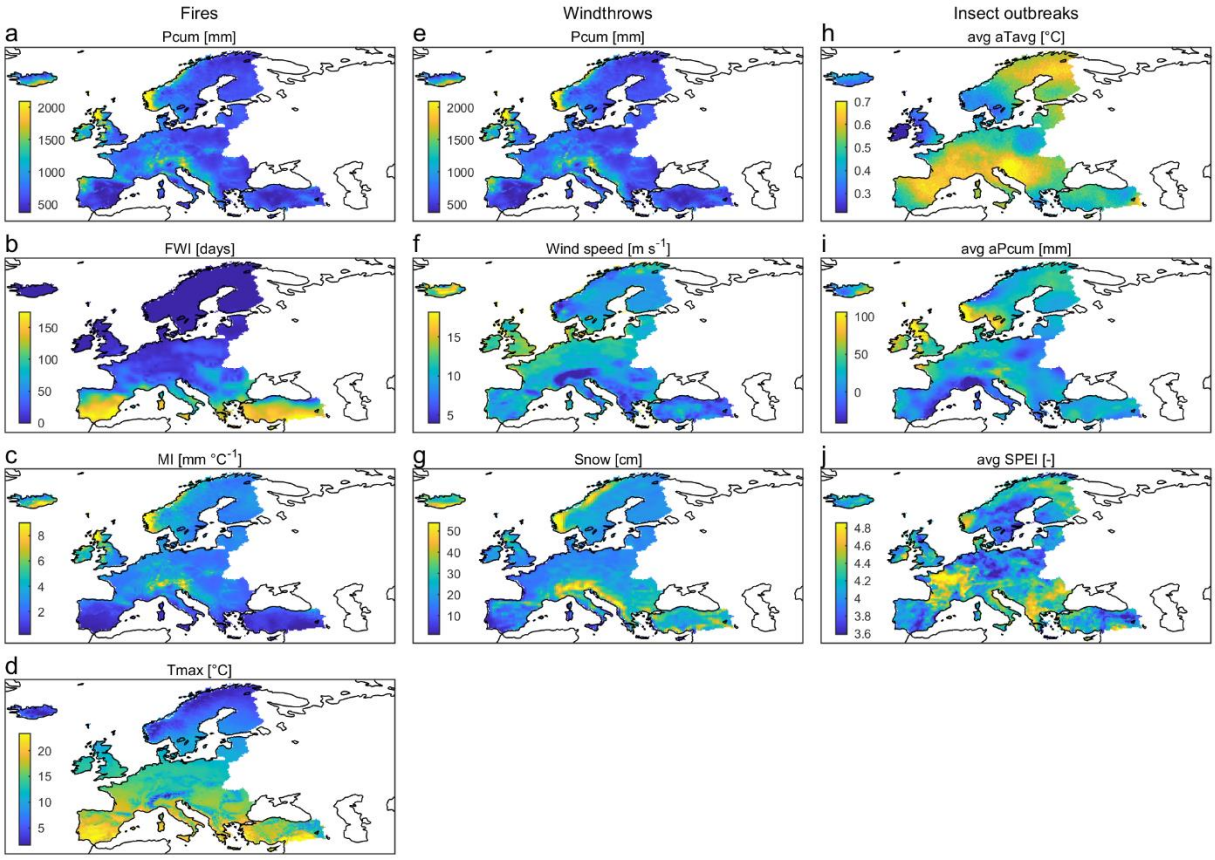


**Figure S3. Spatial variations in climate drivers of natural disturbances.** Annual averages of climate drivers (1979-2018). Maps are grouped per natural disturbance. Predictor acronyms are listed in Table S6.

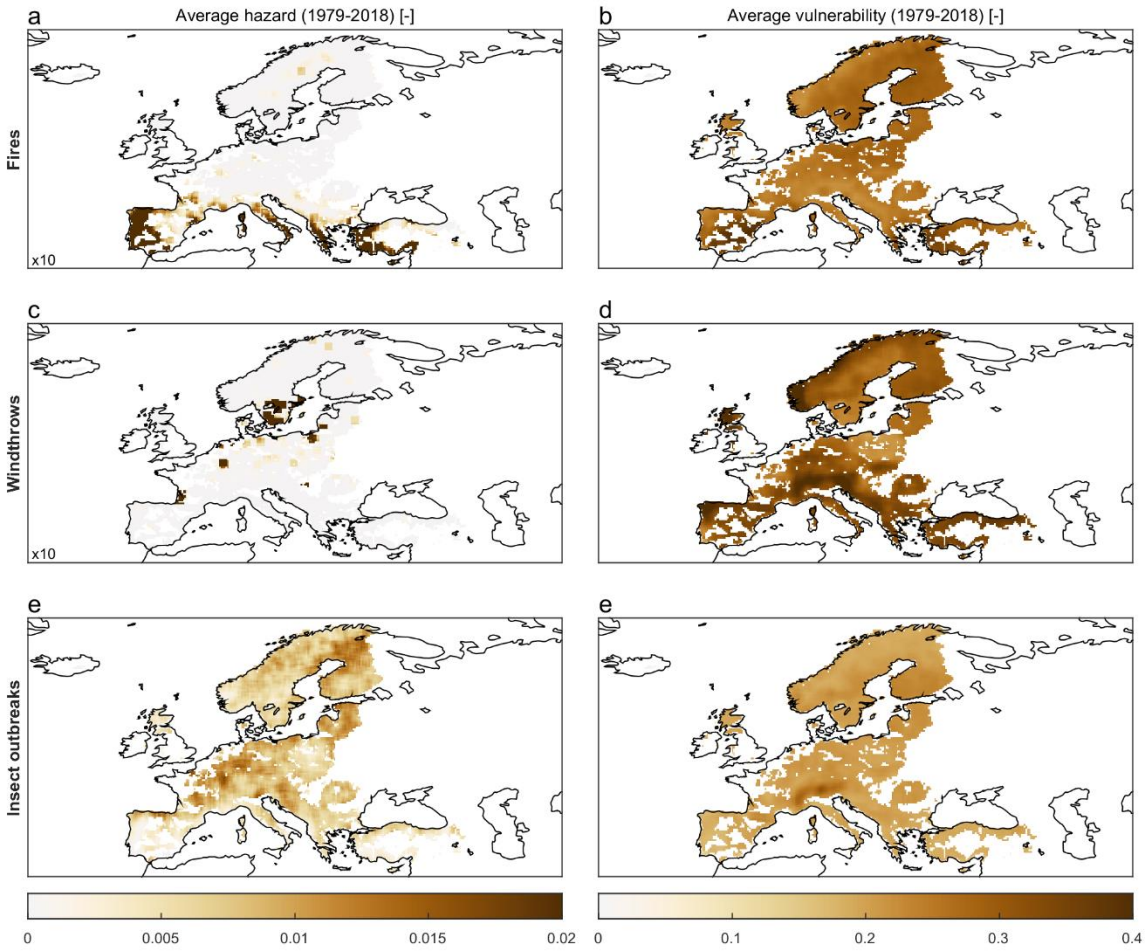


**Figure S4. Spatial variations of hazard and vulnerability of European forests to climate-driven risks.** Hazard (**a**) and vulnerability (**b**) of European forests to fires (averaged over the 1979-2018 period). (**c-d**) and (**e-f**) as (**a-b**) but for windthrows and insect outbreaks, respectively. Forests with cover fraction lower than 0.1 are masked in white.

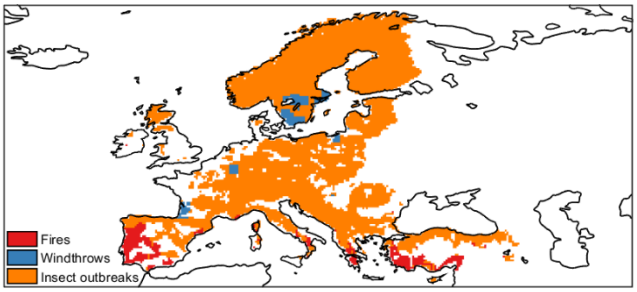


**Figure S5. Dominant climate-driven risks.** Spatial map of dominant climate-driven risk computed as the disturbance leading to the largest annual average biomass loss. Forests with cover fraction lower than 0.1 are masked in white.

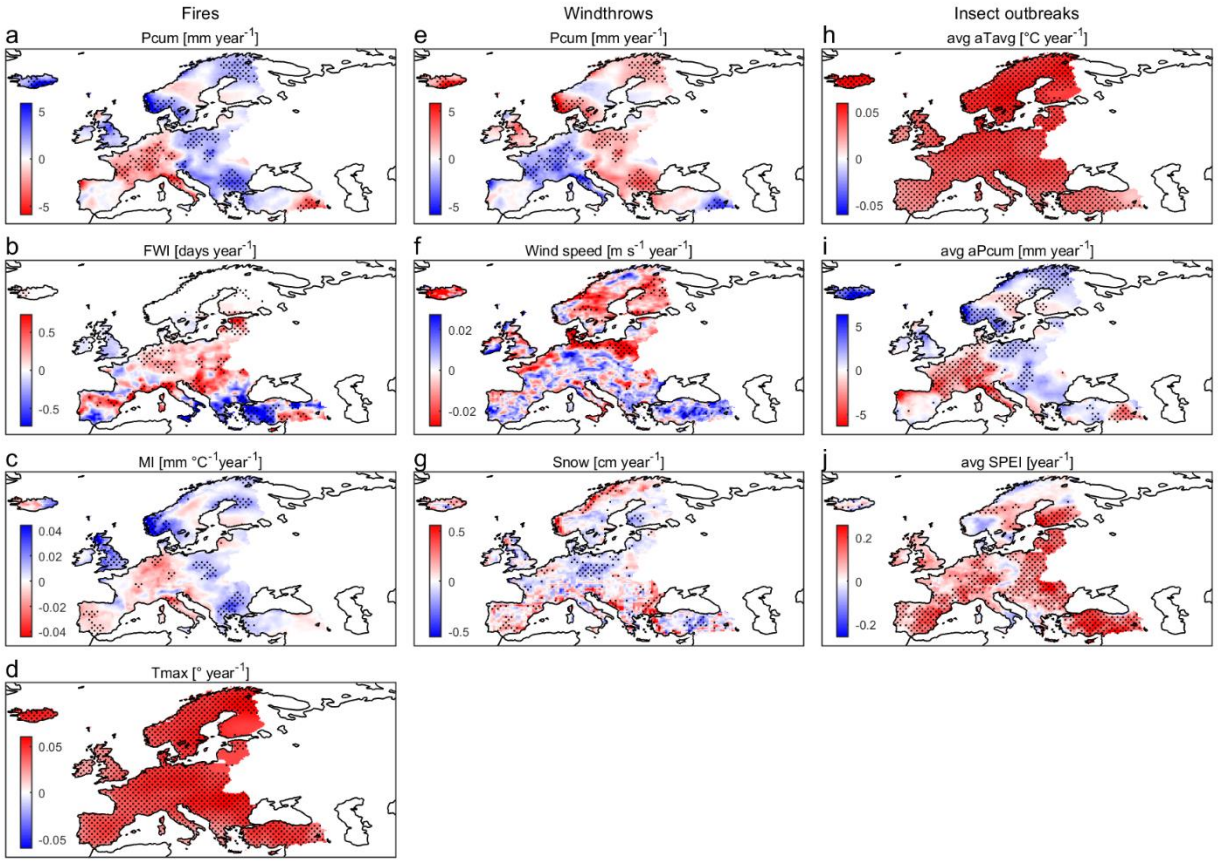


**Figure S6. Temporal variations in climate drivers of natural disturbances.** Temporal trends in climate drivers (1979-2018). Black dots show pixels where trends are significant (two-sided modified Mann–Kendall test; p value <0.05). Maps are grouped per natural disturbance. Predictor acronyms are listed in Table S6.

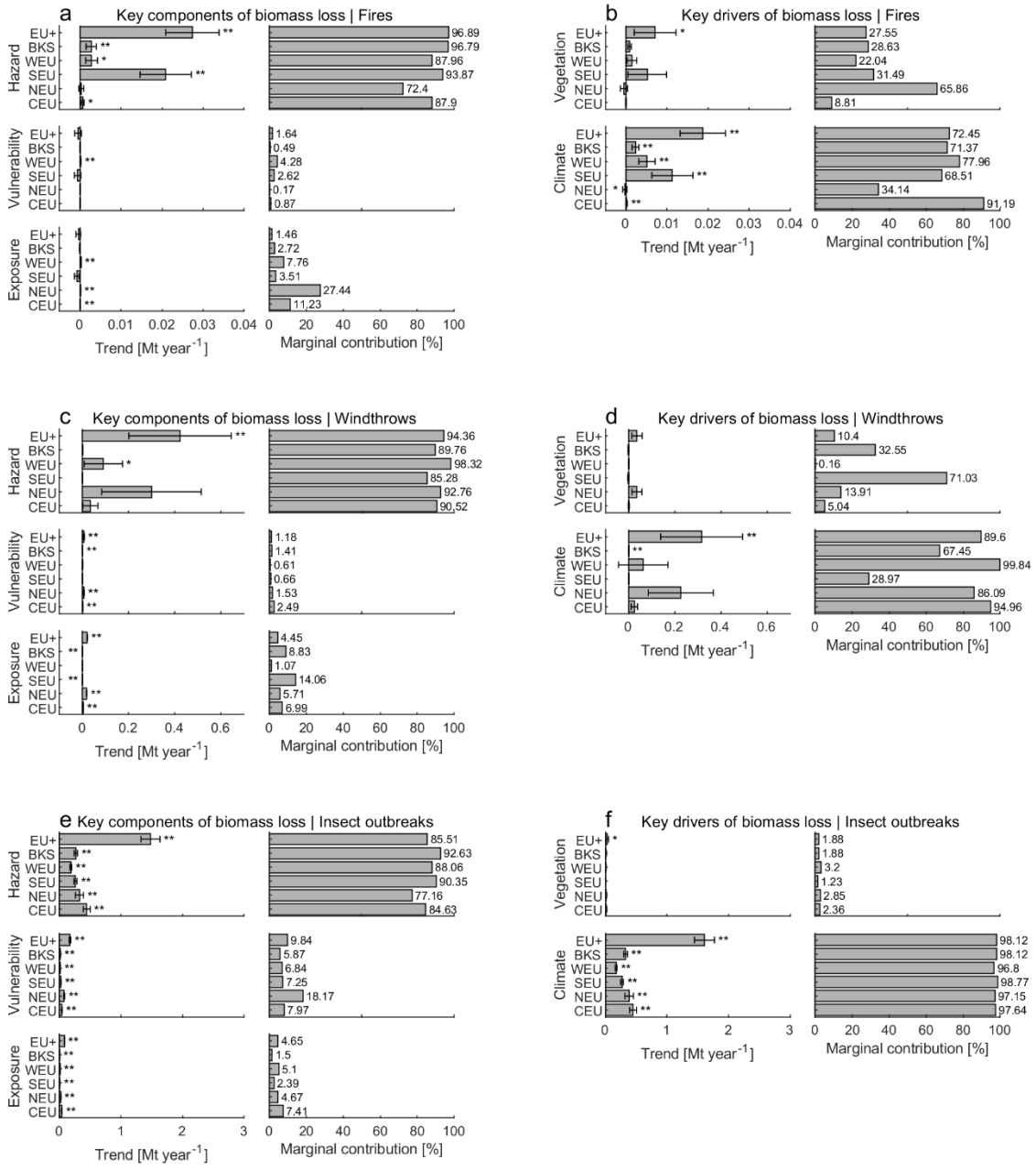


**Figure S7. Key determinants of natural disturbances for European macro-regions.** (**a**) Long-term trend in biomass loss due to fires, aggregated per macro-regions and for the full spatial domain (EU+), owning to changes in each risk component (hazard/vulnerability/exposure) and corresponding marginal contribution to the overall trend (left and right panel, respectively). Symbols "**" and "*" indicate trend statistically significant with p-value <0.05 and <0.1, respectively (two-sided modified Mann–Kendall test). (**b**) as (**a**) but for trend in biomass loss due to fires owning to changes in the underlying drivers (vegetation/climate). (**c**,**d**) and (**e**,**f**) as (**a**,**b**) but for windthrows and insect outbreaks, respectively. Macro-regions are shown in Figure S17.

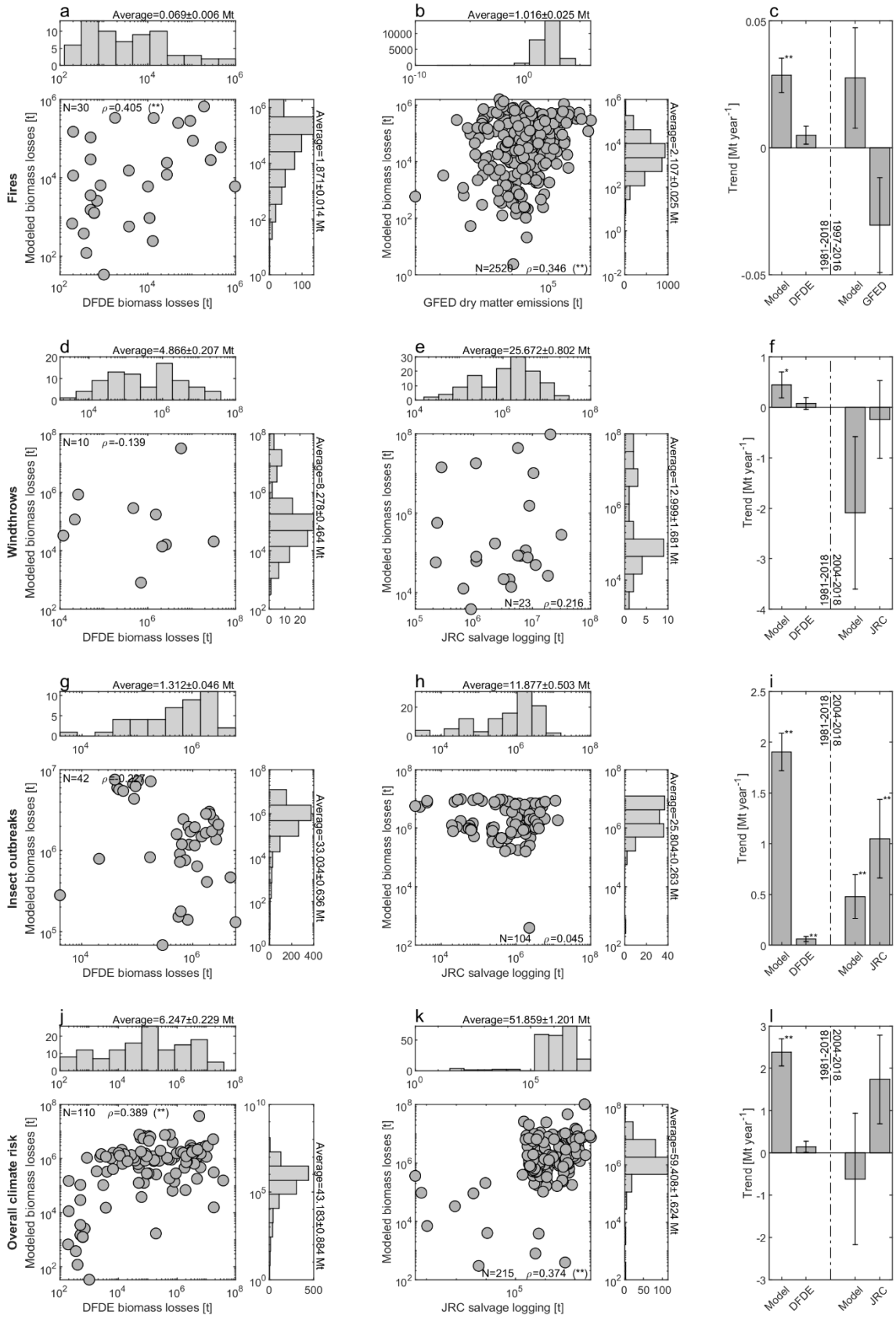
a
Average=0.069±0.006 Mt
N=30 ρ=0.405 (**)
Modeled biomass losses [t]
DFDE biomass losses [t]
Average=1.871±0.014 Mt
b
Average=1.016±0.025 Mt
N=2526 ρ=0.346 (**)
GFED dry matter emissions [t]
Average=2.107±0.025 Mt
c
Trend [Mt year-1]
1981-2018
1997-2016
Model
DFDE
GFED
Fires
d
Average=4.866±0.207 Mt
N=10 ρ=-0.139
Average=8.278±0.464 Mt
e
Average=25.672±0.802 Mt
N=23 ρ=0.216
JRC salvage logging [t]
Average=12.999±1.681 Mt
f
2004-2018
JRC
Windthrows
g
Average=1.312±0.046 Mt
N=42 ρ=0.227
Average=33.034±0.636 Mt
h
Average=11.877±0.503 Mt
N=104 ρ=0.045
Average=25.804±0.263 Mt
i
Insect outbreaks
j
Average=6.247±0.229 Mt
N=110 ρ=0.389 (**)
Average=43.183±0.884 Mt
k
Average=51.859±1.201 Mt
N=215 ρ=0.374 (**)
Average=59.408±1.624 Mt
l
Overall climate risk

**Figure S8. Cross-comparison of modeled climate-driven risks and independent disturbance databases.** (**a**) DFDE versus modeled biomass losses due to fires. Each circle represents an annual-country risk estimate, number of binned records (*N*) and Spearman rank correlation ($\rho$) are shown in labels. The histograms above and on the right of the main panel describe the frequency distribution of DFDE and modeled data, respectively, with their average value reported in label. (**b**) as (**a**) but with GFED biomass losses as independent comparative dataset. (**c**) Trend in biomass losses due to fires derived from model estimates, DFDE and GFED datasets over the overlapping temporal windows. Confidence intervals reflect the standard error of slope, symbols "**" and "*" indicate trend statistically significant with p-value <0.05 and <0.1, respectively (two-sided modified Mann–Kendall test). (**d-f**) as (**a-c**) but for biomass losses due to windthrows and with DFDE and JRC as independent comparative datasets. (**g-i**) as (**a-c**) but for biomass losses due to insect outbreaks and with DFDE and JRC as independent comparative datasets. (**j-l**) as (**a-c**) but for overall biomass losses due to multiple natural disturbances and with DFDE and JRC as independent comparative datasets.

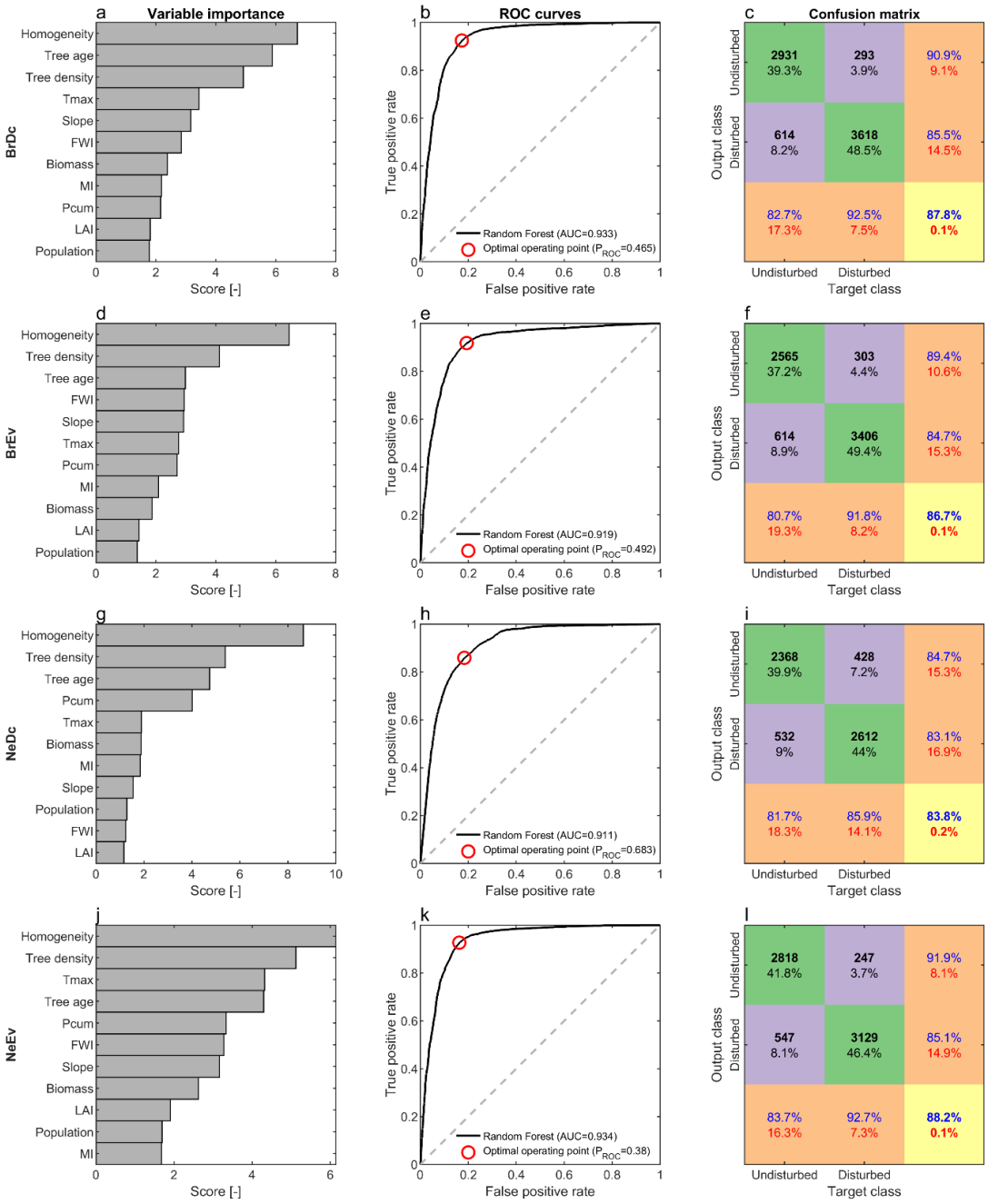


**Figure S9. Performance of random forest classification model of fire occurrence.** (**a-c**) Model performance for broadleaved deciduous (BrDc). (**a**) Selected predictors of disturbance occurrence and corresponding variable importance based on the random forest (RF) classification model, acronyms reported in Table S6. (**b**) Receiver Operating Characteristic (ROC) curve generated from the random forest classification shown in black line and corresponding Area Under the Curve (AUC) metric reported in label. The optimal operating point is shown in red circle and the corresponding probability threshold ($P_{ROC}$) reported in label. (**c**) Confusion matrix. (**d-f**), (**g-i**) and (**m-o**) as (**a-c**) but for broadleaved evergreen (BrEv), needle leaf deciduous (NeDc) and needle leaf evergreen (NeEv), respectively.

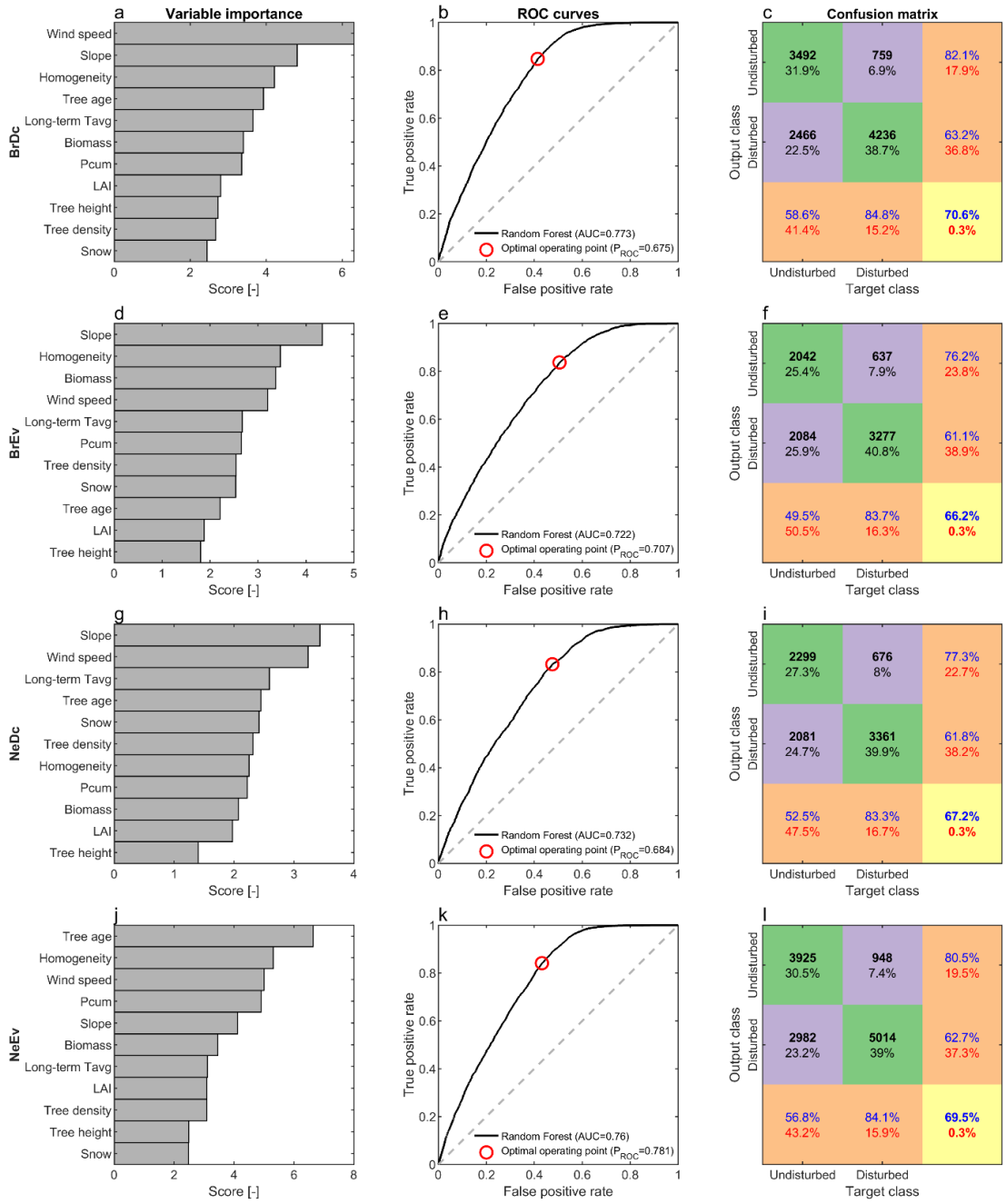


**Figure S10. Performance of random forest classification model of windthrow occurrence.** As Figure S9 but for windthrows.

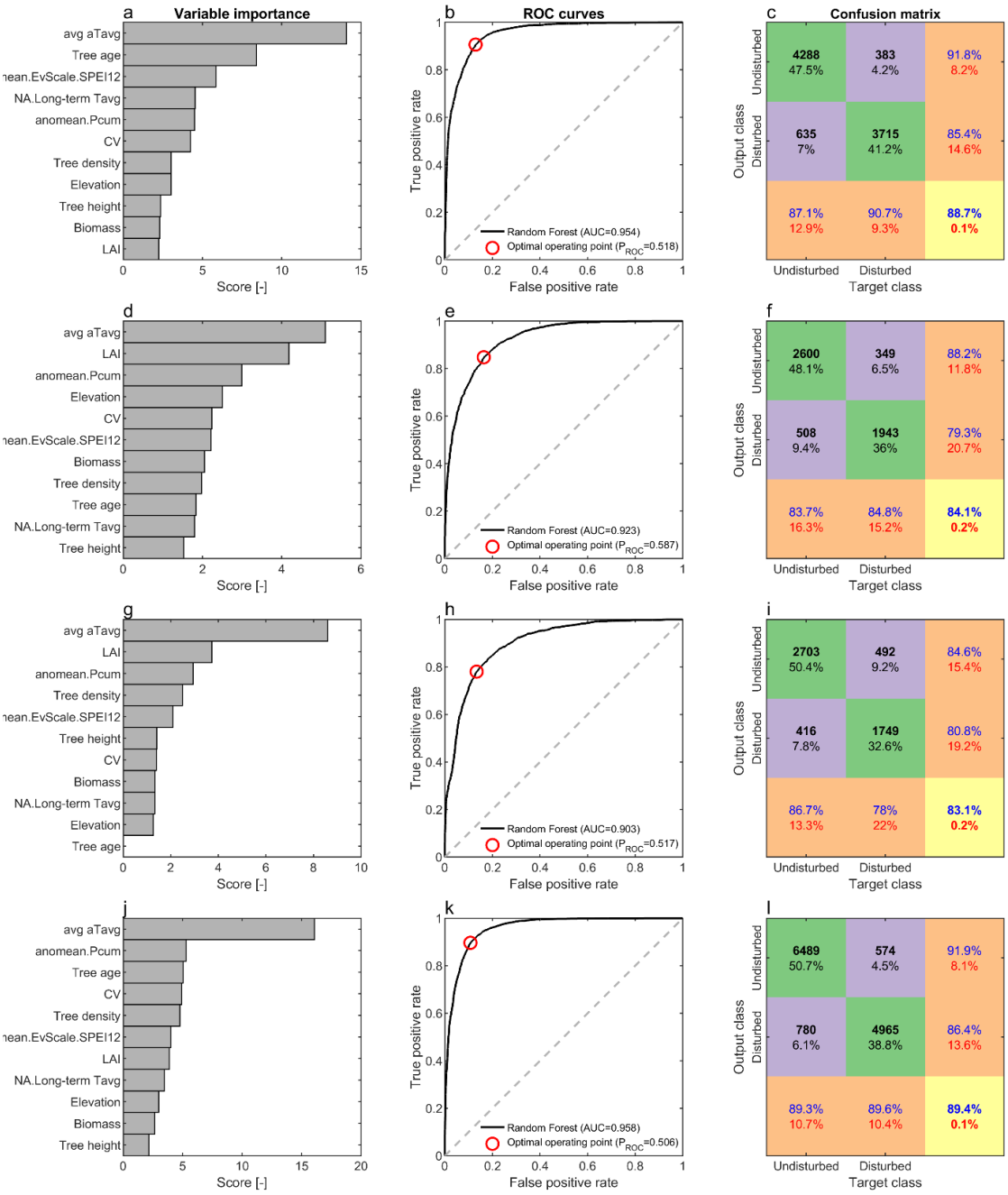


**Figure S11. Performance of random forest classification model of insect outbreak occurrence.** As Figure S9 but for insect outbreaks.

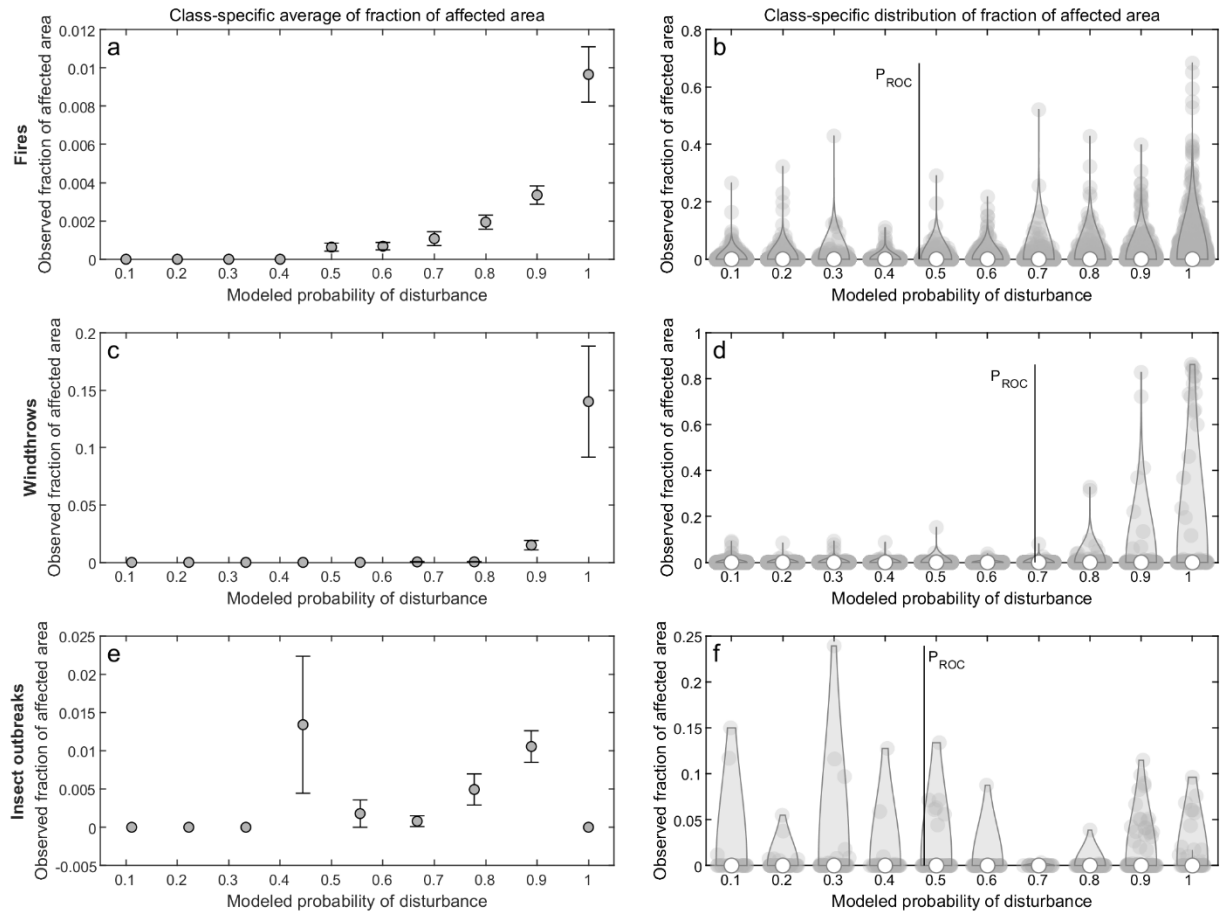


**Figure S12. Relationships between modeled probability of disturbance occurrence and observed fraction of affected forest area.** (**a**) Average fraction of affected forest area binned as a function of modeled probability of fire occurrence. Circle and confidence intervals represent the bin-specific average and standard error, respectively. (**b**) Violin plots representing the frequency distribution of observed fraction of affected areas within each probability class (bin). The probability threshold reflecting the optimal operating point ($P_{ROC}$) is shown in black line. (**c,d**) and (**e,f**) as (**a,b**) but for windthrows and insect outbreaks, respectively.

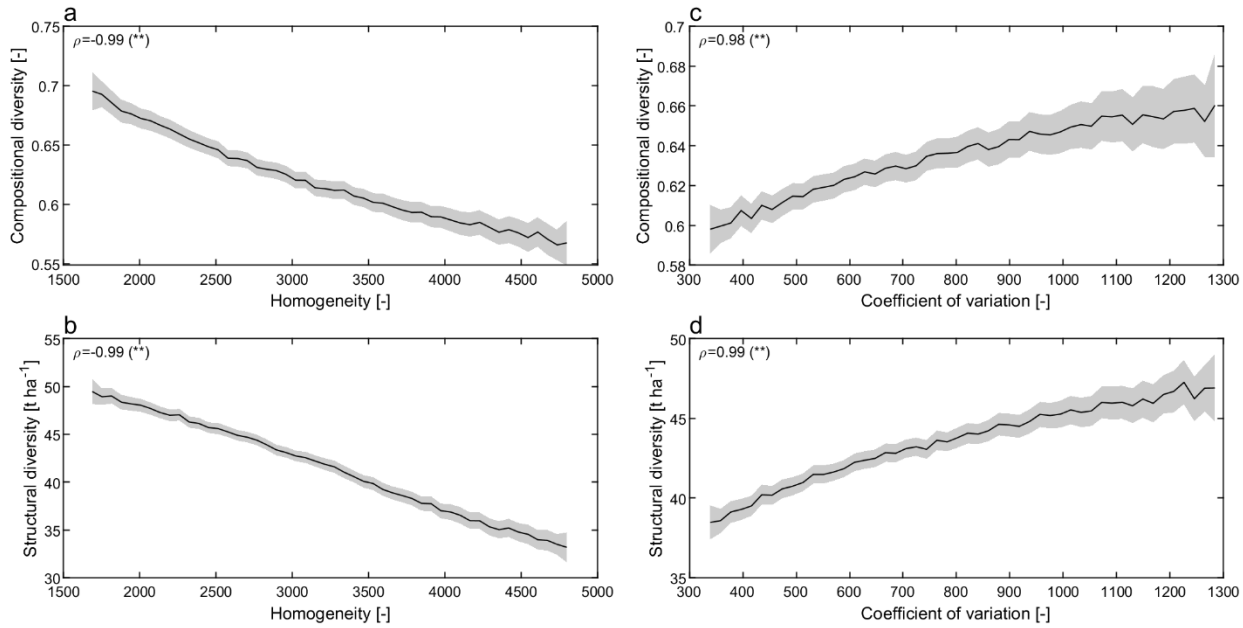


**Figure S13. Relationships between texture-based metrics of ecosystem heterogeneity and forest compositional/structural diversity.** (**a**) Compositional diversity values are binned as a function of texture-based homogeneity (average±5·SE). The strength of the relationship is quantified in terms of Spearman rank ($\rho$) and the symbol "**" indicates a correlation statistically significant with p-value < 0.05. (**b**) as (**a**) but for structural diversity. (**c**) as (**a**) and (**d**) and (**b**) but for the texture-based coefficient of variation.

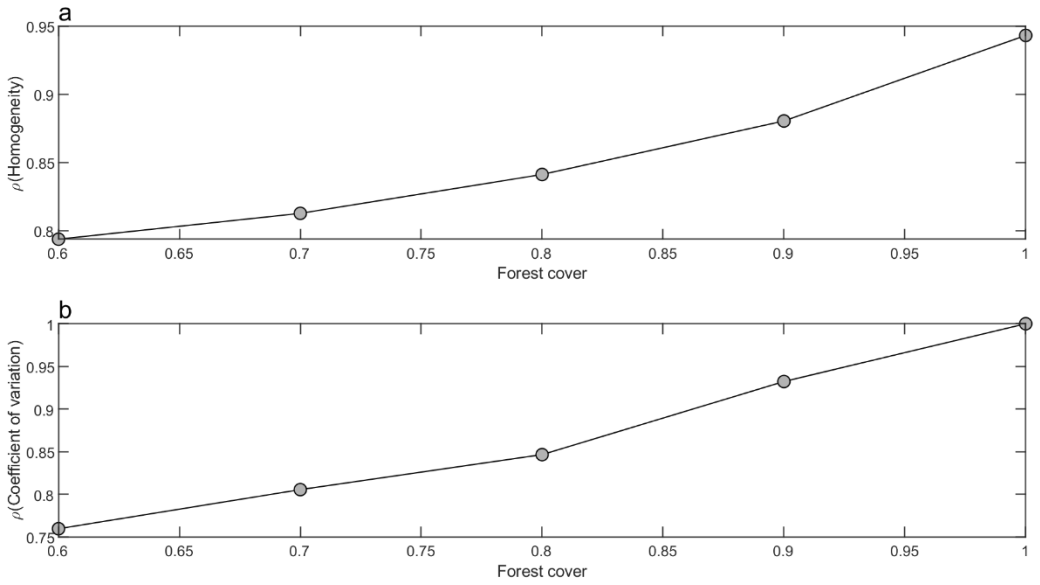


**Figure S14. Correlation between texture heterogeneity metrics derived by masking and without masking non-forest pixels.** Correlation values are expressed in terms of Spearman rank and are analyzed separately for homogeneity (**a**) and coefficient of variation (**b**) along a gradient of forest cover. All correlation values reported in figure have p-value < 0.05. Consistently with the approach described in ref. (ref. [7]), texture metrics were derived for 4x4 pixels boxes with at least nine finite value pixels. Therefore, the correlation analysis has been quantified for forest cover greater than 0.56.

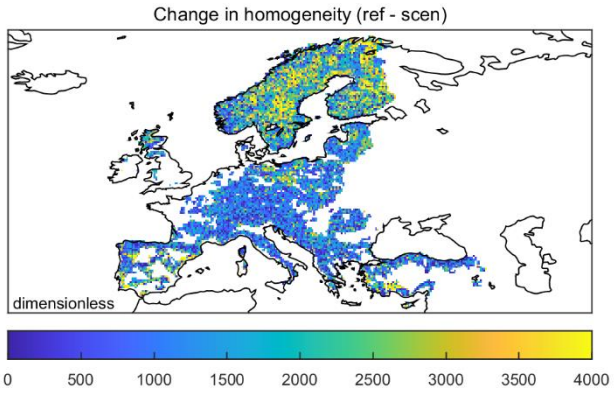


**Figure S15. Change in homogeneity owning to an idealized scenario of enhanced ecosystem heterogeneity.**

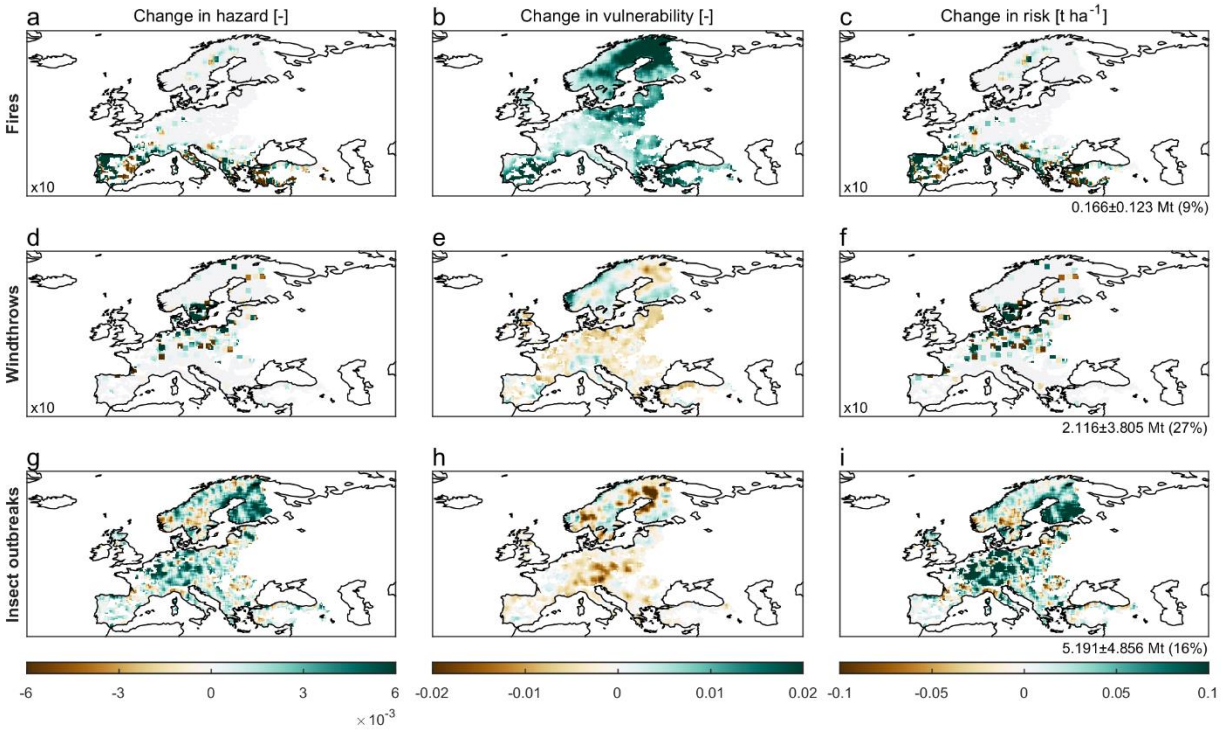


**Figure S16. Effects of enhanced ecosystem heterogeneity on hazard, vulnerability, and risk to natural disturbances.** Changes in fire hazard (**a**), vulnerability to fires (**b**) and biomass losses due to fires (**c**) owning to an increase in ecosystem heterogeneity consistent with local environmental conditions. Avoided biomass loss and relative change compared to the actual scenario are reported in labels. (**d-f**) and (**g-i**) as (**a-c**) but for windthrows and insect outbreaks, respectively.

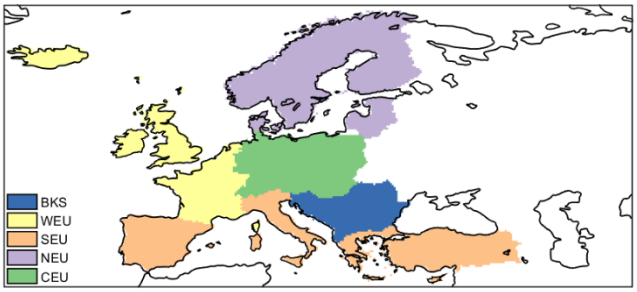


**Figure S17. European regions.** Grouping of countries in macro-areas shown in different colors. Central Europe (CEU) includes Austria, Czech Republic, Luxembourg, Germany, Liechtenstein, Poland, Slovakia and Switzerland. Northern Europe (NEU) includes Denmark, Estonia, Finland, Hungary, Latvia, Lithuania, Norway and Sweden. Southern Europe (SEU) includes Cyprus, Greece, Italy, Malta, Portugal, Spain, and Turkey. Western Europe (WEU) includes Belgium, France, Iceland, Ireland, Netherlands and United Kingdom Balkans (BKS) includes Albania, Bosnia and Herzegovina, Bulgaria, Croatia, Kosovo, Montenegro, Republic of Macedonia, Romania, Serbia and Slovenia.

**Supplemental references**


1. Xu, L., Saatchi, S.S., Yang, Y., Yu, Y., Pongratz, J., Bloom, A.A., Bowman, K., Worden, J., Liu, J., Yin, Y., et al. (2021). Changes in global terrestrial live biomass over the 21st century. Sci. Adv. *7*, eabe9829. https://doi.org/10.1126/sciadv.abe9829.

2. Santoro, M., Cartus, O., Carvalhais, N., Rozendaal, D.M.A., Avitabile, V., Araza, A., de Bruin, S., Herold, M., Quegan, S., Rodríguez-Veiga, P., et al. (2021). The global forest above-ground biomass pool for 2010 estimated from high-resolution satellite observations. Earth Syst. Sci. Data *13*, 3927–3950. https://doi.org/10.5194/essd-13-3927-2021.

3. Simard, M., Pinto, N., Fisher, J.B., and Baccini, A. (2011). Mapping forest canopy height globally with spaceborne lidar. J. Geophys. Res. Biogeosciences *116*. https://doi.org/10.1029/2011JG001708.

4. Poulter, B., Aragão, L., Andela, N., Bellassen, V., Ciais, P., Kato, T., Lin, X., Nachin, B., Luyssaert, S., Pederson, N., et al. (2018). The global forest age dataset (GFADv1.0), link to NetCDF file. https://doi.org/10.1594/PANGAEA.889943 https://doi.org/10.1594/PANGAEA.889943.

5. Zhu, Z., Bi, J., Pan, Y., Ganguly, S., Anav, A., Xu, L., Samanta, A., Piao, S., Nemani, R.R., and Myneni, R.B. (2013). Global Data Sets of Vegetation Leaf Area Index (LAI)3g and Fraction of Photosynthetically Active Radiation (FPAR)3g Derived from Global Inventory Modeling and Mapping Studies (GIMMS) Normalized Difference Vegetation Index (NDVI3g) for the Period 1981 to 2011. Remote Sens. *5*, 927–948. https://doi.org/10.3390/rs5020927.

6. Glick, H.B., Bettigole, C., Maynard, D.S., Covey, K.R., Smith, J.R., and Crowther, T.W. (2016). Spatially-explicit models of global tree density. Sci. Data *3*, 160069. https://doi.org/10.1038/sdata.2016.69.

7. Tuanmu, M.-N., and Jetz, W. (2015). A global, remote sensing-based characterization of terrestrial habitat heterogeneity for biodiversity and ecosystem modelling. Glob. Ecol. Biogeogr. *24*, 1329–1339. https://doi.org/10.1111/geb.12365.

8. Abatzoglou, J.T., Dobrowski, S.Z., Parks, S.A., and Hegewisch, K.C. (2018). TerraClimate, a high-resolution global dataset of monthly climate and climatic water balance from 1958–2015. Sci. Data *5*, 170191. https://doi.org/10.1038/sdata.2017.191.

9. De Martonne, E. (1926). Une nouvelle fanction climatologique: l'indice d'aridité. La Météorologie *2*, 449–458.

10. Vicente-Serrano, S.M., Beguería, S., and López-Moreno, J.I. (2009). A Multiscalar Drought Index Sensitive to Global Warming: The Standardized Precipitation Evapotranspiration Index. J. Clim. *23*, 1696–1718. https://doi.org/10.1175/2009JCLI2909.1.

11. Field, R.D., Spessa, A.C., Aziz, N.A., Camia, A., Cantin, A., Carr, R., Groot, W.J. de, Dowdy, A.J., Flannigan, M.D., Manomaiphiboon, K., et al. (2015). Development of a Global Fire Weather Database. Nat. Hazards Earth Syst. Sci. *15*, 1407–1423. https://doi.org/10.5194/nhess-15-1407-2015.

12. Kanamitsu, M., Ebisuzaki, W., Woollen, J., Yang, S.-K., Hnilo, J.J., Fiorino, M., and Potter, G.L. (2002). NCEP–DOE AMIP-II Reanalysis (R-2). Bull. Am. Meteorol. Soc. *83*, 1631–1644. https://doi.org/10.1175/BAMS-83-11-1631.

13. Pesaresi, M., Ehrlich, D., Ferri, S., Florczyk, A., Carneiro Freire Sergio, M., Halkia, S., Julea Andreea, M., Kemper, T., Soille, P., and Syrris, V. (2016). Operating procedure for the production of the Global Human Settlement Layer from Landsat data of the epochs 1975, 1990, 2000, and 2014 (Publications Office of the European Union) https://doi.org/10.2788/253582 (online).

14. Kloster, S., Mahowald, N.M., Randerson, J.T., Thornton, P.E., Hoffman, F.M., Levis, S., Lawrence, P.J., Feddema, J.J., Oleson, K.W., and Lawrence, D.M. (2010). Fire dynamics during the 20th century simulated by the Community Land Model. Biogeosciences *7*, 1877–1902. https://doi.org/10.5194/bg-7-1877-2010.

15. Pechony, O., and Shindell, D.T. (2010). Driving forces of global wildfires over the past millennium and the forthcoming century. Proc. Natl. Acad. Sci. *107*, 19167–19170. https://doi.org/10.1073/pnas.1003669107.

16. Poulter, B., MacBean, N., Hartley, A., Khlystova, I., Arino, O., Betts, R., Bontemps, S., Boettcher, M., Brockmann, C., Defourny, P., et al. (2015). Plant functional type classification for earth system models: results from the European Space Agency's Land Cover Climate Change Initiative. Geosci Model Dev *8*, 2315–2328. https://doi.org/10.5194/gmd-8-2315-2015.

17. Moesinger, L., Dorigo, W., de Jeu, R., van der Schalie, R., Scanlon, T., Teubner, I., and Forkel, M. (2020). The global long-term microwave Vegetation Optical Depth Climate Archive (VODCA). Earth Syst. Sci. Data *12*, 177–196. https://doi.org/10.5194/essd-12-177-2020.

18. Schelhaas, M.-J., Nabuurs, G.-J., and Schuck, A. (2003). Natural disturbances in the European forests in the 19th and 20th centuries. Glob. Change Biol. *9*, 1620–1633. https://doi.org/10.1046/j.1365-2486.2003.00684.x.

19. Patacca, M., Lindner, M., Lucas-Borja, M.E., Cordonnier, T., Fidej, G., Gardiner, B., Hauf, Y., Jasinevičius, G., Labonne, S., Linkevičius, E., et al. (2023). Significant increase in natural disturbance impacts on European forests since 1950. Glob. Change Biol. *29*, 1359–1376. https://doi.org/10.1111/gcb.16531.

20. Camia, A., Giuntoli, J., Jonsson, K., Robert, N., Cazzaniga, N., Jasinevičius, G., Avitabile, V., Grassi, G., Barredo Cano, J.I., and Mubareka, S. (2020). The use of woody biomass for energy production in the EU (Publications Office of the European Union).

21. van der Werf, G.R., Randerson, J.T., Giglio, L., van Leeuwen, T.T., Chen, Y., Rogers, B.M., Mu, M., van Marle, M.J.E., Morton, D.C., Collatz, G.J., et al. (2017). Global fire emissions estimates during 1997–2016. Earth Syst. Sci. Data *9*, 697–720. https://doi.org/10.5194/essd-9-697-2017.

22. Forzieri, G., Pecchi, M., Girardello, M., Mauri, A., Klaus, M., Nikolov, C., Rüetschi, M., Gardiner, B., Tomaštík, J., Small, D., et al. (2020). A spatially explicit database of wind disturbances in European forests over the period 2000–2018. Earth Syst. Sci. Data *12*, 257–276. https://doi.org/10.5194/essd-12-257-2020.

23. Taszarek, M., Allen, J., Púčik, T., Groenemeijer, P., Czernecki, B., Kolendowicz, L., Lagouvardos, K., Kotroni, V., and Schulz, W. (2019). A Climatology of Thunderstorms across Europe from a Synthesis of Multiple Data Sources. https://doi.org/10.1175/JCLI-D-18-0372.1.

24. Pettit, J.L., Pettit, J.M., Janda, P., Rydval, M., Čada, V., Schurman, J.S., Nagel, T.A., Bače, R., Saulnier, M., Hofmeister, J., et al. (2021). Both Cyclone-induced and Convective Storms Drive Disturbance Patterns in European Primary Beech Forests. J. Geophys. Res. Atmospheres *126*, e2020JD033929. https://doi.org/10.1029/2020JD033929.

25. Forzieri, G., Girardello, M., Ceccherini, G., Spinoni, J., Feyen, L., Hartmann, H., Beck, P.S.A., Camps-Valls, G., Chirici, G., Mauri, A., et al. (2021). Emergent vulnerability to climate-driven disturbances in European forests. Nat. Commun. *12*, 1081. https://doi.org/10.1038/s41467-021-21399-7.

26. Breiman, L. (2001). Random Forests. Mach. Learn. *45*, 5–32. https://doi.org/10.1023/A:1010933404324.

27. Forzieri, G., Dutrieux, L.P., Elia, A., Eckhardt, B., Caudullo, G., Taboada, F.Á., Andriolo, A., Bălăcenoiu, F., Bastos, A., Buzatu, A., et al. (2023). The Database of European Forest Insect and Disease Disturbances: DEFID2. Glob. Change Biol. *29*, 6040–6065. https://doi.org/10.1111/gcb.16912.

28. Senf, C., and Seidl, R. (2021). Mapping the forest disturbance regimes of Europe. Nat. Sustain. *4*, 63–70. https://doi.org/10.1038/s41893-020-00609-y.

29. Senf, C., and Seidl, R. (2021). Storm and fire disturbances in Europe: Distribution and trends. Glob. Change Biol. *27*, 3605–3619. https://doi.org/10.1111/gcb.15679.

30. Sebald, J., Senf, C., and Seidl, R. (2021). Human or natural? Landscape context improves the attribution of forest disturbances mapped from Landsat in Central Europe. Remote Sens. Environ. *262*, 112502. https://doi.org/10.1016/j.rse.2021.112502.

31. Runge, J., Gerhardus, A., Varando, G., Eyring, V., and Camps-Valls, G. (2023). Causal inference for time series. Nat. Rev. Earth Environ. *4*, 487–505. https://doi.org/10.1038/s43017-023-00431-y.

32. Marini, L., Ayres, M.P., and Jactel, H. (2022). Impact of Stand and Landscape Management on Forest Pest Damage. Annu. Rev. Entomol. *67*, 181–199. https://doi.org/10.1146/annurev-ento-062321-065511.

33. Aukema, B.H., Carroll, A.L., Zhu, J., Raffa, K.F., Sickley, T.A., and Taylor, S.W. (2006). Landscape Level Analysis of Mountain Pine Beetle in British Columbia, Canada: Spatiotemporal Development and Spatial Synchrony within the Present Outbreak. Ecography *29*, 427–441.

34. Raffa, K.F., Aukema, B.H., Bentz, B.J., Carroll, A.L., Hicke, J.A., Turner, M.G., and Romme, W.H. (2008). Cross-scale Drivers of Natural Disturbances Prone to Anthropogenic Amplification: The Dynamics of Bark Beetle Eruptions. BioScience *58*, 501–517. https://doi.org/10.1641/B580607.

35. Seidl, R., Müller, J., Hothorn, T., Bässler, C., Heurich, M., and Kautz, M. (2016). Small beetle, large-scale drivers: how regional and landscape factors affect outbreaks of the European spruce bark beetle. J. Appl. Ecol. *53*, 530–540. https://doi.org/10.1111/1365-2664.12540.

36. Tudoran, M.-M., Marquer, L., and Jönsson, A.M. (2016). Historical experience (1850–1950 and 1961–2014) of insect species responsible for forest damage in Sweden: Influence of climate and land management changes. For. Ecol. Manag. *381*, 347–359. https://doi.org/10.1016/j.foreco.2016.09.044.

37. de Groot, M., Diaci, J., and Ogris, N. (2019). Forest management history is an important factor in bark beetle outbreaks: Lessons for the future. For. Ecol. Manag. *433*, 467–474. https://doi.org/10.1016/j.foreco.2018.11.025.

38. Rigot, T., van Halder, I., and Jactel, H. (2014). Landscape diversity slows the spread of an invasive forest pest species. Ecography *37*, 648–658. https://doi.org/10.1111/j.1600-0587.2013.00447.x.

39. Nelson, K.N., Rocca, M.E., Diskin, M., Aoki, C.F., and Romme, W.H. (2014). Predictors of bark beetle activity and scale-dependent spatial heterogeneity change during the course of an outbreak in a subalpine forest. Landsc. Ecol. *29*, 97–109. https://doi.org/10.1007/s10980-013-9954-1.

40. Nunes, P., Branco, M., Van Halder, I., and Jactel, H. (2021). Modelling Monochamus galloprovincialis dispersal trajectories across a heterogeneous landscape to optimize monitoring by trapping networks. Landsc. Ecol. *36*, 931–941. https://doi.org/10.1007/s10980-020-01188-1.

41. Campbell, E.M., MacLean, D.A., and Bergeron, Y. (2008). The Severity of Budworm-Caused Growth Reductions in Balsam Fir/Spruce Stands Varies with the Hardwood Content of Surrounding Forest Landscapes. For. Sci. *54*, 195–205. https://doi.org/10.1093/forestscience/54.2.195.

42. Lloret, F., Calvo, E., Pons, X., and Díaz-Delgado, R. (2002). Wildfires and landscape patterns in the Eastern Iberian Peninsula. Landsc. Ecol. *17*, 745–759. https://doi.org/10.1023/A:1022966930861.

43. Turner, M.G., Donato, D.C., and Romme, W.H. (2013). Consequences of spatial heterogeneity for ecosystem services in changing forest landscapes: priorities for future research. Landsc. Ecol. *28*, 1081–1097. https://doi.org/10.1007/s10980-012-9741-4.

44. Seidl, R., Schelhaas, M.-J., and Lexer, M.J. (2011). Unraveling the drivers of intensifying forest disturbance regimes in Europe. Glob. Change Biol. *17*, 2842–2852. https://doi.org/10.1111/j.1365-2486.2011.02452.x.

45. Mitchell, S.J. (2013). Wind as a natural disturbance agent in forests: a synthesis. For. Int. J. For. Res. *86*, 147–157. https://doi.org/10.1093/forestry/cps058.

46. Gardiner, B. (2021). Wind damage to forests and trees: a review with an emphasis on planted and managed forests. J. For. Res. *26*, 248–266. https://doi.org/10.1080/13416979.2021.1940665.

47. Gardiner, B., Schuck, A., Schelhaas, M.J., Orazio, C., Blennow, K., and Nicoll, B. (2013). Living with storm damage to forests (European Forest Institute).

48. Gohli, J., Krokene, P., Flo Heggem, E.S., and Økland, B. (2024). Climatic and management-related drivers of endemic European spruce bark beetle populations in boreal forests. J. Appl. Ecol. *61*, 809–820. https://doi.org/10.1111/1365-2664.14606.

49. Guyot, V., Jactel, H., Imbaud, B., Burnel, L., Castagneyrol, B., Heinz, W., Deconchat, M., and Vialatte, A. (2019). Tree diversity drives associational resistance to herbivory at both forest edge and interior. Ecol. Evol. *9*, 9040–9051. https://doi.org/10.1002/ece3.5450.

50. Jamieson, M.A., Trowbridge, A.M., Raffa, K.F., and Lindroth, R.L. (2012). Consequences of Climate Warming and Altered Precipitation Patterns for Plant-Insect and Multitrophic Interactions. Plant Physiol. *160*, 1719–1727. https://doi.org/10.1104/pp.112.206524.

51. Migliavacca, M., Dosio, A., Kloster, S., Ward, D.S., Camia, A., Houborg, R., Houston Durrant, T., Khabarov, N., Krasovskii, A.A., San Miguel-Ayanz, J., et al. (2013). Modeling burned area in Europe with the Community Land Model. J. Geophys. Res. Biogeosciences *118*, 265–279. https://doi.org/10.1002/jgrg.20026.